University of Stavanger

**FACULTY OF SCIENCE AND TECHNOLOGY**

# BACHELOR'S THESIS

| | |
|---|---|
| Study programme / specialisation:<br>Petroleum Geology Engineering<br>Bachelor's Degree<br>Programme | Spring semester, 2021<br><br>Open |
| Author:<br>Charish Mae Araneta | ……<br>(signature of author) |
| Programme coordinator:<br>Supervisors: Pål Ø. Andersen, Raoof Gholami | |
| Title of bachelor's thesis:<br>A review of energy produces and storage in geothermal energy, and geothermal wells and drilling | |
| Credits: 20 | |
| Keywords:<br>Geothermal<br>Energy<br>Well<br>Drilling | Number of pages: 73<br>+ supplemental material/other: 8<br><br>Place: Stavanger<br>Date: 15.05.2021 |

# A review of energy produces and storage in geothermal energy, and geothermal well and drilling

**by**

**Charish Mae Araneta**

**BSc Thesis**

Presented to the Faculty of Science and Technology

The University of Stavanger

**The University of Stavanger**

**May 2021**

# Abstract

## A review of energy produces and storage in geothermal energy, and geothermal wells and drilling

*Geothermal energy is one of the most rapidly growing renewable energy sources today. It is a fundamental renewable resource since heat is continually generated throughout the earth and is still available throughout the year. It can help minimize the use of fossil fuels, this being a high priority on the political agenda of many countries around the world. Geothermal energy is one of the oldest and most well-known sources of energy to generate electricity. The primary source of geothermal energy is hydrothermal resources. It is found at a shallower depth, and hot dry rock resources are normally found in a deeper formation.*

*With all the technology we have today, it is good to research where to have all we need. Therefore, this thesis aims to give us two overviews of how energy is produced and stored: geothermal energy and geothermal wells and drilling. Geothermal energy is renewable- and environmentally friendly energy because energy is the extraction of natural thermal energy from within the earth. It summarizes general knowledge about geothermal energy; it includes the functions and challenges of using geothermal energy and its benefit and drawbacks. Likewise, it will explain the heat transfer theory. It classifies into three types which are heat convection, heat conduction, and heat radiation. With the help of its conceptual and numerical modelling, it will give us a better understanding of the over-all heat transfer coefficient.*

*Further to this thesis, it is important to analyse any possible problems by operating in the geothermal field. This thesis will present an informative overview of how to separate the two significant roles, which are "planning" and "designing" a geothermal well drilling. It will give a great variety of information about the two roles. On the other hand, it explains a general assessment of geothermal drilling and well, such as the typical drilling rigs and geothermal wells. Finally, it is undoubtedly in current research projects in Norway and other countries, such as the Philippines and Iceland.*

# Acknowledgment

*This thesis is submitted to the Department of Energy and Petroleum Engineering at the University of Stavanger as a Bachelor´s in Science degree requirement. I want to thank my supervisors, Pål Ø. Andersen and Raoof Gholami, for your endless guidance and help throughout this project. Thank you for your time and effort in assisting me with this thesis. Even in your busy schedule, you are always available to give back feedback and advice.*

*I would also like to express my very profound gratitude to my family, especially my parents, for supporting and allowing me to chase after my dreams. Last year was a challenging year for all of us and a tough year for my family and me. Last October of 2020, we found out that I have lymphoma cancer. I thought that I was not able to finish my study due to my sickness. God knows how much I worked hard to pass all my exams, meet the requirements that I needed, and finish writing this thesis. Last month, April 2021, I went to visit my doctor. After months of recovery, observation, blood tests, and CT scans. My doctor finally declared that "I AM CANCER FREE." The radiation treatment went well, and they cannot see any tumours have gone back. Therefore, I thank God for helping, guiding, comforting and giving me and my family strength when we needed it the most.*

*Without God and my family, this accomplishment would not have been possible. All glory and honour belong to my living God, Jesus Christ!*

*Charish Mae Araneta*
*University of Stavanger, Norway*
*May 2021*

# List of Contents

**ABSTRACT** ..... **5**

**ACKNOWLEDGMENT** ..... **6**

**LIST OF FIGURES** ..... **10**

**LIST OF TABLES** ..... **11**

**NOMENCLATURE** ..... **12**

**ABBREVIATIONS** ..... **14**

**1 INTRODUCTION** ..... **15**

1.1 Background ..... 15
1.2 Objective of the thesis ..... 16
1.3 Structure of the thesis ..... 16

**2 GEOTHERMAL ENERGY** ..... **17**

2.1 Introduction to Geothermal Energy ..... 17
2.2 Geothermal system ..... 18
2.3 Geothermal reservoir ..... 18
2.4 Geothermal Energy Occurrence ..... 19
*2.4.1 Tectonic plate boundaries ..... 19*
*2.4.2 Hot spot ..... 21*
2.5 Geothermal Energy Challenges ..... 22
2.6 Geothermal Energy Advantage and Disadvantage ..... 24
2.7 Geothermal Energy Worldwide Review ..... 25
2.8 Geothermal Energy Different types ..... 26
*2.8.1 Geothermal Heat Pumps ..... 26*
*2.8.2 Space Heating and Cooling ..... 28*
*2.8.3 Greenhouse and Covered Ground Heating ..... 28*
*2.8.4 Aquaculture Pond and Raceway Heating ..... 28*
*2.8.5 Agricultural Crop Drying ..... 29*
*2.8.6 Industrial Process Heat ..... 29*
*2.8.7 Snow Melting and Space Cooling ..... 29*
*2.8.8 Bathing and Swimming ..... 30*
*2.8.9 Other Uses ..... 30*

**3 THEORY** ..... **31**

3.1 Heat flow ..... 31
3.2 Heat Transfer Mechanisms ..... 31

*3.2.1 Heat conduction* ..... *31*
*3.2.2 Heat convection* ..... *32*
*3.2.3 Heat Radiation* ..... *33*
3.3 HEAT FLOW RATE ..... 33

**4 MODELLING ..... 34**

4.1 HEAT TRANSFER MODELLING ..... 34
*4.1.1 Over-all Heat Transfer* ..... *34*
*4.1.2 Heat Transfer between flowing fluid and inside tubing wall* ..... *35*
*4.1.3 Heat Transfer* ..... *36*
*4.1.4 Estimating $h_r$ and $h_c$* ..... *38*
*4.1.5 Natural Convection ($h_c$)* ..... *38*
4.2 CALCULATION PROCEDURE ..... 39
4.3 RESULT OF HEAT TRANSFER ..... 41

**5 GEOTHERMAL WELL DRILLING ..... 42**

5.1 GEOTHERMAL WELL DRILLING PLANNING ..... 42
*5.1.1 Classification of geothermal wells* ..... *43*
*5.1.2 Well costs* ..... *43*
*5.1.3 Geothermal well different types* ..... *43*
5.2 GEOTHERMAL CHEMISTRY ..... 44
*5.2.1 Corrosion* ..... *45*
*5.2.2 Scaling* ..... *49*
*5.2.3 Material Selection* ..... *49*
*5.2.4 Metallic Materials* ..... *50*
*5.2.5 Non-Metallic Selection* ..... *50*
5.3 GEOTHERMAL WELL DRILLING DESIGN ..... 51
5.4 GEOTHERMAL WELL DRILLING DIFFERENT TYPES ..... 53
*5.4.1 Cable Tool* ..... *53*
*5.4.2 Rotary drilling* ..... *55*
*5.4.3 Types of bits* ..... *56*
5.5 GEOTHERMAL WELL WORLDWIDE REVIEW 2010 – 2014 ..... 57
*5.5.1 Well drilled* ..... *57*
*5.5.2 Person-years of professional personnel working* ..... *57*
*5.5.3 Total investment* ..... *58*

**6 PROJECTS ..... 59**

6.1 NORWEGIAN PROJECTS ..... 59
*6.1.1 Geothermal energy in the Iddefjord granite in Østfold Norway* ..... *59*
*6.1.2 Hot Dry Rock Project in State Hospital in Oslo* ..... *63*
*6.1.3 Kontiki project and HeatBar project in Norway* ..... *63*
6.2 THE PHILIPPINES PROJECT ..... 67

6.3 ICELAND PROJECT ..... 69
**7 CONCLUSION ..... 74**
**REFERENCES ..... 75**
**APPENDIX ..... 77**

# List of Figures

Figure 1 Larderello Italy 1868 ..... 15
Figure 2 Geothermal steam field with its elements: recharge area, impermeable cover, reservoir and heat source, (González-Acevedo & García-Zarate, 2018) ..... 17
Figure 3 Geothermal resources temperatures (Sircar et al., 2017) ..... 18
Figure 4 Tectonic controls, (Finger & Blankenship, 2010) ..... 20
Figure 5 Risk and investment on geothermal projects, (Fraser, Calcagno, Jaudin, Vernier, & Dumas, 2013) ..... 22
Figure 6 The installed direct-use geothermal capacity and annual utilization from 1995 to 2015 ..... 25
Figure 7 Comparison of worldwide direct-use geothermal energy in TJ/yr from 1995, 2000, 2005, 2010 and 2015, (Lund & Boyd, 2015) ..... 26
Figure 8 Simple stylized diagram of the vapor-compression refrigeration cycle of a heat pump (Ehrlich & Geller, 2017) ..... 27
Figure 9 Outline of different snow storages, in a building, in a pit and underground,(Nordell, 2015) ..... 30
Figure 10 Temperature boundary conditions for a slab, (Nathan Amuri, 2017) ..... 32
Figure 11 Heat convection through two media,(Nathan Amuri, 2017) ..... 32
Figure 13 Natural convection in the casing annulus, (Willhite, 1967) ..... 36
Figure 12 Temperature distribution in annular completion (Willhite, 1967) ..... 37
Figure 14 Variation of $Uto$ with tubing temperature for parameters of Table 3, (Willhite, 1967) ..... 40
Figure 15 Typical composition of geothermal waters, (Povarov, Tomarov, & Semenov, 2000) ..... 45
Figure 16 Electrochemical process (Kristanto, Kusumo, & Abdassah, 2005) ..... 45
Figure 17 Uniform corrosion (Bellarby, 2009) ..... 47
Figure 18 Overall reaction, (Shadravan & Shine, 2015) ..... 47
Figure 19 Carbon steel tubing (Bellarby, 2009) ..... 48
Figure 20 Calcite scaling (Fridriksson & Thórhallsson, 2007) ..... 49
Figure 21 Typical geothermal well design, (Suryanarayana, Bowling, Sathuvalli, & Krishnamurthy) ..... 52
Figure 22 Geothermal well design, (Finger & Blankenship, 2010) ..... 52
Figure 23 Basic elements of a cable tool drilling, (Culver, 1998) ..... 54
Figure 24 Schematic diagram of a direct rotary, (Culver, 1998) ..... 55
Figure 26 PDC bits, (Ngugi, 2008) ..... 56
Figure 27 Drag bit, (Ngugi, 2008) ..... 56
Figure 25 Tri-cone roller bits, (Ngugi, 2008) ..... 56
Figure 28 Bit body (single leg) with cone and bearing in place, (Ngugi, 2008) ..... 57
Figure 29 Bit bearing, (Ngugi, 2008) ..... 57
Figure 30 Bit cone, (Ngugi, 2008) ..... 57
Figure 31, A: Bore hole localities in Østfold Norway. Dotted area: Iddefjord granite. B: Temperature gradient (°C/km) and heat flow (hfu) from the same localities, (Grønlie et al., 1980) ..... 60

Figure 32, Temperature verses depth plots from 9 of the location in Figure 33 A. Note the good results in holes Nos. 12 and 14 and the high temperature gradients, (Grønlie, Johansen, Karlstad, & Heier, 1980) ..... 62
Figure 33 Drilling tools used for the HDR project at the State Hospital in Oslo,(Midttømme, 2005) ..... 63
Figure 34 Heat flow map of Norway from 1970s, (Pascal, Elvebakk, & Olesen, 2010) ..... 64
Figure 35 Modern heat flow map of Norway. Note that the newly determined heat flow values exceed by 10 to 20 $mW/m^2$,(Pascal et al., 2010) ..... 65
Figure 36 Estimated temperatures at 5 km depth below the surface, (Pascal et al., 2010) ..... 66
Figure 37 Location of the Tiwi Geothermal Field, (Menzies et al., 2010) ..... 67
Figure 38 Reservoir Top and Major Structures in the Tiwi Geothermal Field, (Menzies et al., 2010) ..... 68
Figure 39 Initial State Conceptual Model of Tiwi, (Menzies, Villaseñor, & Sunio, 2010) ..... 69
Figure 40 Geological map of Reykjanes. It shows the drillhole locations, potential drill sites for deep drilling, depth contours to high resistivity core and hydrothermal surface manifestations,(Fridleifsson & Albertsson, 2000) ..... 70
Figure 41 Reykjanes, the landward extension of the Reykjanes ridge. The drill fields at Reykjanes, Eldvörp and Svartsengi can be seen,(Fridleifsson & Albertsson, 2000) ..... 71
Figure 42 The Nesjavellir drill field, (Fridleifsson & Albertsson, 2000) ..... 72
Figure 43 A temperature profile of well NJ-11 during drilling. The boiling point depth curve for pure water is shown for comparison,(Fridleifsson & Albertsson, 2000) ..... 73

# List of Tables

Table 1 - Summary of direct-use data worldwide in 2015, (Lund & Boyd, 2015) ..... 78
Table 2 - Summary of the various categories of direct-use worldwide for the period of 2015, 2010, 2005, 2000 and 1995, (Lund & Boyd, 2015) ..... 78
Table 3 - Parameters for Variation of $Uto$, (Willhite, 1967) ..... 78
Table 4 - Thermal Conductivity of Wellbore Materials, (Willhite, 1967) ..... 78
Table 6 - Temperature gradient, conductivity and heat flow from 11 holes in the Iddefjord granite, Østfold, Norway. Conductivity only measured in holes Nos. 12 and 14 (*: estimated conductivity), (Grønlie et al., 1980) ..... 78
Table 5 - Estimated temperatures at 5km depth below the surface for each selected heat flow site in Norway, (Midttømme, 2005) ..... 78
Table 7 - Hydrothermal section along the rift axes at Reykjanes, inclunding all deep drill holes,(Fridleifsson & Albertsson, 2000) ..... 78
Table 8 - Hydrothermal cross section across the rift zone at Nesjavallir, including well NJ-11,(Fridleifsson & Albertsson, 2000) ..... 78
Table 11 - Steam Well Borehole Profile, (Finger & Blankenship, 2010) ..... 78
Table 10 - Steam Well Bit Summary, (Finger & Blankenship, 2010) ..... 78
Table 12 - Brine Well Borehole Profile (Finger & Blankenship, 2010) ..... 78
Table 9 - Brine Well Bit Summary, (Finger & Blankenship, 2010) ..... 78

# Nomenclature

$A = energy\ generated\ per\ unit\ volume\ per\ unit\ volume\ per\ second$

$A_j = characteristic\ surface\ area, sq\ ft (subscript\ j\ identifies\ the\ surface)$

$COP_{(max)} = coefficient\ of\ performance$

$D = the\ product\ of\ depth$

$DA = heat\ generated\ by\ radioactive\ decay\ in\ the\ shallow\ crust$

$f(t) = transient\ time\ function, dimensionless$

$F_{tci} = view\ factor\ based\ on\ outside\ tubing\ and\ inside\ casing\ surfaces,$
$dimensionless$

$\overline{F_{tci}} = over - all\ interchange\ factor\ between\ the\ outside\ tubing\ and$
$inside\ casing\ surfaces, dimensionless$

$G = Grashoft\ number, dimensionless$

$h_c = heat\ transfer\ coefficient\ for\ natural\ convection\ based\ on$
$the\ outside\ tubing\ surface\ and\ the\ temperature\ difference$
$between\ the\ outside\ tubing\ and\ inside\ casing\ surfaces,$
$Btu/hr\ ft\ °F$

$h_f = film\ coefficient\ for\ heat\ transfer\ or\ condesation\ coefficient\ based\ on$
$inside\ tubing\ or\ casing\ surface\ and\ temperature\ difference\ between$
$the\ flowing\ fluid\ and\ either\ of\ these\ surfaces, Btu/hr\ ft\ °F$

$h_r = heat\ trasnfer\ coefficient\ for\ radiation\ based\ on\ the\ outside\ tubing$
$surface\ and\ the\ temperature\ difference\ between\ the\ outside$
$tubing\ and\ inside\ casing\ surfaces, Btu/hr\ ft\ °F$

$k_{cas} = thermal\ conductivity\ of\ the\ casing\ material\ at\ the\ average$
$casing\ temperature\ , Btu/hr\ ft\ °F$

$k_{cem} = thermal\ conductivity\ the\ cement\ at\ the\ average\ cement\ temperature$
$and\ pressure, Btu/hr\ ft\ °F$

$k_e = thermal\ conductivity\ of\ the\ formation, Btu/hr\ ft\ °F$

$k_{hc} = equivalent\ thermal\ conductivity\ of\ the\ annular\ fluid\ with\ natural$
$convection\ effects, evaluated\ at\ the\ average\ temperature\ and\ pressure$
$of\ the\ annulus, Btu/hr\ ft\ °F$

$k_{tub} = thermal\ conductivity\ of\ the\ tubing\ material\ at\ the\ average\ tubing$
$temperature, Btu/hr\ ft\ °F$

$Pr = Prandtl\ number, dimensionless$

$Q = heat\ flow\ through\ the\ wellbore, Btu/hr$

$Q_c = heat\ flow\ in\ the\ annulus\ by\ natural\ convection\ and\ conduction, Btu/hr$

$Q_r = heat\ flow\ in\ the\ annulus\ due\ to\ radiation, Btu/hr$

$r = radius, ft$

$r_{oi} = inside\ radius\ of\ casing, ft$
$r_{co} = outside\ radius\ of\ casing, ft$
$r_h = radius\ of drill\ hole, ft$
$r_{ins} = radius\ of\ the\ outside\ insultation\ surface, ft$
$r_{ti} = inside\ radius\ of\ tubing, ft$
$r_{to} = outside\ radius\ of\ tubing, ft$
$t = time, hours\ or\ units\ consitent\ of\ \alpha$
$T = temperature,$ °F
$T* = absolute\ temperature, °R =$ °F + 460
$T_{ci} = temperature\ of\ inside\ casing\ surface,$ °F
$T_{co} = temperature\ of\ outside\ casing\ surface,$ °F
$T_e = undisturbed\ temperature\ of\ the\ formation,$ °F
$T_f = temperature\ of\ flowing\ fluid,$ °F
$T_G = ground\ temperature\ in\ Kelvins,$ °F
$T_H = high\ temperatures\ in\ Kelvins,$ °F
$T_h = temperature\ at\ cement\ formation\ interface,$ °F
$T_{ins} = temperature\ of\ the\ outside\ surface\ of\ the\ insulation,$ °F
$T_{ti} = temperature\ of\ inside\ tubing\ surface,$ °F
$T_{to} = temperature\ of\ outside\ tubing\ surface,$ °F
$U_{ci} = overall\ heat\ transfer\ coefficient\ based\ on\ the\ inside\ casing\ surface\ and\ the\ temperature\ difference\ between\ the\ fluid\ and\ cement\ formation\ interface, Btu/hr\ sq\ ft$ °F
$U_j = overall\ heat\ transfer\ coefficient\ based\ on\ the\ characteristic\ surface\ area\ A_j\ and\ characteristi\ temperature\ difference\ \Delta T_j, , Btu/hr\ sq\ ft$ °F
$U_{to} = overall\ heat\ transfer\ coefficient\ based\ on\ the\ outside\ tubing\ surface\ and\ the\ temperature\ difference\ between\ fluid\ and\ cement\ formation\ interface, , Btu/hr\ sq\ ft$ °F
$z = depth, ft$
$\alpha = thermal\ diffusivity\ of\ the\ earth, sq\ ft/hr$
$\beta = thermal\ volumetic\ expansion\ coefficient\ of\ the\ fluid\ in\ the\ annulus,$
$°R^{-1} = \frac{1}{T_{an}^*}\ for\ an\ ideal\ gas, or\ generally = -\frac{1}{\rho_{an}}\left(\frac{\partial \rho_{an}}{\partial T}\right)_{\rho}$
$where\ P\ is\ the\ annulus\ pressure$
$\Delta L = increment\ of\ tubing\ or\ casing\ length, ft$
$\Delta r = insulation\ thickness, ft$
$\Delta T_j = characteristic\ temperature\ difference\ related\ to\ U_j\ and\ the\ surface\ area\ A_j,$ °F
$\varepsilon_{to} = emissivity\ of\ outside\ tubing\ surface, dimensionless$

$\varepsilon_{ci} = emissivity\ of\ inside\ casing\ surface, dimensionless$
$\sigma = Stefan - Boltzmann\ constant, 1.713\ X\ 10^{-9}/sq\ ft\ hr\ °R^4$
$\rho_{an} = density\ of\ the\ fluid\ in\ the\ annulus\ at\ T_{an} and\ pressure\ P, lb/cu\ ft$
$\mu_{an} = viscosity\ of\ the\ fluid\ in\ the\ annulus\ at\ T_{an} and\ P, lb\ mass/ft\ hr$

# Abbreviations

℃ $(/km) =\ unit\ of\ temperature\ on\ the\ Celsius\ scale\ (per\ kilo\ meter)$
℉ $=\ unit\ of\ themperature\ on\ the\ Fahrenheit\ scale$
$CaCO_3 = Calcite\ (Calcium\ Carbonate)$
$CO_2 = Carbon\ dioxide$
$FeS = Iron\ sulphide$
$GW, GW_e = Giga\ Watt\ (Equivalent)$
$HCl = Hydrogen\ Chloride$
$H_2S = Hydrogen\ Sulphide$
$H_2SO_4 = Sulphric\ Acid$
$km =\ Kilometer$
$m =\ Meter$
$MWt = Mean\ Waiting\ time$
$NaCl = Sodium\ Chloride\ (Brine)$
$NORSOK = NORsk\ SOkkels\ Konkurranseposisjon$
$pH = Power\ of\ Hydrogen$
$SiO_2 = Silicon\ Oxide\ (Silica)$
$TJ/yr\ = Terajoules\ per\ year$
$WGC2010 = The\ World\ Geothermal\ Congress\ 2010$

# 1 Introduction

Geothermal energy is among the most rapidly developing renewable energy sources. It is a fundamental renewable resource since heat is continually generated throughout the earth and is still available throughout the year. It refers to the thermal energy that has been deposited underneath the planet for millions of years as a result of the earth´s formation. It makes use of a considerable volume of untapped energy stored under the earth´s surface.

## 1.1 Background

Due to the appearance of volcanoes, hot springs, and other thermal phenomena, our forefathers must have concluded that areas of the Earth´s interior were hot (Dickson & Fanelli, 2013). Native American have been using geothermal heat for over ten thousand years ago. They have used it for cooking and were drawn for hot springs for theological as well as functional purposes. In ancient time, Greek and Romans saw hot springs as sites of healing imbued with divine influence, as well as places of heating for houses.

In 1740, the first thermometer measurements were made in a mine near Belfort, France. A small town called Larderello in the Tuscan region of Italy (Figure 1) was the first to generate electricity using geothermal energy in 1818. The first geothermal heat plants were built in Boise, Idaho, in 1892 (USA). In 2015, geothermal energy was used to generate electricity in more than 80 countries around the world (Lund & Boyd, 2015).

*Figure 1 Larderello Italy 1868*

Geothermal energy, for example, is one of these renewables. Using thermal energy from the Earth´s interior to generate other value sources of energy (such as electricity). It requires the extraction of high temperature fluids such as water, methane, or a combination of both.

## 1.2 Objective of the thesis

The objectives for this thesis are the following:

- To review how much energy is produced and stored in geothermal energy. To analyse how geothermal energy works; the challenges it faces, advantages and disadvantages. To recognize what type of- and which part of the world are using the most geothermal energy
- To learn how heat is transfer. To interpret the heat transfer theory and master the three types. By its conceptual and modelling, we will have a better understanding of the over-all heat transfer coefficient
- To distinguish the two significant roles, "planning" and "designing" on operating a geothermal well drilling. We will examine the different types of drilling rigs and geothermal wells
- To recognize some industrial projects in Norway and other countries such as the Philippines and Norway. We will determine how the different findings are and the results they got

## 1.3 Structure of the thesis

- **Chapter 2 Geothermal Energy** – This chapter contains a summary of general knowledge about geothermal energy. It contains its functions, the challenges it faces, and its benefit and drawbacks. It also represents different types of geothermal energy and review worldwide
- **Chapter 3 Theory** – This chapter contains the theory of heat flow, heat transfer and heat flow rate
- **Chapter 4 Modelling** – This chapter presents the model developed of heat transfer
- **Chapter 5 Geothermal Well** – This chapter represents the generic information about geothermal wells and drilling. It explains about planning, chemistry, designing, different types of drilling equipment and review worldwide regardless to geothermal well drilling
- **Chapter 6 Projects -** This chapter represents some industrial projects in Norway and other countries in the world such as the Philippines and Iceland
- **Chapter 7 Conclusion**– This chapter, a conclusion of the summary of all we have learned

# 2 Geothermal Energy

This chapter contains general information about geothermal energy. It also includes the functions, challenges, advantages, and disadvantages of the use of geothermal energy. And represents different types of geothermal energy worldwide.

## 2.1 Introduction to Geothermal Energy

Geothermal energy is the extraction of natural thermal energy from within the earth. The word geothermal comes from the Greek words; geo means "earth" and thermal means "heat". Geothermal energy is stored in rocks and fluids in the centre of the earth. It can be found from the shallow ground to several miles below the surface and even farther down to the scorching molten rock called *magma*. Geothermal energy forms of energy exploitation which is renewable and environmentally friendly. Figure 2 shows an image of the geothermal steam field, it manifests on the surface in the form of volcanoes, geysers, fumaroles, hot springs etc.

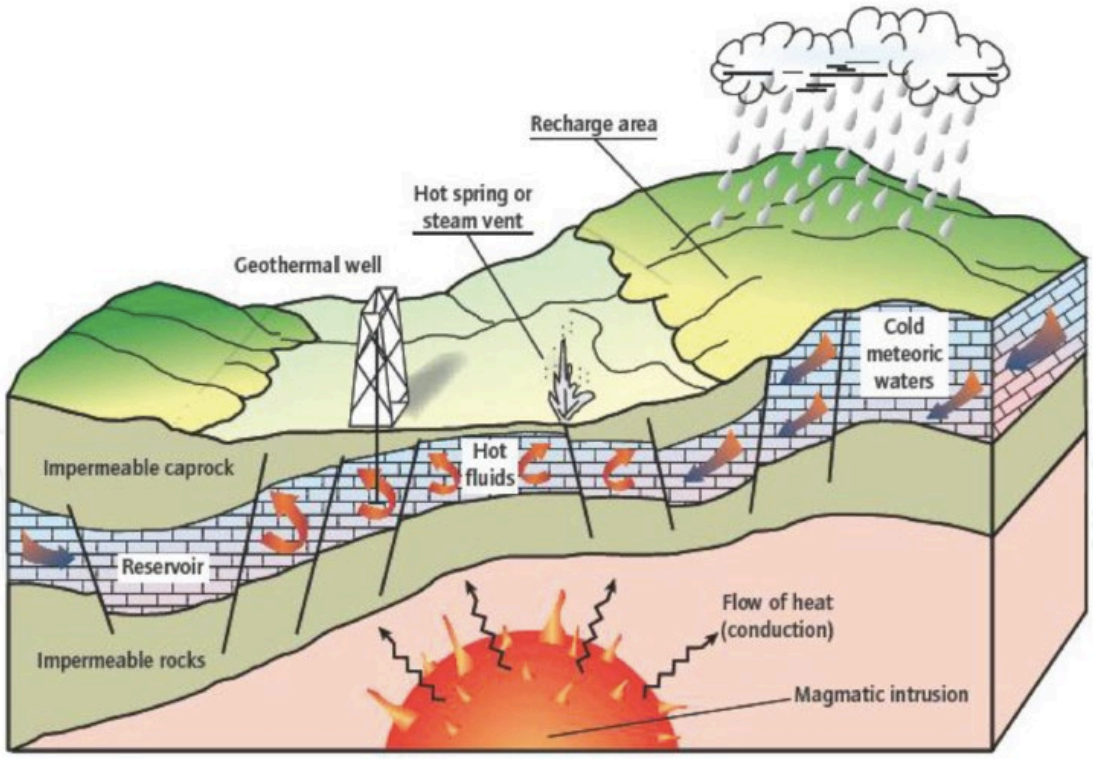


*Figure 2 Geothermal steam field with its elements: recharge area, impermeable cover, reservoir and heat source, (González-Acevedo & García-Zarate, 2018)*

According to (Matek, 2016), in 2016, a total of 13.1 GWe of conventional geothermal energy has been installed worldwide. The average temperature increases at 25ºC/km approximately

with depth (Finger & Blankenship, 2010). The heat source with a temperature below 100ºC (212ºF) at an economic centre is defined as low-temperature systems. For example, an island in the southwest in Iceland called Reyjhanes, is an area with magmatic intrusions that could reach more than of 400ºC (752ºF).

The most common definitions and classifications of geothermal energy are the Enthalpy (Lee, 1996), which carries the heat from the deep hot rocks into the surface. *Enthalpy* is the sum of the internal energy and the product of the pressure and volume of a thermodynamic system. It is used to heat content of fluids that are transported from the geothermal reservoir to the surface. Researchers divided enthalpy into three temperatures: low, medium, and high. Figure 3 explains the different types of geothermal resource temperature, low-, medium-, and high enthalpy resources. It explains from different research from different authors.

| **Classification Schemes** | (a) Muffler and Cataldi (1978) | (b) Hochstein (1990) | (c) Benderitter and Cormy (1990) | (d) Nicholson (1993) | (e) Axelsson and Gunnlaugsson (2000) |
|---|---|---|---|---|---|
| Low Enthalpy resources | <90 | <125 | <100 | <=150 | <=190 |
| Intermediate Enthalpy resources | 90–150 | 125–225 | 100–200 | - | - |
| High Enthalpy resources | >150 | >225 | >200 | >150 | >190 |

*Figure 3 Geothermal resources temperatures (Sircar et al., 2017)*

## 2.2 Geothermal system

Geothermal system defines, according to Dr. Manfred Hochstein (Lee, 1996), "convective water" in the upper crust of the Earth, which, in a confined space. It transfers heat from a heat source to heat sink, usually the free surface. It contains three main elements: *a heat source, a reservoir* and *a fluid (Lee, 1996)*.

The heat source can be a very high temperature (>600ºC) magmatic intrusion that has reached relatively shallow depth (5-10 km). It can be also a low temperature, like the Earth´s average temperature, which increases with depth. It can use heat to produce electricity.

## 2.3 Geothermal reservoir

The *reservoir* is a volume of hot permeable rocks with circulating fluids extract heat. It is cover by impermeable stones which are connected to a surficial recharge area.

Geothermal reservoirs which are suitable to produce electricity need a temperature above 150ºC(320ºF). The geothermal fluid is water. It originates from the reservoir. However,

some reservoir has low permeability. It could inject cooler fluid into the reservoir and produce it later. This water carries with its chemicals and gases such as $CO_2$, $H_2S$, etc. Figure 2 shows geothermal reservoir is located.

## 2.4 Geothermal Energy Occurrence

Geothermal energy is usually found along with the areas of hydrothermal resources. Temperature increases with depth within the Earth at an average of about 25ºC/km (Finger & Blankenship, 2010). The average surface temperature is about 20ºC, and the temperature of 3 km is the only 95ºC.

The heat of the Earth flows differently from different parts of the world. According to (Finger & Blankenship, 2010), in the Rocky Mountains (North America) heat flows around 40 to 60 $mWm^{-2}$. This heat flow, in the Rocky Mountain, flows within the thermal conductivity of the rocks. It is located on the upper part which is 4km of the crust yields with subsurface temperatures of 90º to 110ºC at 4km.

Geothermal energy can use temperatures low as 35ºC, well the minimum temperature suitable for electrical generation is about 135ºC. Therefore, most of the geothermal energies are usually found along major tectonic plate boundaries where most volcanoes are located.

### *2.4.1 Tectonic plate boundaries*

The heat of the Earth can also be related to the movement of the *magma.* It moves in the crust or deep circulation of water in active zones of faulting. Plate tectonics provides an overview of the geological process where we can see identified the heat flow and geothermal development. The brittle and moving plates of the lithosphere, the crust, and upper mantle, are driven by the convection of plastic rocks below.

Convection causes the crustal plates to break and move away from zones of hot upwelling material (Finger & Blankenship, 2010). The magma moves upward into a zone of separation brings with its substantial amounts of thermal energy. However, the area where the most spreading happens is in ocean basins and unsuitable for geothermal development.

Plate boundaries are divided into three main types: convergent-, divergent- and transform boundaries. Figure 4 explains the tectonic control. It contains line of spreading boundaries, subducting boundaries haunches on upper plates, translational or diffuse boundaries and areas with geothermal potential.

First are the convergent boundaries. It is where two plates are colliding. Subduction zones occur when one or both of the tectonic plates are composed of oceanic crust. It can happen when, are the following: oceanic crust meets ocean crust, oceanic crust meets continental crust, or continental crust meets continental crust. Many of the world´s most critical geothermal regions are associated with these features: Indonesia, Japan, Mexico, New Zealand, the Philippines, and the fields in Central and South America (Finger & Blankenship, 2010).

The second is the divergent boundaries. It is where two plates are moving apart. The space created can fill with new crustal material sourced from molten magma that forms below. Or it can develop within continents but will open up and become an ocean basin. It can happen on land, where the continents produce rifts which produce rift valleys or under the sea, where the most active is between oceanic plates and are called mid-oceanic ridges. Rifting of the Earth´s crust can also occur in continental blocks (Finger & Blankenship, 2010).

Two examples are the East African Rift and the Rio Grand Rift in New Mexico. It contains young volcanism and hosts several geothermal systems such as Olkaria in Kenya and the Valles Caldera in New Mexico.

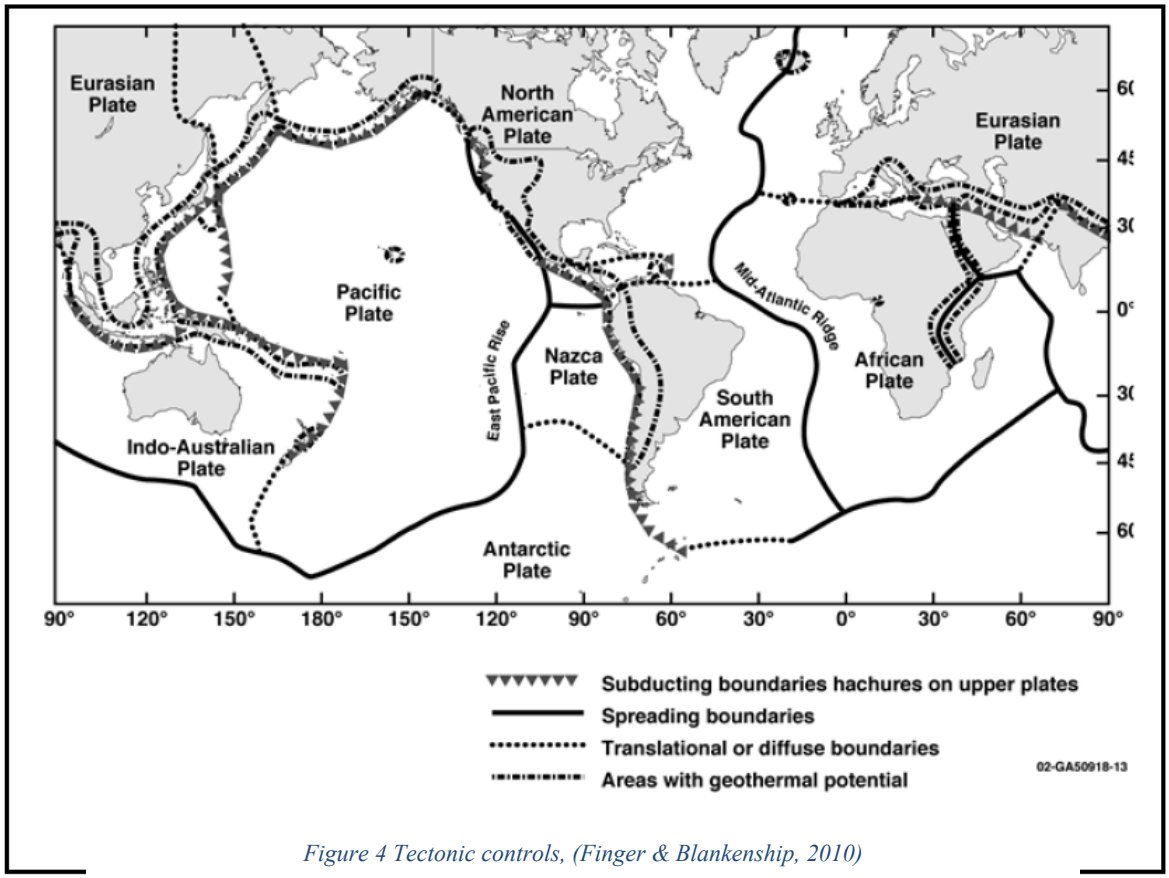


*Figure 4 Tectonic controls, (Finger & Blankenship, 2010)*

Lastly are the transform boundaries. It is where plates slide past each other. The relative motion of the plates is horizontal. They can occur underwater or on land, and the crust is either destroyed or created. Because of friction, the plates glide past each other. If not, stress builds up in both plates, and when it exceeds the threshold of the rocks, the energy is released and will cause a massive earthquake.

This type of boundary is also known as pull-apart basins in the Salton Trough of Southern California. Volcanism associated with the Salton Trough generated the heat in the Salton Sea, Cerro Prieto, and Imperial Valley geothermal fields. Researchers believed what happened in San Andreas fault may be the primary source of the heat source in the Greysers geothermal area, not far, about 90 miles north of San Francisco.

### *2.4.2 Hot spot*

A third source elevates heat flow and volcanism, which is the "*hot spot*". A hot spot is fed by a region deep within the Earth´s mantle from which heat rises through the process of convection. It is from the lithosphere base, where the brittle, upper portion of the mantle meets the Earth´s crust.

Scientists were amazed because the hot spot volcano is unique. After all, it does not occur at the boundaries of Earth´s tectonic plates. Instead, it appears at abnormally hot centres called mantle plumes. According to Canadian geophysicist J. Tuzo Wilson, he had a theory about that hot spots' volcanoes are created by hot areas fixed deep below the Earth´s mantle.

Most scientists believed around 40 to 50 hot spots exist around the world. Several critical geothermal systems are associated with recent volcanism caused by hotspots, such as Yellowstone, USA, the geothermal fields in Iceland, and those of the Azores (Finger & Blankenship, 2010).

## 2.5 Geothermal Energy Challenges

Geothermal energy can describe by properties as reliability, sustainability, and flexibility. We can find it around the globe and is a renewable energy source. However, the advancement of the development of geothermal systems for deep geothermal is slow. The barriers for deep and shallow geothermal systems are high investment costs, lack of public understanding, and the inherent resistance to change and profound geothermal systems-related risk and uncertainty related to resource quality and reservoir productivity.

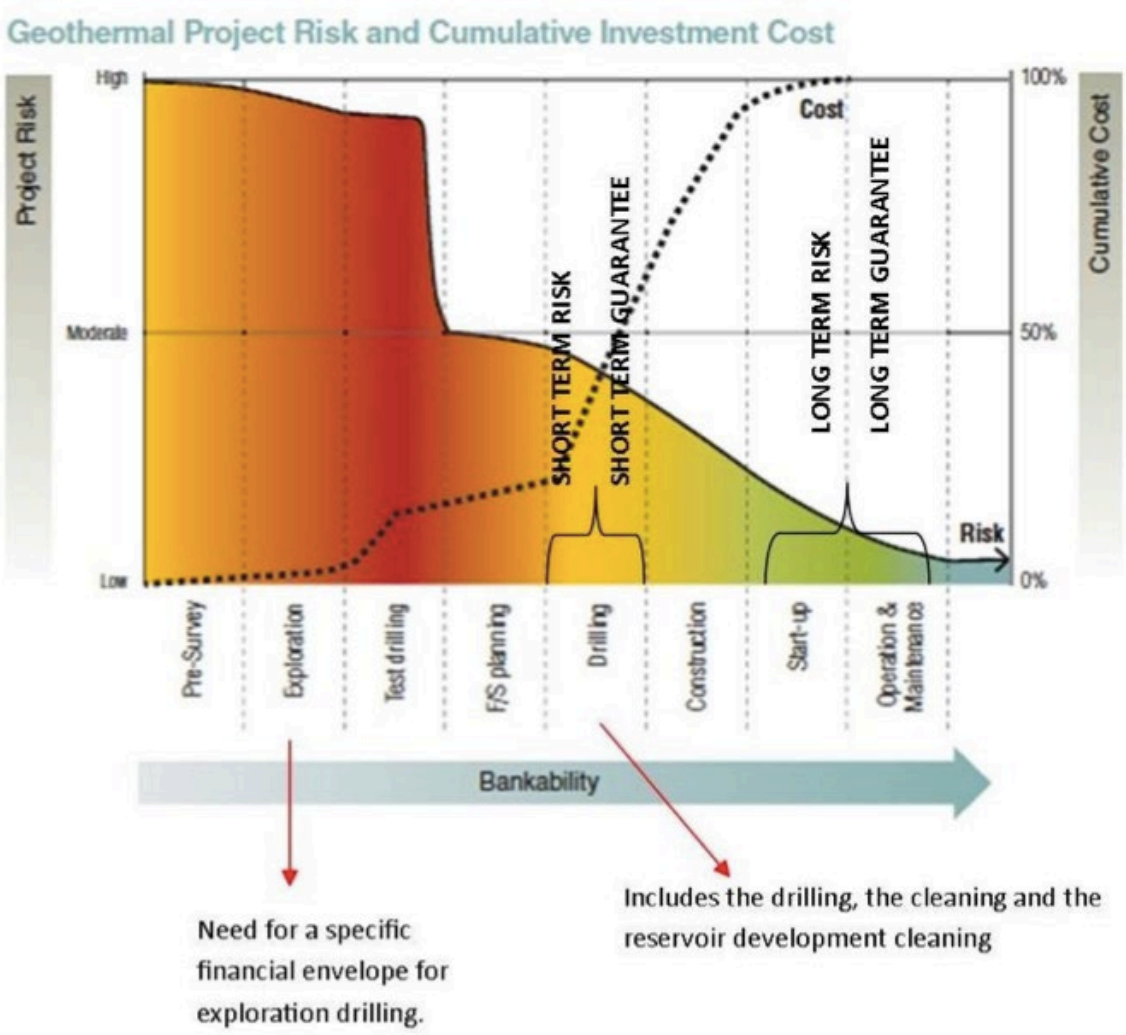


*Figure 5 Risk and investment on geothermal projects, (Fraser, Calcagno, Jaudin, Vernier, & Dumas, 2013)*

According to (Kabeyi, 2019) discovering and exploiting subsurface energy resources while mitigating their impact constitutes significant technical and socio-political challenges. Some geothermal fields in the world have challenges in supplying steam for stable operation. The

depletion of the geothermal fluid can cause cooling, vaporization, and acidification. Figure 5 shows the main high upfront costs and risks. It contains of short term- risk and guarantee and long term- risk and guarantee.

Discovering, and exploiting subsurface energy resources while mitigating their impact constitute a major technical and socio-political challenges. Among other challenges are the following (Kabeyi, 2019):

- Discovering, Characterizing, and Predicting
- Accurately characterizing the subsurface using integrated geophysical and geochemical technologies
- Quantitatively inferring subsurface evolution under current and future engineered conditions
- Finding variable, low-risk geothermal resources
- Challenges of accessing geothermal resources in terms of cost. It essential is to develop safe, cost-effective drilling and completions with properly managed wellbore integrity
- Engineering challenges in the form of general difficulty in creating or constructing desired subsurface conditions in challenging high-pressure and high-temperature environments like supercritical geothermal resources
- Challenge of sustaining the resources in terms of maintaining optimal subsurface conditions over multi-decadal or more extended time frames through complex geothermal system evolution
- Challenges of monitoring the resources in the form of improving observational methods to advance the understanding of the complex geothermal systems

Another factor affecting the drilling time increase is unexpected problems that may occur during the drilling operations. The most common issue is the loss of fluid circulation, especially in geothermal well drilling operations are:

- Increasing the drilling time
- Loss of expensive drilling fluid material
- Poor cementing

The loss of circulation is a common and expensive problem encountered during oil and geothermal drilling (Allan & Kukacka, 1995). Loss zones are known as drilling fluid that is lost to fractured or permeable formations. Plugging loss zones are achieved by cementing the zone with bridging agents. It is widespread in geothermal well drilling and will increase the drilling time and receptivity cost.

## 2.6 Geothermal Energy Advantage and Disadvantage

Like any other energy resource, geothermal energy has its own set of advantages and disadvantages. The benefits to using it directly or indirectly are the following (Kabeyi, 2019):

- There is increasing public awareness and appreciation of geothermal energy as a renewable energy resource
- There are advances in modelling and characterization of leading to better management of shallow and low enthalpy geothermal resources
- Advances in drilling technology and management have led to reduced upstream costs of a geothermal project
- Development in reservoir characterization techniques have led to better estimation of geothermal reservoir geometry and properties hence more success rates in drilling
- Effect of directional as opposed to vertical drilling has increased yield and success rates
- Geothermal has more positive environmental benefits compared to fuel-based power plants

The disadvantages to using it directly or indirectly are the following (Kabeyi, 2019):

- The process of injecting high-pressure streams of water into the Earth can result in minor seismic activity or small earthquakes
- It has been linked to subsidence or the slow sinking of land. The underground fractures collapse and can lead to damaged pipelines, roadways, buildings, and natural drainage systems
- Water that flows through underground reservoirs can pick up trace amounts of toxic elements such as arsenic, mercury, and selenium. These harmful substances can be leaked to water sources if the geothermal system is not properly insulated
- The initial cost of installing geothermal technology is expensive

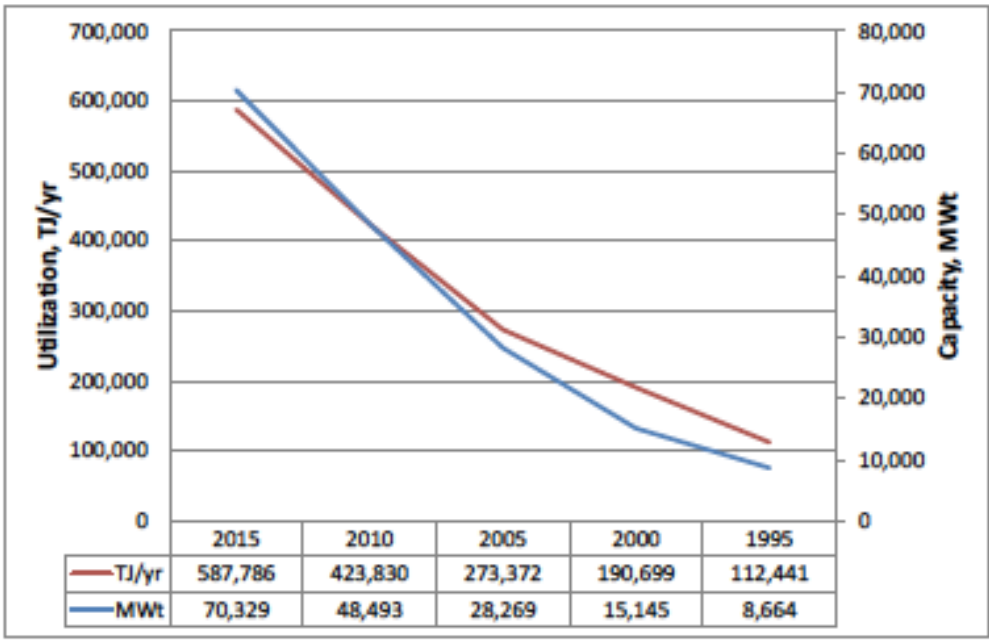


*Figure 6 The installed direct-use geothermal capacity and annual utilization from 1995 to 2015*

## 2.7 Geothermal Energy Worldwide Review

Direct use of geothermal energy is one of the oldest, most versatile, and common forms of utilizing geothermal energy. According to (Lund & Boyd, 2015), 82 countries in the world have increased from 78 reports from 2010. In 2010, around 587,786 TJ/yr (163,287 GWh/yr) was used in thermal energy.

About 55.3% for ground-source heat pumps, 20.3% for bathing and swimming, 15.0% for space heating (89% is for district heating), 4.5% for greenhouses and open ground heating, 2.0% for aquaculture pond and raceway heating, 1.8% for industrial process heating, 0.4% for snow melting and cooling, 0.4% for agricultural drying, and 0.3% for other uses. Around 2,218 wells were drilled in 42 countries, 34,000 person-years of effort were allocated in 52 countries, and about US$20 billion was invested in projects by 49 countries (Lund & Boyd,

2015). Table 1 show the summary of direct-use data worldwide in 2016 and Figure 6 show the installed direct-use of geothermal from 1995 until 2015 with Utilization and Capacity.

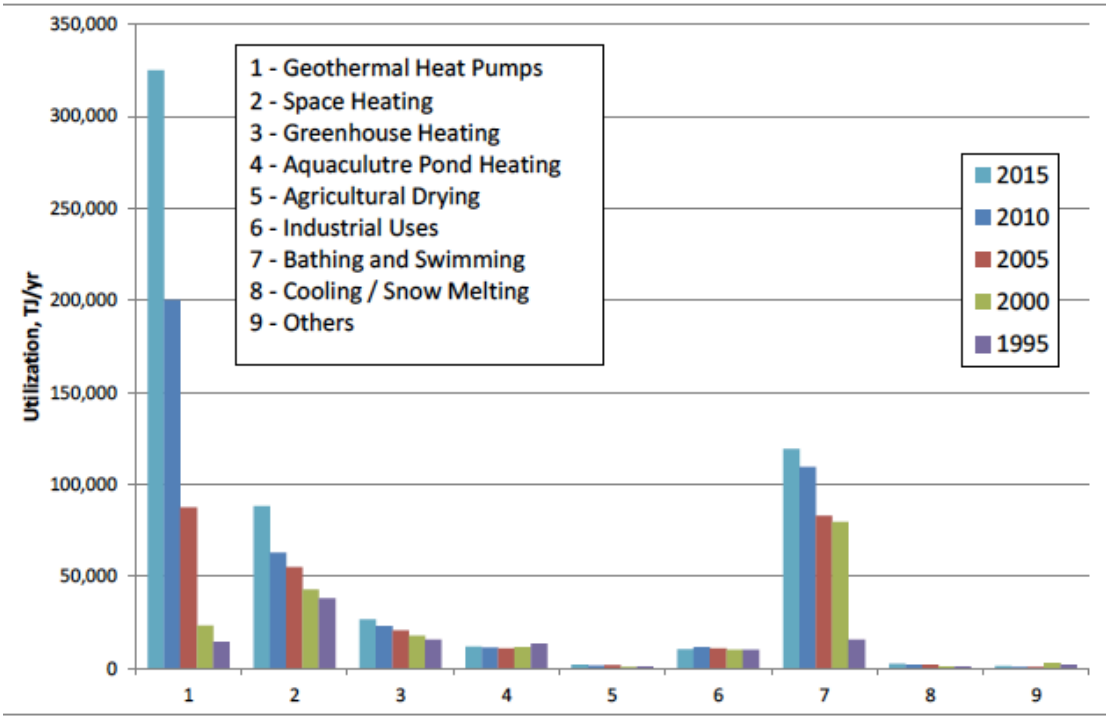


*Figure 7 Comparison of worldwide direct-use geothermal energy in TJ/yr from 1995, 2000, 2005, 2010 and 2015, (Lund & Boyd, 2015)*

## 2.8 Geothermal Energy Different types

Figure 7, are the data from 1995, 2000, 2005, 2010 and 2015 among the various uses in terms of capacity, energy utilization and capacity factor. The district heating represents 88% of the installed capacity and 89% of the annual energy use. Snow melting represents the majority of the snow melting/air-conditioning category.

While "other" is a category that covers a variety of uses, that includes animal husbandry and carbonation of soft drinks. Table 2, shows the summary of various types of direct-use worldwide for 2015, 2010, 2005, 2000, and 1995. Figure 7 shows the comparison of worldwide direct use from 1995, 2000, 2005, 2010, and 2015. The numbers of different types of Geothermal energy are published by (Lund & Boyd, 2015).

### *2.8.1 Geothermal Heat Pumps*

Geothermal heat pumps have the most extensive energy use and installed capacity worldwide. It is more efficient than conventional ones. Since they extract thermal energy

from the ground rather than the outside air and the ground below a few meters of depth is warmer than the outside air in winter (Ehrlich & Geller, 2017). The reason why is that the circulating fluid is a liquid, not air, which has a lower specific heat. The installed capacity of geothermal heat pumps is 49,898 MWt, and the annual energy use is 325,028 TJ/yr with a capacity factor 0.21 (Lund & Boyd, 2015). Figure 8 show a vapor-compression refrigeration cycle of a heat pump. In a conventional heat pump, a volatile fluid in its vapor state is compressed by a compressor, so that is releases heat to its surroundings in the process of liquefying – the left coils in the figure. The high-pressure liquid then passes through a valve where the pressure drop allows it to vaporize and cool below the temperature of the ground which acts to heat it – the section of the coil on the right. The cyclic process continues as long as electrical energy is supplied to the compressor.

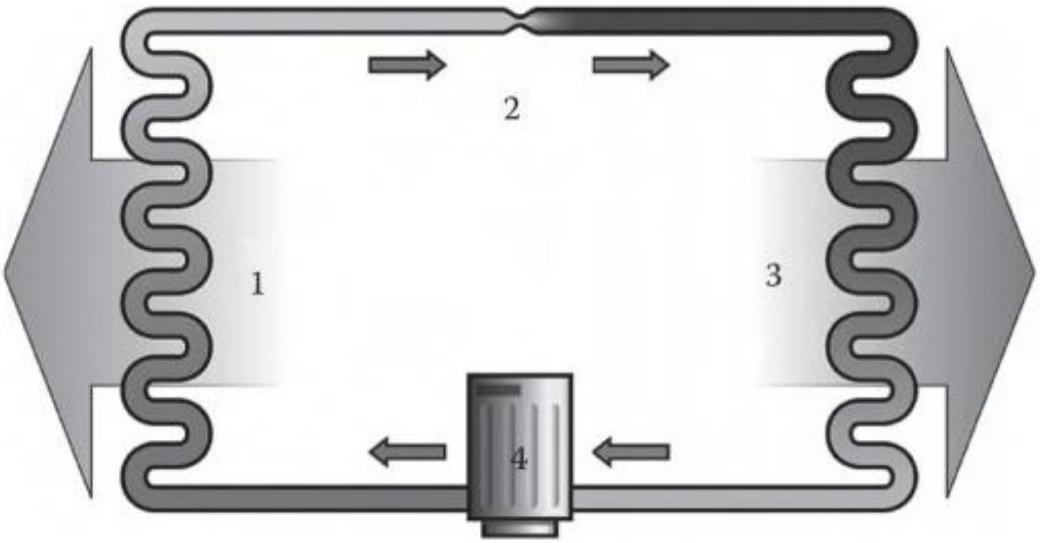


*Figure 8 Simple stylized diagram of the vapor-compression refrigeration cycle of a heat pump (Ehrlich & Geller, 2017)*

1: condenser; 2: expansion valve; 3: evaporator; 4: compressor expelling heat of the left (hot) side and absorbing heat or expelling cold on the right (cold) side

The performance of a heat pump is measured in terms of its coefficient of performance (COP) (Ehrlich & Geller, 2017). The coefficient of performance becomes more incredible the smaller the difference between the ground and home temperatures, with the maximum possible (Carnot) value described as:

| | |
|---|---|
| (1) | $$COP_{max} = \frac{T_H}{T_H - T_G}$$ |

Both the high (H) and ground (G) temperatures must be in Kelvins. Many homes use electric heat pumps that use heat extracted from the cold outside air to heat the house. According to

(Lund & Boyd, 2015), the average coefficient of performance (COP) of 3.5% allows for one unit of energy input to 2.5 units of energy output for a geothermal component of 71% of the rated capacity.

### *2.8.2 Space Heating and Cooling*

Space heating and cooling of the building represent the most significant single-energy expenditure for the homeowner. It has increased 44% in installed capacity and annual energy use over WGC2010. The installed capacity in space heating and cooling has 7.556 MWt, and the annual energy use is 88,222 TJ/yr. In comparison, 88% of the total installed capacity and 89% of the annual energy use is in district heating (Lund & Boyd, 2015).

### *2.8.3 Greenhouse and Covered Ground Heating*

The economical choice for geothermal heating in most countries is with low-temperature heat. Because it offers a reasonable payback, which is typical in ten years, depending on the system design and the cost of fossil fuel replaced. It is essential to calculate the retribution and to implement energy conservation measures. Such as: reducing air infiltration, installing energy curtains, insulating sidewalls and the foundation perimeter, making good use of growing space, and installing electronic environmental controls.

According to (Lund & Boyd, 2015), it has increased by 19% in installed capacity and 16% in annual energy use. The installed capacity is 1.839 MWt and 26,662 TJ/yr in energy use. It was reported about 13 countries that used geothermal greenhouse heating, such as Turkey, Russia, Hungary, China, and Netherlands.

### *2.8.4 Aquaculture Pond and Raceway Heating*

Aquaculture pond and raceway heating are among the most common uses of geothermal resources (Boyd & Lund, 2006). Because of the significant heating requirements of these facilities and their ability to use low-temperature fluids (30°C and above), they are a natural application.

Aquaculture involves raising freshwater or marine organisms in a controlled environment to enhance production rates (Boyd & Lund, 2006). The main species are carp, catfish, bass, Tilapia, frogs, mullet, eels, salmon, sturgeon, shrimp, lobster, crayfish, crabs, oysters, scallops, alligators, mussels, and abalone.

According to (Lund & Boyd, 2015), t has increased over WGC2010, amounting to a 6.7% increase in installed capacity and a 2.7% increase in annual energy use. The installed capacity

is 695 MWt, and the annual energy use is 11,958 TJ/yr. Around 20 countries were reported to use this type of energy resources. Countries such as USA, China, Iceland, Italy, and Israel.

### *2.8.5 Agricultural Crop Drying*

Agricultural crops are essential for the human diet, depending upon their nature, including vitamins, minerals, and fibers (Gunathilake, 2018). Some crops are highly seasonal and are available in plenty. There are many techniques for the use of drying.

The most common techniques are air, in which heat is applied by convection and carries away the vapor as humidity from the product. Sun-drying and artificial drying are used via air. Vacuum drying and fluidized bed drying are kept in vacuum conditions, and water is used to evaporate and fluidize the material. Drum drying is used to provide energy on a heated surface, and spray drying atomizes the liquid particles to remove moisture. And final special drying and curing techniques are used for the preservation of big onion crops.

According to (Lund & Boyd, 2015), it has increased 28.8% and 24.2% compared to WGC2010 and has a total of 161 MWt, and 2,030 TJ/yr are being utilized. About 15 countries in the world were reported to dry various grains, vegetables, and fruit crops. Countries such as Iceland (seaweed), USA (onions), Serbia (wheat and other cereals), El Salvador, Guatemala and Mexico (fruit), New Zealand (Lucerne), Philippines (coconut meat), and Mexico, New Zealand, and Romania (timber).

### *2.8.6 Industrial Process Heat*

Industrial Process Heat is defined as geothermal energy used directly to prepare materials used to produce manufactured goods. According to (Lund & Boyd, 2015), it has 18% increase and 12% decrease compared WGC2010. The installed capacity is 610 MWt, and the annual energy use is 10,453 TJ/yr. It has applications in 15 countries in the world.

Countries are the following Guatemala and Slovenia (concrete during), Bulgaria, Serbia and USA (bottling of water and carbonated drinks), Romania and New Zealand (milk pasteurization), Serbia and Slovenia (leather industry), Bulgaria, Poland, and Russia (chemical extraction), Iceland and Turkey (CO2 extraction), New Zealand (pulp and paper processing, Vietnam (iodine and salt extraction) and last Italy (borate and boric acid production). It needs the following: preheat for boiler feedwater, hot water for various processes, hot air for drying, steam production, and direct heating.

### *2.8.7 Snow Melting and Space Cooling*

According to (Nordell, 2015) snow and ice have extraordinary properties for cooling applications. Its melting point at 0°C together with its very high latent heat of fusion. It

makes it more suitable for space cooling and cooling of food supplies. All snow and ice storage have methods that insulated the mass of ice/snow stored until later use. There are three types of thermal energy storage systems using snow and ice:

(a) Snow storage in thermally insulated buildings
(b) Snow storage in a thermally insulated pit
(c) Underground snow storage (without thermal insulation)

According to (Lund & Boyd, 2015), the installed capacity is 360 MWt, and the annual energy use is 2,600 TJ/yr. An estimated 2.5 million square meters of pavement are heated worldwide, and the primary user is in Iceland for 74%. Figure 9 show the outline of different snow storages. It describes the storages types, different cold carries like air, water and the snow itself are used to transport the cold to the cold load.

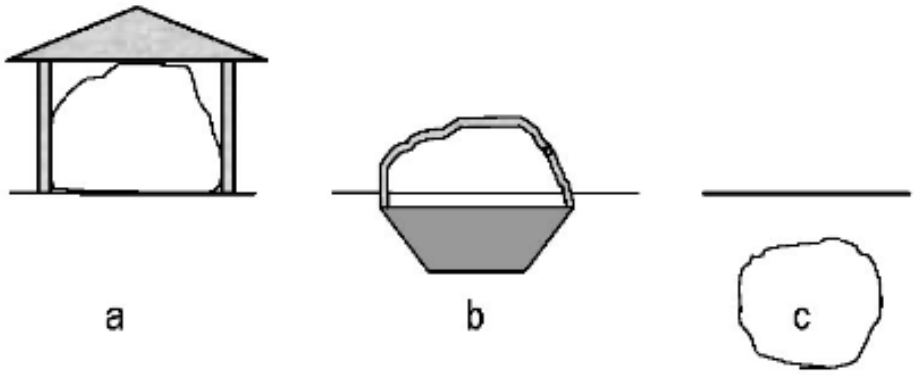


*Figure 9 Outline of different snow storages, in a building, in a pit and underground,(Nordell, 2015)*

### *2.8.8 Bathing and Swimming*

About 70 countries in the world have spas and resorts that have swimming pools heated with geothermal energy. The installed capacity is 9,140 MWt, and the annual energy use is 119,381 TJ/yr, and in 2010 it was up to 36.4% and 9.1% (Lund & Boyd, 2015).

### *2.8.9 Other Uses*

This category was reported in 13 countries. It includes animal farming, spirulina cultivations, desalination, and sterilization of bottles. It has increased in 88 and 52% in 2010 and contains 79 MWt and 1,452 TJ/yr (Lund & Boyd, 2015).

# 3 Theory

This chapter of the thesis presents the theory of heat flow, heat transfer, and heat flow rate, which is explain on the Chapter 4 Modelling. According to (Finger & Blankenship, 2010), the heat of the Earth is divided into two groups: the heat generated by the formation of the Earth and the heat generated by subsequent radioactive decay of elements in the upper parts of the Earth.

## 3.1 Heat flow

Heat flow is the rate of thermal energy flow per unit surface area of the heat transfer surface. The main parameter to calculate the heat transfer and heat flux vector is lower temperature regions.

According to a study (Birch, Roy, & Decker, 1968), found the *heat flux* can be expressed as an equation:

| | |
|---|---|
| (2) | $Q = DA$ |

where Q is defined as the component of heat flow that originates from the lower crust, and DA is the heat generated by radioactive decay in the shallow crust. DA is well the product of depth (D) and the energy generated per unit volume per second (A). Because A varies with depth, the calculation of heat flow and the temperature with the depth is complex.

## 3.2 Heat Transfer Mechanisms

Heat transfer is the transfer of thermal energy due to a temperature change. The movement of heat is from hot to cold surfaces. Heat transfer can classify into three types: *heat convection, heat conduction*, and *heat radiation.* These three are indecent of each other, but they all result in the overall heat transfer system.

### *3.2.1 Heat conduction*

Heat conduction is the transfer of energy, in other words, internal energy. From higher internal energy to the neighbouring lesser less energetic. Figure 10 shows the Heat transfer through a plane slab. The temperature on one side is higher than the other side (T1 > T2). For one-dimensional, the heat transfer flow is proportional to the change in temperature and inversely proportional to the distance between the showed in equation (3).

To explain the heat flow (convective flux) is proportional to the temperature difference between solid, liquid, and gas, the equation is written as:

| | |
|---|---|
| (3) | $$Q_{cd} = -k\frac{dT}{dx} = -k\frac{T_2 - T_1}{L}$$ |

Where $Q_{cd}$is the conductive heat flux, $T$ is the temperature, $k$is thermal conductivity, $L$ is the length

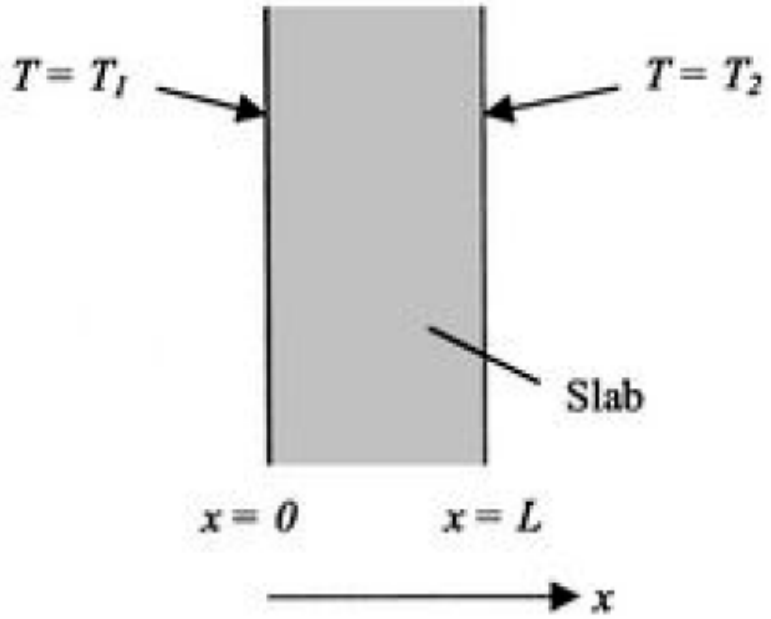


*Figure 10 Temperature boundary conditions for a slab, (Nathan Amuri, 2017)*

### *3.2.2 Heat convection*

Heat convection is the mode of heat transfer through a liquid or gas medium in motion. It can be from a solid surface to liquid or gas. When an external source causes the motion of a medium, then the convection is called forced convection. Figure 11 explains the motion as a pump or wind. On the other hand, buoyancy forces cause the so-called natural convection, caused by density differences within the fluid, owing to the temperature variation within the fluid.

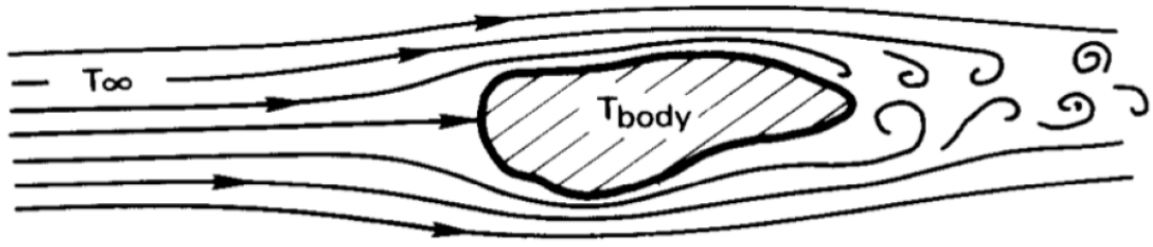


*Figure 11 Heat convection through two media,(Nathan Amuri, 2017)*

Under heat conduction, the heat flux vector is proportional to the temperature gradient vector. With the help of Newton´s law of cooling, it represents the convection heat flux as:

| | |
|---|---|
| (4) | $Q_{cv} = -kA_s(T_s - T_\infty)$ |

Where $T_s$is the temperature of the heat source and $T_\infty$is the temperature of the surrounding fluid, $Q_{cv}$convectional heat flux, $k$ is thermal conductivity.

### *3.2.3 Heat Radiation*

Heat radiation is the energy released by an object in the form of electromagnetic waves owing to changes in the electronic distribution of the atoms. Radiative heat flux is a contrast to convection and heat conduction. The heat emitted by radiation an object depends on many factors, such as hot is an object.

The object can absorb heat and the color of an object. Stefan-Boltzmann law represents as:

| | |
|---|---|
| (5) | $Q_{rd} = \sigma A_s T_s^4$ |

Where $Q_{rd}$ the radiation heat flux, $\sigma$ Stefan-Boltzmann constant, $A_s$ area of radiated surface and $T$ is the absolute temperature.

## 3.3 Heat Flow Rate

The rate of heat flow is defined as the heat flow per unit length of the wellbore. It is known as overall heat transfer or heat exchange.

The rate of heat flow described as (Ichim, Teodoriu, & Falcone, 2017):

| | |
|---|---|
| (6) | $Q = -2\pi r_{to} U_{to}(T_f - T_{wb})$ |

Where $U_{to}$the overall heat transfer coefficient in $[BTU/hr - ft^2 - °\text{F}]$, $(T_f - T_{wb})$ is the temperature difference between the wellbore interface and wellbore fluid and $2\pi r_{to}$ is the tubing outside area. A positive heat exchange implies that heat flows from the wellbore to the formation and a negative heat exchange implies the opposite.

# 4 Modelling

This chapter of the thesis represents the modelling for heat transfer coefficients. The analysis is based on the classical paper published by (Willhite, 1967). Casing temperatures and well-bore heat losses are critical variables in steam and hot water injection wells. The over-all heat transfer coefficient for a well-bore is developed from its component terms to understand the concept better.

Specific methods have been selected from the heat transfer literature for estimating the size of each heat transfer component. The simplified calculation produces suggested for determining the over-all heat transfer coefficient. Comparison of calculated and measured casing temperatures during steam injection confirms the basic formulation and applicability of the recommended products for engineering calculations.

"A good understanding of the important aspects of the structure of the system and the most significant (physical and chemical) aspects in it is referred to as its "conceptual model" (O'Sullivan, Pruess, & Lippmann, 2001). The "conceptual model" consists of two or three sketches of several horizontal and vertical sections of the geothermal systems. And it contains information about the geological structure, temperature, geochemistry, resistivity, and surface activity (Ganguly & Kumar, 2012).

## 4.1 Heat Transfer Modelling

Casing temperatures and wellbore heat loses are critical variables in steam and hot water injection wells (Willhite, 1967). Plenty of authors have been written about wellbore heat losses and casing temperatures only if the overall heat transfer coefficient is known. Over-all heat transfer can translate as the net resistance for flowing fluid, tubing, insulating material, casing completion fluid, casing wall and cement sheath to the flow of heat. The analysis of heat transfer model is published by (Willhite, 1967).

### *4.1.1 Over-all Heat Transfer*

Over-all heat transfer coefficient is found by the heat transfer mechanisms between the flowing fluid and the cement-formation interface.

Over-all heat transfer is described as:

| | |
|---|---|
| (7) | $Q = U_j A_j \Delta T_j$ |

where $U_j$ is the over-all heat transfer, $A_j$ is the area and $\Delta T_j$ is the temperature difference. In theory, any radial surface could be used to determine the characteristic area

#### 4.1.1.1 Outside tubing surface

The outside tubing surface area is described as:

| | |
|---|---|
| (8) | $Q = 2\pi r_{to} \cdot U_{to} \cdot (T_f - T_h) \cdot \Delta L$ |

where $2\pi r_{to}\Delta L$is an incremental length of injection tubing, $\Delta T_j$ is the difference between the temperature of the flowing fluid $T_f$and the temperature at the cement-formation interface (the drill hole) $T_h$

#### 4.1.1.2 Inside tubing surface

The inside casing surface area is described as:

| | |
|---|---|
| (9) | $Q = 2\pi r_{ci} \cdot U_{oi} \cdot (T_f - T_h) \cdot \Delta L$ |

where $U_j$ is the over-all heat transfer, $A_j$ is the area and $\Delta T_j$ is the temperature difference. A expression for the over-all heat transfer coefficient for any well completion can be found by considering the heat transfer mechanisms between the flowing fluid and the cement-formation interface.

### *4.1.2 Heat Transfer between flowing fluid and inside tubing wall*

The rate of heat transfer between the flowing fluid and inside tubing wall is described as:

| | |
|---|---|
| (10) | $Q = 2\pi r_{fi} \cdot h_f \cdot (T_f - T_{ti}) \cdot \Delta L$ |

Where $h_f$ is the film coefficient for heat transfer based on the inside surface area of the tubing and the temperature difference between the flowing fluid and the inside tubing wall $T_f - T_{ti}$

According to (baron de Fourier, 1822), he discovered the rate of heat flow through a body is directly proportional to the temperature gradient in the medium. The radial system of the wellbore is described as:

| | |
|---|---|
| (11) | $Q = -2\pi r \cdot k_h \cdot \frac{dT}{dr} \cdot \Delta L$ |

$k_h$ is the proportionality factor is termed the thermal conductivity of the medium

The heat transfer $Q$ is described as (Willhite, 1967):

| | |
|---|---|
| (12) | $Q = 2\pi r_{ins}^{o} \cdot (h_c + h_r) \cdot (T_{ins}^{o} - T_c^{i}) \cdot \Delta L$ |

Where the combined effect of natural convection, conduction $h_c$ and radiation $h_r$

### *4.1.3 Heat Transfer*

Heat transfer through conduction (Willhite, 1967):

Tubing:

| | |
|---|---|
| (13) | $$Q = \frac{2\pi k_{tub}(T_{ti} - T_{to})\Delta L}{\ln \frac{r_{to}}{r_{ti}}}$$ |

Casing:

| | |
|---|---|
| (14) | $$Q = \frac{2\pi k_{cas}(T_{ci} - T_{co})\Delta L}{\ln \frac{r_{co}}{r_{ci}}}$$ |

Cement:

| | |
|---|---|
| (15) | $$Q = \frac{2\pi k_{cem}(T_{co} - T_{h})\Delta L}{\ln \frac{r_{h}}{r_{co}}}$$ |

Three modes of heat transfer are present in the casing annulus. The amount of radiant energy transported between the tubing and casing depends on the surfaces' view and the emitting and absorbing characteristics of their surfaces. The cause of the heat transfer by natural convection in the annulus between the tubing and casing is by the fluid motion, resulting from the variation of density with temperature. The three modes are independent heat transfer mechanisms. Figure 13 is an interpretation of fluid motion in the casing annulus.

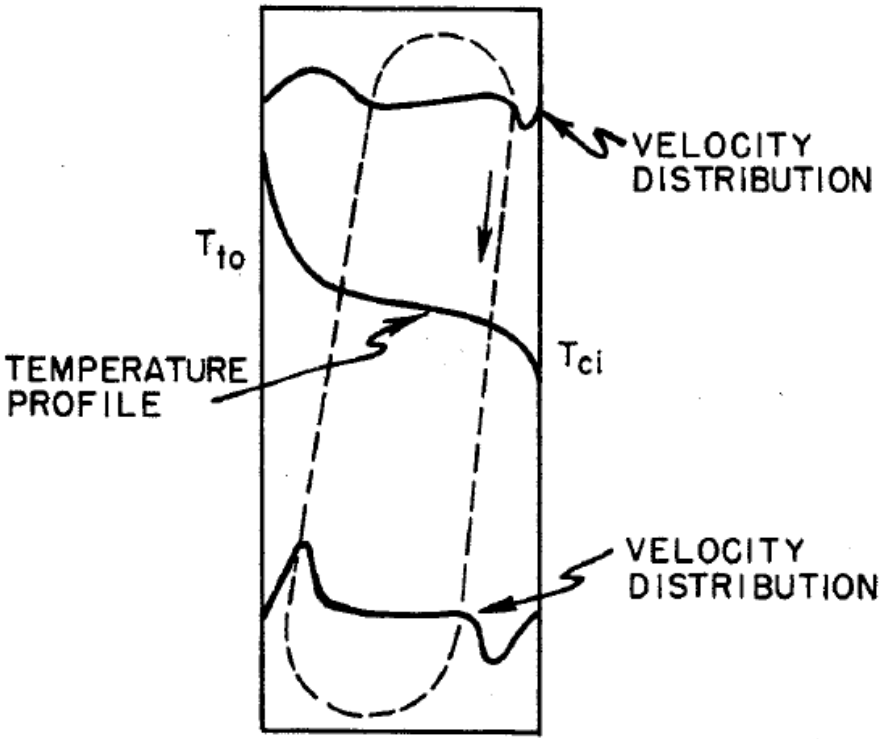


*Figure 12 Natural convection in the casing annulus, (Willhite, 1967)*

Heat transfer rate through the annulus in terms of the heat transfer coefficient $h_c$ (natural convection and conduction) and $h_r$ (radiation). The outside surface area of the tubing $(2\pi r_{to}, \Delta L)$ and the temperature difference between the outside tubing surface and the inside casing surface, is described as:

| | |
|---|---|
| (16) | $Q = 2\pi r_{to} \cdot (h_c + h_r) \cdot (T_{to} - T_{ci}) \cdot \Delta L$ |

The temperature difference between the well and the formation as the sum of the temperature difference and is described as:

| | |
|---|---|
| (17) | $T_f - T_h = (T_f - T_{ti}) + (T_{ti} - T_{to}) + (T_{to} - T_{ci}) + (T_{ci} - T_{co}) + (T_{co} - T_h)$ |

Inserting temperature differences obtained and we get:

| | |
|---|---|
| (18) | $T_f - T_h = \frac{Q}{2\pi\Delta L}\left[\frac{1}{r_{ti}h_f} + \frac{\ln\frac{r_{to}}{r_{ti}}}{k_{tub}} + \frac{1}{r_{to}(h_c + h_r)} + \frac{\ln\frac{r_{co}}{r_{ci}}}{k_{cas}} + \frac{\ln\frac{r_h}{r_{co}}}{k_{cem}}\right]$ |

With the comparison with Equation (18) and we get:

| | |
|---|---|
| (19) | $U_{to} = \left[\frac{r_{to}}{r_{ti}h_f} + \frac{r_{to}\ln\frac{r_{to}}{r_{ti}}}{k_{tub}} + \frac{1}{(h_c + h_r)} + \frac{r_{to}\ln\frac{r_{co}}{r_{ci}}}{k_{cas}} + \frac{r_{to}\ln\frac{r_h}{r_{co}}}{k_{cem}}\right]^{-1}$ |

Figure 12 shows the thermal conductivity of the tubing and casing steel is higher than for the other materials in the wellbore.

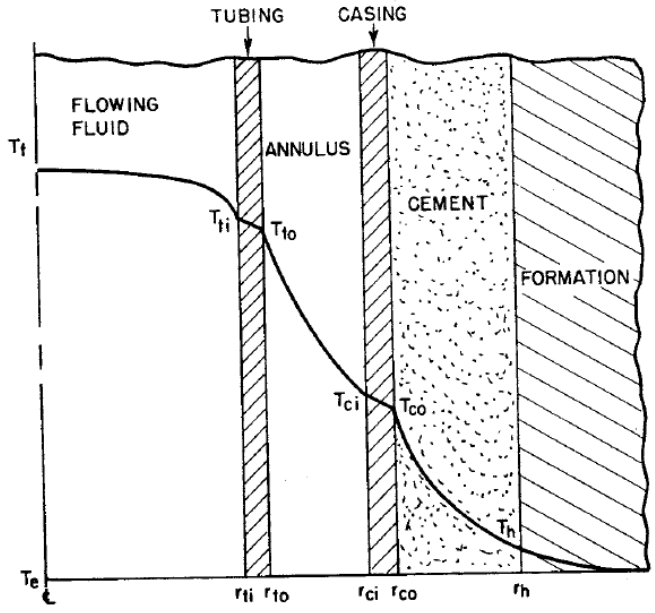


*Figure 13 Temperature distribution in annular completion (Willhite, 1967)*

### *4.1.4 Estimating $h_r$ and $h_c$*

The radiant heat flux $Q_r$ between the outer surface of the tubing at temperature $T_{to}$ and the inside surface of the casing at $T_{oi}$ is described as:

| | |
|---|---|
| (20) | $Q_r = 2\pi r_{to}\sigma F_{tci}(T_{to}^{*4} - T_{ci}^{*4})\Delta L$ |

Where $\sigma$is the Stefan-Boltzmann constant $(1.713 * 10^{-9})$BTU/sq ft hour), $F_{tci}$is the view factor of the fraction of the radiation emitted from the external surface area of tubing $A_{to}$which is by the inner casing surface area $A_{ci}$.

A concentric annulus is described as:

| | |
|---|---|
| (21) | $\frac{1}{F_{tci}} = \frac{1}{\overline{F_{tci}}} + \left(\frac{1}{\varepsilon_{to}} - 1\right) + \frac{A_{to}}{A_{ci}}(\frac{1}{\varepsilon_{ci}} - 1)$ |

Where $\varepsilon_{to}$and $\varepsilon_{ci}$are the emissivities of the external tubing and internal casing surfaces, and $F_{tci}$is the over-all interchange factor between the two surfaces

A heat transfer coefficient for radiation $h_r$, can be describe by factoring Eq (30) and substituting the following equations:

| | |
|---|---|
| (22) | $Q_r = 2\pi r_{to}h_r(T_{to}^{*} - T_{ci}^{*})\Delta L$ |
| (23) | $Q_r = 2\pi r_{to}h_r(T_{to} - T_{ci})\Delta L$ |

Where

| | |
|---|---|
| (24) | $h_r = \sigma F_{tci}(T_{to}^{*2} + T_{ci}^{*2})(T_{to}^{*} + T_{ci}^{*})$ |

$h_r$ can be calculated if $T_{to} and\ T_{ci}$ are known

### *4.1.5 Natural Convection ($h_c$)*

Heat transfer by conduction and natural convection between the inside casing surface and the outside tubing surface is described as:

| | |
|---|---|
| (25) | $Q_c = \frac{2\pi k_{hc}(T_{ci} - T_{to})\Delta L}{\ln\frac{r_{ei}}{r_{to}}}$ |

Where $Q_c$ is heat transfer rate due to conduction and natural convection, Btu/hour and $k_{hc}$ is equivalent thermal conductivity of the annular fluid, Btu/hour ft °F.

The thermal conductivity of the fluid in the annulus is described as:

| | |
|---|---|
| (26) | $Q_o = 2\pi r_{to}h_c(T_{ci} - T_{to})\Delta L$ |
| (27) | $h_c = \frac{k_{hc}}{r_{to}\ln\frac{r_{ei}}{r_{to}}}$ |

Dropkin and Sommerscales measured values of $k_{hc}$between enclosed vertical plates (Willhite, 1967). The correlation of Dropkin and Sommerscales in terms of the nomenclature of the wellbore is described as:

| | |
|---|---|
| (28) | $$\frac{k_{hc}}{k_{ha}} = 0.049(GrPr)^{0.333}Pr^{0.074}$$ |

Where

| | |
|---|---|
| (29) | $$Gr = \frac{(r_{ci} - r_{to})^3 \delta \rho_{an}^2 \beta (T_{to} - T_{ci})}{\mu_{an}^2}$$ |

And

| | |
|---|---|
| (30) | $$\mathrm{Pr} = \frac{c_{an}\mu_{an}}{k_{ha}}$$ |

The product of GrPr in the wells with high-pressure gas in the annulus ranges from $10^5$ to $10^9$.

## 4.2 Calculation Procedure

The casing temperature is calculated using (30) which derived by combining Equations (7), (13) and (14), described as:

| | |
|---|---|
| (31) | $$T_{oi} = T_h + (\frac{\ln\frac{r_h}{r_{co}}}{k_{cem}} + \frac{\ln\frac{r_{co}}{r_{ci}}}{k_{cas}}) r_{to} U_{to} (T_f - T_h)$$ |

By neglecting the thermal resistance of the film, tubing and casing, Equation (30) reduces (31)

| | |
|---|---|
| (32) | $$T_{oi} = T_h + \frac{r_{to} U_{to} \ln\frac{r_h}{r_{co}}}{k_{cem}} (T_{to} - T_h)$$ |

The heat flow in the well completion Equation (7), is equated to the radial heat flow into the cement formation. By the help of Rameys´producere, equation (32) can be described as:

| | |
|---|---|
| (33) | $$Q = \frac{2\pi k_e (T_k - T_e)\Delta z}{f(t)}$$ |

Equating Equation (7) and (32) with $\Delta z = \Delta L$ and then solving for $T_h$ gives:

| | |
|---|---|
| (34) | $$T_h = \frac{T_f f(t) + \frac{k_e}{r_{to}U_{to}} T_e}{f(t) + \frac{k_e}{r_{to}U_{to}}}$$ |

Where $T_e$= undisturbed temperature of the formation at depth z, °F

$k_e$= thermal conductivity of the formation at the depth z, Btu/hour ft °F

$f(t)$ = transient heat conduction function

The transient heat conduction function $f(t)$enters into wellbore heat loss calculations because heat flow in the calculations because heat flow in the surrounding formation varies with time. Heat loses to these formations are large but decrease with time as thermal resistance to the flow of heat builds up in the formation.

The calculation procedure discussed in the preceding paragraph was used to prepare for Figure 14 a plot of $U_{to}$ vs tubing temperature for several modifications of an annular completion. The parameters used to calculate $U_{to}$ are summarized in Table 3. The five completions presented on Figure 14 were selected to illustrate the heat transfer mechanisms in the annuli of steam and hot water injection wells. In this completion, radiation is the primary heat transfer mechanism. Since radiation varies with the emitting properties of the

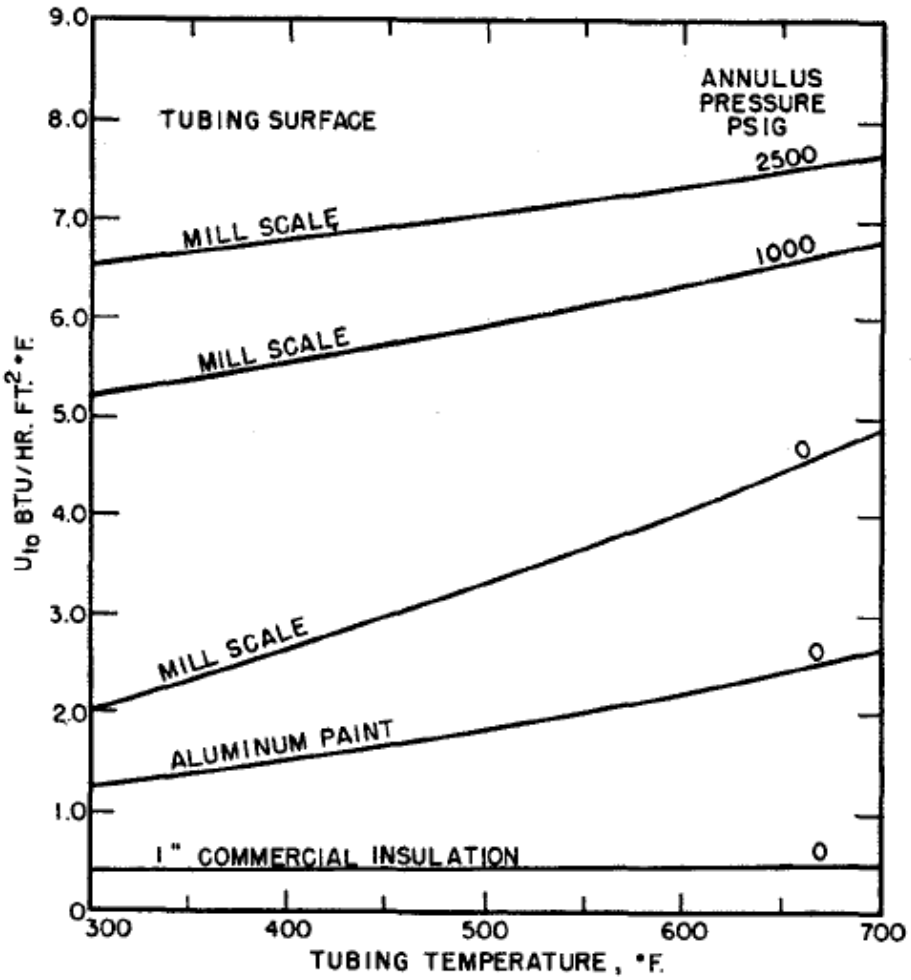


*Figure 14 Variation of $U_{to}$ with tubing temperature for parameters of Table 3, (Willhite, 1967)*

tubing surface. The radiation heat transfer coefficient $h_r$ can be lowered by coating the tubing surface with a highly reflective material.

Another completion technique is to use high-pressure air or nitrogen to eliminate the down-hole packer. The natural convection coefficient is larger by one or two orders of magnitude because the density of the gas in the annulus increases.

On the other hand, radiation and natural convection can be minimized by insulating the injection tubing. They are based on the outer surface of the insulation can be large, but their effect on $U_{to}$is small. Since they are in series with the high thermal resistance. Figure 14 is useful in estimating the over-all heat transfer coefficient for wells with parameters. (Willhite, 1967), suggested the following procedure:

1) Select a value of $U_{to}$ corresponding to the temperature of the fluid or tubing from Figure 14 for the corresponding well completion
2) Determine $f(t)$ from Table 4
3) Calculate $T_h$ using Equation (33)
4) Calculate $T_{oi}$ from Equation (31)
5) Then estimate $h_r$ and $h_c$
6) Determine a new value of $U_{to}$ from Equation (16) or (17)
7) Compare the calculate value of $U_{to}$ with the value used in Step 2 through Step 5 and repeat Steps 2 through 6 until agreement is obtained between two successive trials

## 4.3 Result of Heat Transfer

Casing temperatures were calculated by using $k_e = 1.0 \frac{Btu}{hour} ft$ °F, $k_{cem} = 0.2 \frac{Btu}{hour} ft$ and drill hole diameter of 12 in (Willhite, 1967). The temperatures were measured during steam injection in one of our steam injections projects. The over-all heat transfer coefficient can be estimated from the process variable. In an over-all heat transfer coefficient includes how various heat transfer mechanisms. A simplified calculation procedure was outlined for determining the over-all heat transfer coefficient. Comparison of predicted and field casing temperatures confirms the basic formulation and applicability of the suggested produces for engineering calculations.

# 5 Geothermal Well Drilling

This chapter represents the generic information about geothermal wells and drilling. It explains about planning, chemistry, and designing a geothermal wells and drilling. It discusses also the different types of drilling rigs, wells and worldwide review.

Preparing for a drilling project separate two significant roles - *planning* the well and *designing* the well. "Planning" means to list, define, schedule and budget for all the multitude of individual activities required to drill a well, and "designing" means to specify all the physical parameters such as depth, diameter, etc. that define the well itself (Finger & Blankenship, 2010).

## 5.1 Geothermal Well Drilling Planning

Planning a geothermal well should list and define all the activities required to complete the well, with their related costs and times. It should give sufficient descriptions of individual tasks to clarify the sequence they must perform (Finger & Blankenship, 2010).

Planning is essential for any drilling operations to reduce the risk of injury or property damage from unexpected events. All the contractors and service companies should meet and agree to assign the responsibilities for the various activities and not have any confusion each step. The main objective of planning a well is to drill safely, minimize costs and drill a usable well (Ngugi, 2008).

A plan can write like an outline, in list format, of the various activities, and be more specific and in active electronic format. Management software ranges from simple spreadsheets, through freeware available on the Web, to sophisticated planning tools such as Microsoft Project. Overall, the geothermal well planning must be flexible enough to accommodate unexpected events or trouble during the project.

To specify drilling an interval between two given depths and running casing, are the following (Finger & Blankenship, 2010):

- Hole size and suggested bit type (include weight on bit and rotary speed, if available from similar wells)
- Definition of all components of the bottom-hole assembly and whether downhole motors are to be used
- Expected rate of penetration and bit life (thus, expected time to drill the interval)
- Any directional drilling instructions
- Drilling fluid type and flow rate

- Any required logging during drilling or before causing is run
- Size, weight, and grade of casing
- Proposed cementing program
- Any problems expected in that interval or special precautions to be taken

### *5.1.1 Classification of geothermal wells*

Wells can be categorized as follows (Ngugi, 2008):

- Exploration/discovery wells – No geological data or previous drilling records exist
- Appraisal wells – Delineates the reservoir´s boundary, drilled after the exploration wells
- Production wells – Drill the known productive portions of the reservoir
- Work-over wells – Re-entry of already drilled wells to deepen, clean etc.

Planning for the drilling of exploration wells takes more effort than appraisal wells and production drilling.

### *5.1.2 Well costs*

It is impossible to have a proper universal guideline for estimating well drilling, and completion costs. However, in general, drilling costs depend on depth, diameter, and difficulty. The formation to be drilled has a large effect on drilling costs. For low-to-moderate temperature wells, the cost can be estimated on a dollar per inch of diameter per foot of depth according to the following (Culver, 1998):

| **Depth (ft)** | **Cost ($/inch/ft)** | |
|---|---|---|
| 0 – 500 | 1.80 soft | 5.00 hard |
| 500 - 1200 | 3.00 soft | 6.25 hard |
| 1200 – 2000 | 4.75 soft | 9.00 hard |
| 2000 - 3000 | 8.50 soft | 11.00 hard |

The actual drilling costs represent between 40 and 60% of the total completed cost, depending on the casing program, mud costs, cement and cementing aids (example cementing shoes and centralizers), well head equipment etc.

### *5.1.3 Geothermal well different types*

According to (Finger & Blankenship, 2010), there were two particular wells were drilled: “steam well” and “brine well” in the mid-1990s.

### 5.1.3.1 Steam Well

Steam well has a two-leg well with casing to around 1500 m and two open-hole branches to around 3000 m. However, the first leg encountered no steam entries. It was plugged back, and two additional branches were drilled (three holes drilled from around 1350 to around 3000 m). The hole was drilled with mud to the 1500 m casing points; then all branches were air-drilled. With the total time was over the hole around 90 days and total well cost was around $3 million. Lucky, there was no significant of lost circulation in the mud-drilled part of the hole. And it steams well is considered as a success. Table 11 shows the steam well borehole profile and Table 10 shows the steam well bit summary.

### 5.1.3.1 Brine Well

Brine well is a self-energized geothermal production well drilled in sedimentary formations. The well is cased to around 640 m and has an open hole production interval from there down to around 1500 m. The corrosive nature of brine requires titanium casing, but standard practice is to avoid drilling inside this expensive tubular. Produce is to drill 37.5 cm to TD and flow test well through a 40.6 cm steel casing. Afterwards, run and cement 34 m titanium production string inside the 40.6 cm casing.

## 5.2 Geothermal Chemistry

Planning a geothermal well with fluids is essential. Geothermal fluid chemistry is characteristics by presence of many chemical elements and compounds in various combinations. It contains a different concentration of dissolved elements and the most critical characteristics of geothermal fluids are (Povarov et al., 2000):

1. Total dissolved solids (TDS) in parts per million (ppm) or milligrams per liter (mg/L). This gives a measure of the number of chemical salts dissolved in the waters
2. pH – the pH of a fluid is a measure of the acidity or alkalinity of the fluid. Neutral fluids have pH = 7 at room temperature. Acid fluids have pH values <7 and alkaline fluids have pH values >7

The total amount of dissolved chemicals depends on the temperature and geology of the reservoir. Within lower temperatures, reservoirs typically have less amount of dissolved chemicals. While in higher temperatures may have expectations. The corrosion-aggressive gases are found in the composition: carbon dioxide (60-95%) and hydrogen sulfide (2-15%) as well the hydrogen, methane, ammonia are also found (Povarov et al., 2000).

Figure 15, shows the typical composition of geothermal waters. The presence of these elements leads to long-term well integrity problems like corrosion, erosion, and scaling of the casings used for well completion.

| Species | Wairakei[2] wells ~ 1.5km | Rotorua[3] springs | Waitoa[4] springs | for comparison | |
|---|---|---|---|---|---|
| | | | | Seawater[5] | River water |
| Cl- | 2156 | 560 | 57 | 19350 | 5.7 |
| Na+ | 1200 | 485 | 220 | 10760 | 4.8 |
| $SiO_2$ | 660 | 490 | 175 | 0.005-0.01 | 13 |
| K+ | 200 | 58.5 | 43 | 399 | 2 |
| $HBO_2^-$ | 115 | 21.6 | 1.2 | 0.004 | - |
| $HCO_3^-$ | 32 | 167 | 3177 | 142 | 23 |
| $SO_4^{2-}$ | 25 | 88 | <1 | 2710 | 6.7 |
| $Ca^{2+}$ | 17.5 | 1.2 | 37 | 411 | 15 |
| Li+ | 13.2 | 4.7 | 0.6 | 0.18 | - |
| F- | 8.1 | 6.4 | 0.3 | 0.0013 | - |
| $NH_3$ | 0.15 | 0.2 | - | - | - |

[1] figures given in ppm, where ppm = mg/kg; [2] "neutral chloride" waters; [3] "acid sulfate" waters; [4] "alkali carbonate" waters; [5] seawater has a pH range of 8.1-8.3 and river water has a pH range of 5-6.5

*Figure 15 Typical composition of geothermal waters, (Povarov, Tomarov, & Semenov, 2000)*

### *5.2.1 Corrosion*

Corrosion can be defined as the wear-off of a material, usually metal, because of a reaction with its environment. It happens where an anode, cathode, electrolyte, and an electrical current are present.

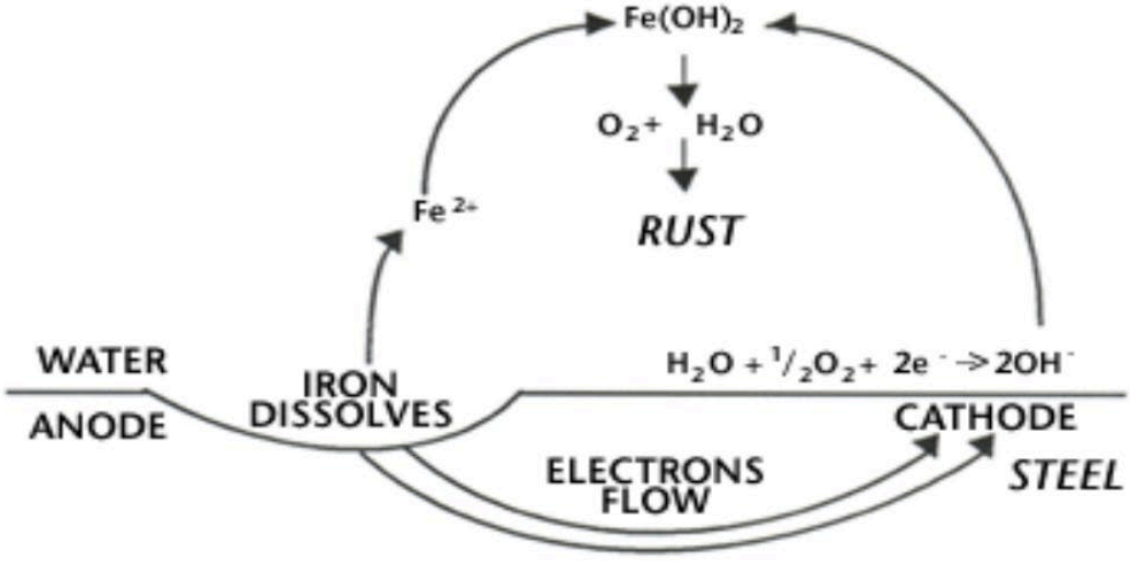


*Figure 16 Electrochemical process (Kristanto, Kusumo, & Abdassah, 2005)*

Figure 16 shows the process of corrosion. shows the process of corrosion. We can find all the different types of corrosion in geothermal equipment. The common types of corrosion

that occur in geothermal wells are the following: uniform corrosion, carbon dioxide, erosion-corrosion, hydrogen sulfide corrosion, pitting, oxygen corrosion etc.

According to (Schweitzer, 1996), temperature can significantly influence the corrosion process. Since an electrochemical reaction and reaction rates do increase with increasing temperature. Metallic and non-metallic parts of geothermal wells can be highly corrosive. With extreme high temperature could produce endogenous corrosive fluids, such as $H_2S$ and requires operators to plan for safety precautions. Because it can create a detrimental environment to cement, production casing and wellhead (Shadravan & Shine, 2015).

Corrosion problems occur in many geothermal operations and have severe equipment damage. The subjects of extreme corrosion within the geothermal steam and brine are production wells, steam and brine gathering systems, injection lines, and wells. (Ocampo-Diaz, Valdez-Salaz, Shorr, Sauceda, & Rosas-González, 2005) have listed the following types of contaminants and conditions in the steam and brine:

- Carbon dioxide, $CO_2$
- Hydrogen sulfide, $H_2S$
- Hydrogen Chloride, HCl
- Iron Sulfide, FeS
- Sulfuric acid, $H_2SO_4$
- Oxygen
- Temperature
- Suspended Solids
- Flow hydrodynamics

### 5.2.1.1 Uniform Corrosion

Uniform Corrosion is the simplest form of "corrosion". It is a rate of metal loss over the exposed surface and is often expressed in terms of metal thickness loss per unit of time (Schweitzer, 1996). It is the basis for most corrosion prediction equations. Figure 17 shows the uniform corrosion reactions. The anode and cathode are both on the surface of the metal. The anode emits electrons, and cathode receives them.

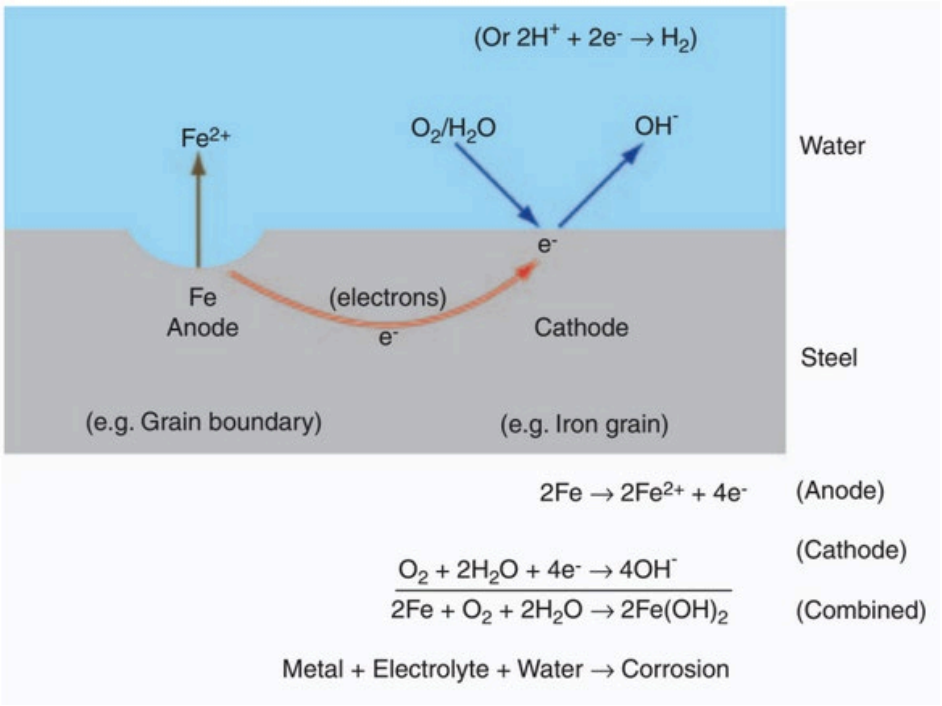


*Figure 17 Uniform corrosion (Bellarby, 2009)*

### 5.2.1.2 Carbon dioxide Corrosion

The acidic nature of dissolved CO2 dissolved helps in the deterioration of metals known as carbon dioxide or sweet corrosion. The level of acidity of the solution depends on the partial pressure of the gas. According to (Bellarby, 2009) sweet corrosion has very high in new

$$H_2CO_3 + e^- \rightarrow H + HCO_3^-$$
$$2H \rightarrow H_2$$

Which can turn iron to ferro

$$Fe \rightarrow Fe^{2+} + 2e^-$$

Therefore the overall reaction is

$$CO_2 + H_2O + Fe \rightarrow FeCO_3 + H_2$$

*Figure 18 Overall reaction, (Shadravan & Shine, 2015)*

environments at very high flow rates. The common mechanisms of $CO_2$ corrosion (Shadravan & Shine, 2015) is shown in Figure 18.

### 5.3.1.3 Oxygen Corrosion

Oxygen can cause problems on production wells by exacerbating stress corrosion cracking (Bellarby, 2009). Oxygen reacts quickly with carbon steel, and most casings use API carbon steel tubing. At the same time, it has the potential to fill the reservoir completion and create plugging to cause failures of tubing/casing. Figure 19 shows an example of corrosion on carbon steel.

*Figure 19 Carbon steel tubing (Bellarby, 2009)*

### 5.2.1.4 Stress Corrosion Cracking

Stress corrosion is caused by localized corrosion combined with tensile stresses (Bellarby, 2009). The presence of $H_2S$ and $CO_2$ in produced fluids leads to the reaction with steal to form semi protective film of rust. The rust can wash away on the surface by the flow of fluid. It can lead to the exposure of more material for chemical attack in the presence of high temperature and pH. The causes of stress cracking are the following: environment, stress and material.

### 5.2.1.5 Erosion Corrosion

Erosion Corrosion happens in flowing systems where turbulence occurs, typically in pipe bends (elbows), tube constrictions, and other structures that alter flow direction or velocity.

The mechanism is the continual flow of water, where it removes any protective film from the metal surface. It also leads to rapid failure.

### *5.2.2 Scaling*

Scaling is the precipitation of salts from geothermal fluid during production. It occurs to the change in pressure, temperature, or pH. Scaling is a challenge in most geothermal wells. According to (Gunnlaugsson, Ármannsson, Thorhallsson, & Steingrímsson, 2014) the most common geothermal scales are silica ($SiO_2$) and calcite ($CaCO_3$). The temperature ranges of scaling depositions are the following (Ármannsson et al., 2014):

- Calcite scaling 180-240°C
- Silica scaling 240-290°C
- Silica and sulphide scaling >290°C

Figure 20 show a picture of calcite inside a slotted liner in Krafla KJ-19. According to (Fridriksson & Thórhallsson, 2007), the most severe calcite scaling was at 280m depth in 210°C well.

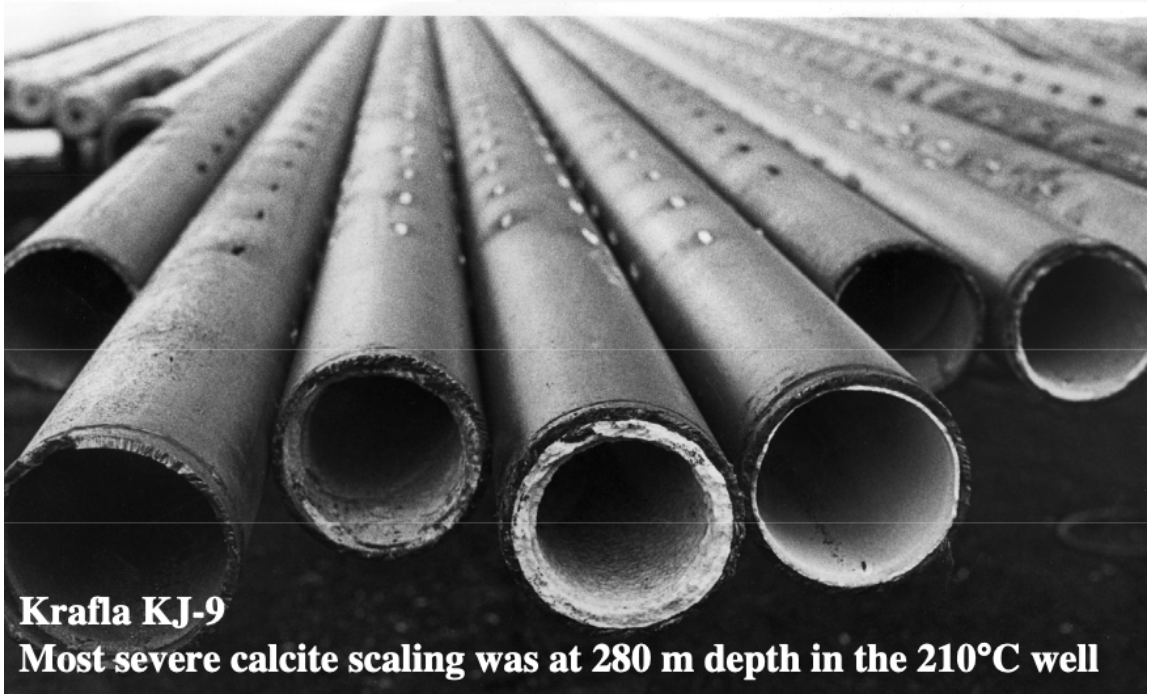


*Figure 20 Calcite scaling (Fridriksson & Thórhallsson, 2007)*

### *5.2.3 Material Selection*

Material selection for geothermal well construction is one factor of importance in the basic design of geothermal utilization schemes, which are expected for long-term service. Not

corrosion is also a problem in geothermal installations and the use of proper material selection, operation, and maintenance.

### *5.2.4 Metallic Materials*

According to NORSOK Standard metallic materials are divided into carbon and low alloyed steels, stainless steel, nickel base alloys etc.

#### 5.2.4.1 Carbon and Low Alloyed Metals

Carbon steels are less expensive and convenient to use in geothermal wells. Sulfur stressed breaking can be seen in steel materials subjected to hydrogen sulfide under stressed conditions in water environments (Ellis, 1985) (Conover, 1982).

It increases when the temperature rises. It decreases in strength, stress, and the concentration of Sulphur and increases in pH. Low alloy steels have corrosion resistance similar to carbon steels (Ellis, 1985).

#### 5.2.4.2 Copper Alloy

Copper alloys show cracks in the presence of high amount of Sulphur in geothermal wells. In Iceland, they experience to indicate for heat exchange service, copper is unsatisfactory, and most brasses (Cu-Zn) and bronzes (Cu-Sn) are still less suitable. The amount of ammoniac and ammonium is low, where the cracks on the metal surfaces are limited (Conover, 1982; Ellis, 1985).

#### 5.2.4.3 Stainless Steel

Unlike copper, stainless steel is not affected by traces of hydrogen sulfide. According to theory, the probability of uniform corrosion decreases in stainless steel in geothermal environments. At the same time, pit corrosion, cracking corrosion, and H2S corrosion may occur depending on which type of stainless steel is used. According to (Conover, 1982), Molybdenum and silica increases the resistance to stressed corrosion.

#### 5.2.4.4 Nickel Based Alloys

Nickel-based alloys are much better than the other materials. Nickel is a good help for other metals in their resistance to a different kind. According to (Sanada et al., 2000), high temperature in geothermal wells, is suitable to use Ni-Co-Mo alloys as material.

### *5.2.5 Non-Metallic Selection*

Metals are used in geothermal well completions. At the same time, non-metallic materials are being used in some particular cases, such as the use of elastomers. An elastomer is a

polymer with viscoelasticity and with weak intermolecular forces. Non-metallic materials are generally strong against corrosive environments as compared to metals and alloys. (Conover, 1982), (Ellis, 1985; Sanada et al., 2000) listed some non-metallic materials that are used in geothermal field:

- Elastomers
- Cements
- Concrete and polymer composition
- Fiber reinforced materials

## 5.3 Geothermal Well Drilling Design

Geothermal wells have extensive diameter drilling by all other industries, and workers require a highly specialized drilling skill. It can design and use different materials and tools depending on the type of geothermal system. The purpose of the geothermal well will require a well-detailed planning of the strength and diameter of the material.

Designing a geothermal well is known as "bottom up" process. The location of the production zone determines the well´s overall length, and the required flow rate determines the diameter at the bottom of the hole (Finger & Blankenship, 2010). The well´s profile above the production zone is set by iteration of the larger casing strings that required drilling or geological considerations.

According to (Ichim et al., 2017) casing fatigue and cement integrity are the key issues for geothermal wells since they have a higher life expectancy than oil and gas wells. The depths and sizes of the tubular are shown. As well the trapped fluid pocket in the tieback section annulus of the well. The APB (annular pressure build-up) in a trapped fluid pocket cannot relieve itself as the cement is enclosed in steel with no access to the formation. The pressure will then develop with heat-up during the first half-cycle (production) and can lead to collapse or an inward bulge of the tieback. Figure 21 shows a typical geothermal well schematic, identifying the region of interest.

Because of the large diameters in geothermal wells, casing and cementing will form a large share of the cost, and eliminating one string of casing would cause an impact on the project. Therefore, the need for directional drilling and the accuracy with which the hole trajectory must be controlled. But if the directional drilling is dictated by the well design, then there are consequences about it.

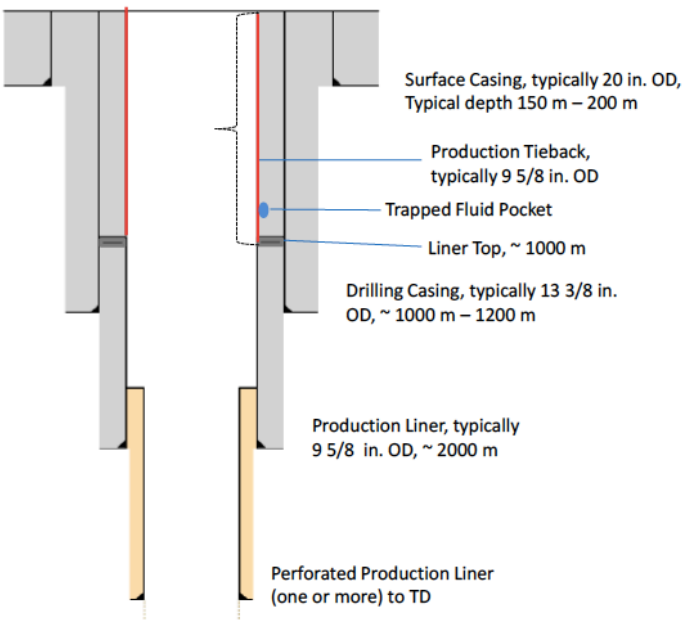


*Figure 21 Typical geothermal well design, (Suryanarayana, Bowling, Sathuvalli, & Krishnamurthy)*

Designing a well needs a great variety of information. Figure 22 shows an example of geothermal well design. The following parameters are important to include in designing a well (Finger & Blankenship, 2010):

- Purpose of the well: production, injection, exploration, or workover
- Reservoir conditions: previous temperature, pressure logs in offset wells, thermal gradient holes, geophysical information, brine chemistry, and significant impact on casing selection and cost

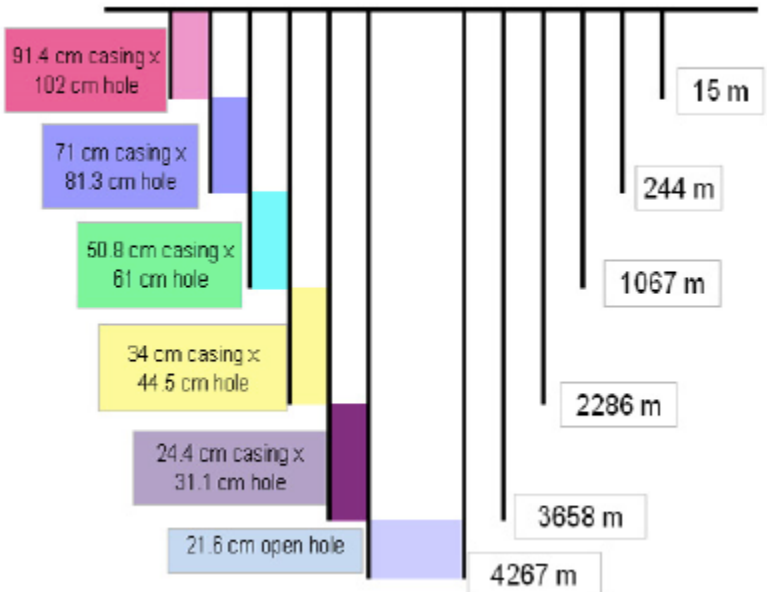


*Figure 22 Geothermal well design, (Finger & Blankenship, 2010)*

- Logistical requirements: the lease, a power sales contract, and other finances requirements
- Problems in drilling: lost circulation material for under pressured formations, appropriate drilling fluid additives for corrosive brines or for exceptionally high temperatures, high temperatures logging or steering tools and drilling motors if those tools will be used in a hot hole; stand-by fishing tools
- Casing requirements: the heart of well design is the specification of the casing program

## 5.4 Geothermal Well Drilling Different types

Geothermal well drilling is more expensive in cost and depth than on-shore oil and gas drilling for three principal reasons (Finger & Blankenship, 2010)

1) Technical challenge: the conditions described above the mean that special tools and techniques are required for the harsh downhole conditions
2) Large diameters: because the produced fluid (hot water or steam) is of intrinsically low value, large flow rates and thus, large holes and casing are required
3) Uniqueness: almost every geothermal well is different, so a new well presents a new learning curve much more often than with oil and gas

Geothermal well and drilling equipment are published by (Culver, 1998), (Ngugi, 2008) and (Finger & Blankenship, 2010). Most of the criteria used to select a drill rig will be derived from well parameters, such as diameter, depth, and casing design. The process of planning and designing the well will have established the diameter to know what kind of rig will be used. There are two types of drilling rigs: cable tool and rotary drilling (Finger & Blankenship, 2010).

### *5.4.1 Cable Tool*

Cable Tool uses a heavy bit that is repeatedly lifted and dropped that crushes and breaks the formation. Figure 23 shows the basic elements of a cable tool. The pitman arm and spudder beam impart an up-and-down motion to the cable and drill bit. The length of cable is adjusted. So that on the down stroke the tools stretch the line as the bit hits the bottom of the hole, striking with a sharp blow and retracting. The twist, or lay, of the cable imparts a slight turning motion to the tools so the bit hits a new face with each stroke. Let clay cable is used so that the twisting action tightens the tools screwed connections on each upstroke. If the borehole is dry, water is added to form a slurry that is bailed out. An experienced driller can drill through any formation, including large cervices and caverns.

With the cable tool rigs, have some advantages such as (Culver, 1998):

1) There is no potential for plugging producing formations with drilling muds
2) Rigs cost less, are simpler to maintain and can be operated by one or two persons. Transportation and step up are easy and less water are required
3) Sampling and formation logging are simple and fairly accurate. There is little chance for contamination by previously drilled zones, especially in consolidated formation. In unconsolidated formations, there is always some chance the cable, tools or bailer will wipe the side walls, carrying material down to be sampled later
4) Qualitative and quantitative data can be obtained during drilling, including good flow estimates, and temperature, static water level, and water chemistry measurements

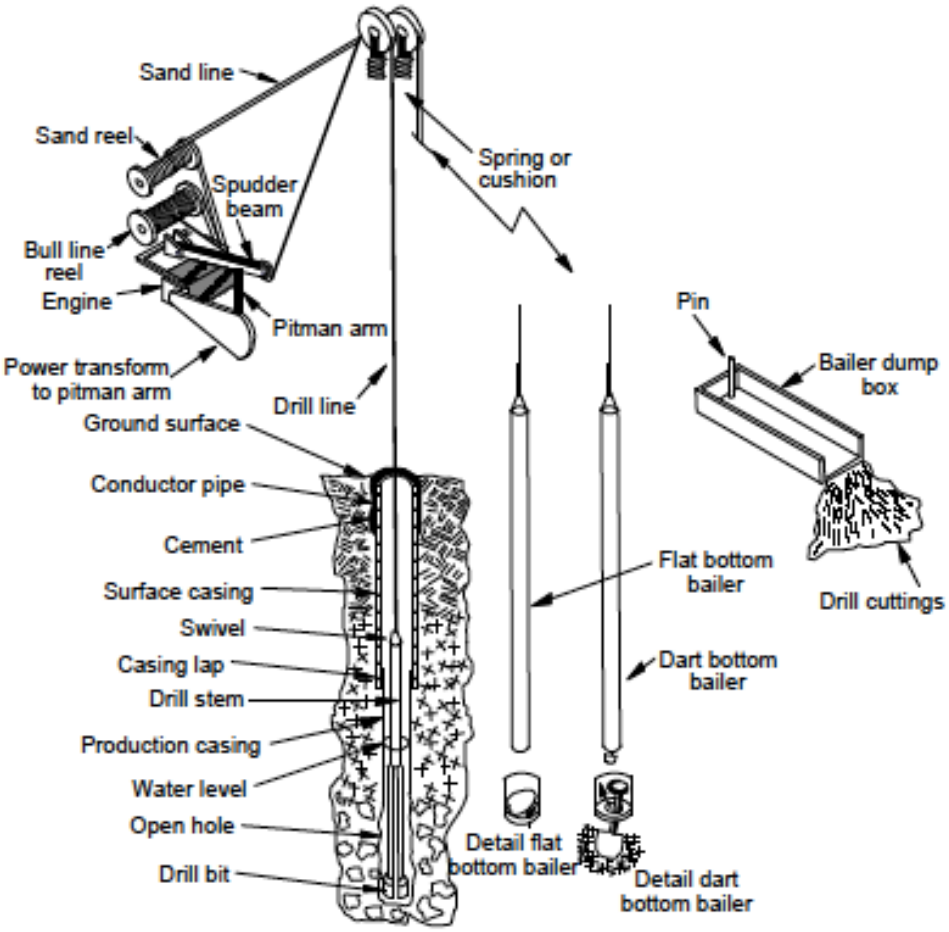


*Figure 23 Basic elements of a cable tool drilling, (Culver, 1998)*

And the disadvantages are (Culver, 1998):

1) Depth and penetration rates are limited
2) Blowout preventers are not easily adapted

3) In unconsolidated formations, casing must be driven as the hole progresses
4) There is a lack of experienced personnel. Cable tool drilling is somewhat of an art and the preponderance of rotary drilling means a cable tool driller with wide experience may be hard to find
5) The method is limited to vertical holes

### *5.4.2 Rotary drilling*

Rotary drilling is the most common drilling method in both water and geothermal well drilling (Culver, 1998). Figure 24 shows the basic elements of a conventional rotary mud rig. The drill bit is rotated by the hollow drill collar and drill pipe. Torque is applied through the rotary table and Kelly. Drilling fluid is circulated down the drill pipe and out openings in the bit where it cleans cuttings from beneath the bit, cools the bit and carries cuttings to the surface where they are separated from the fluid. Weight on the bit is applied by the heavy drill collar assembly. The drill pipe is held in tension by the traveling block.

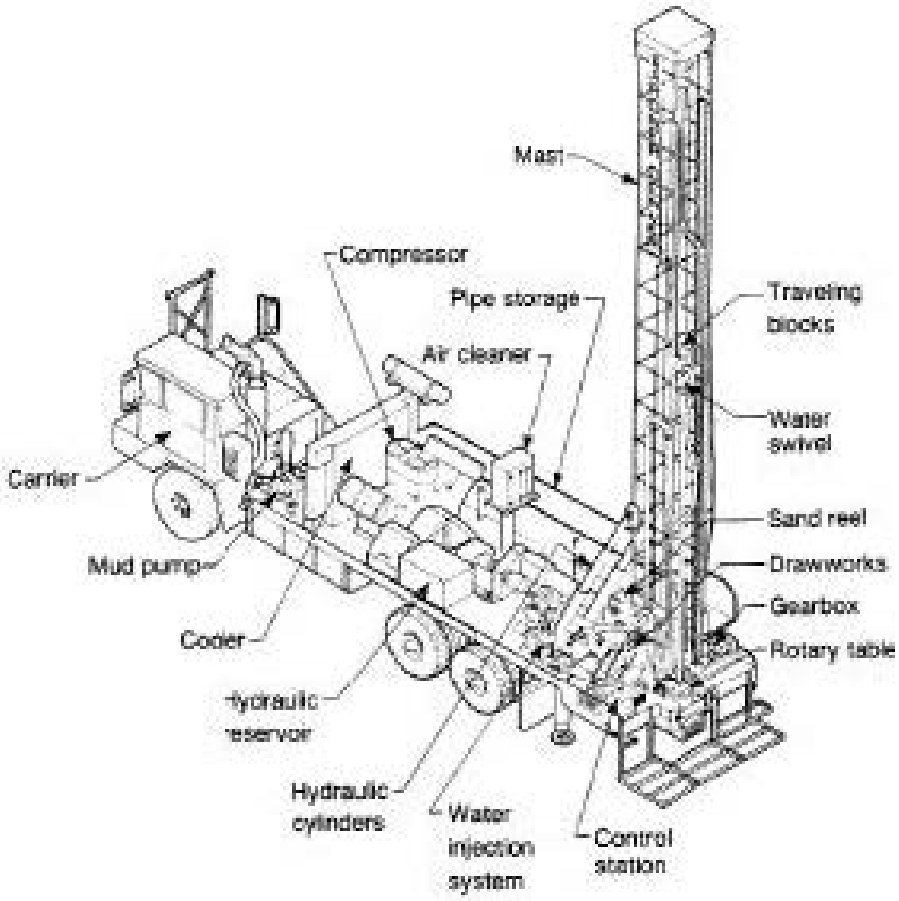


*Figure 24 Schematic diagram of a direct rotary, (Culver, 1998)*

Rigs with top head drive do not use a rotary table and Kelly. Instead, they use a hydraulic motor that travels up and down the mast supplies torque directly to the drill pipe. Rigs with masts and draw works capable of lifting 150,000 lb and with drives producing 140,000 in. lb of toque are available. Drilling fluids can be water, mud (water with additives such as bentonite, polymer, etc), air and water (mists), air, or air and water with foaming agents.

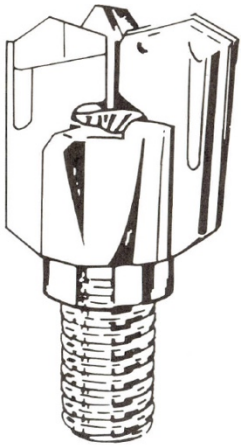

*Figure 26 Drag bit, (Ngugi, 2008)*

*Figure 25 PDC bits, (Ngugi, 2008)*

*Figure 27 Tri-cone roller bits, (Ngugi, 2008)*

### *5.4.3 Types of bits*

#### 5.4.4.3.1 Drag bits

Drag bits is the oldest rotary tool still in use Figure 27 (Ngugi, 2008). The cutting blades are integrally made with the bit body. They are fixed to it and rotate as a unit with the drill string. The bit is used primarily in soft and gummy formations.

#### 5.4.4.3.2 Polycrystalline diamond compacts (PDC) bits

The PDC bits us diamonds inserts embedded on the bit body Figure 26 (Ngugi, 2008). They operate by the diamonds embedding into the formation and dragged across the face of the rock in a ploughing action. The diamond bits drill according to the shear failure mechanism. They are of higher cost, but their long life makes them cost economic in certain circumstances. The bits are hardly used in geothermal drilling, only 5% of the drilling cases in the oil industry.

#### 5.4.4.3.3 Roller cutting bit

More than 95% of the oil field footage is drilled today with tri-cone roller bits Figure 25 (Ngugi, 2008). Roller cones bits have three components groups: the rolling cones, the bearings and the bit body Figure 28, Figure 29 and Figure 30 (Ngugi, 2008). The body is a forged and welded structure, having three pieces, called the legs, with bearings pins on the

lower end of each leg. Each leg has a nozzle boss and a one third circular arc-shaped piece at the top.

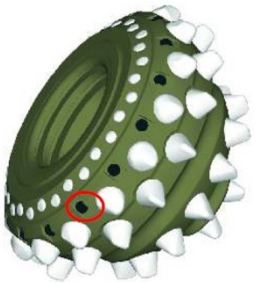

*Figure 30 Bit cone, (Ngugi, 2008)*


*Figure 29 Bit bearing, (Ngugi, 2008)*

*Figure 28 Bit body (single leg) with cone and bearing in place, (Ngugi, 2008)*

## 5.5 Geothermal Well Worldwide Review 2010 – 2014

A worldwide application of geothermal energy for direct utilization review from (Lund & Boyd, 2015). It represents different number regardless to geothermal well drilling.

### *5.5.1 Well drilled*

Around 2.218 well were drilled by 42 countries during the period of 2010 to 2014 for both direct-use and electric power. It has increase in 6.2% over the period of 2005 to 2009 in 37 countries. Countries such as China, Turkey, USA, Kenya, India and New Zealand has drilled more than 100 wells, which the average is 53 wells per country. Around 48.8% were drilled for power generation, 38.7% drilled for direct utilization, 8.6% drilled as combined heat and power wells, and 3.9% drilled as research or gradient wells. This are the regional allocations (Lund & Boyd, 2015):

- 14.7 % in Africa by 4 countries (327 wells)
- 19.2% in North and South America by 9 countries (426 wells)
- 48.4% in Asia by 8 countries (1074 wells)
- 12.6% in Europe by 19 countries (279 wells)
- 5.1% in Oceania by 2 countries (112 wells)

### *5.5.2 Person-years of professional personnel working*

About 34,000 person-years in 52 countries of professional effort was allocated to geothermal development. The average was 654 person-years per country over the five-year period. It has 25% decrease from 2005-2009 in 43 countries. The countries such as USA, China, New Zealand, Turkey, Iceland, Mexico, Belgium, Poland, Norway and South Korea has more than 100 person-years/year. It is categories about: 10.8% by government, 21.9% by public utilities, 10.6% by universities, 1.7% by foreign consultants, 0.2% by contribution through

foreign aid programs, and 54.8% by private industry. This are the regional allocations (Lund & Boyd, 2015):

- 0.8% in Africa by 5 countries (55.0 person-years/year)
- 36.4% in North and South America by 10 countries (2,475.0 person-years/year)
- 31.1% in Asia by 9 countries (2,115.5 person-years/year)
- 21.5% in Europe by 25 countries (1,1466.6 person-years/year)
- 10.2% in Oceania by 3 countries (693.0 person-years/year)

### *5.5.3 Total investment*

Around US$20 billion was invested in geothermal energy by 49 countries during the period of 2010 to 2014. The average for investment per country was US$407 million, however some countries like Turkey, Kenya, China, Thailand, USA, Switzerland, New Zealand, Australia, Italy and South Korea invested over US$500 million. It is categorized by 28.3% was for electric power utilization in 16 countries, 21.8% was for direct use in 32 countries, 25.6% was for field development including production drilling and surface equipment in 32 countries and 24.4% was for R&D including surface exploration and exploratory drilling in 48 countries. This are the regional investments (Lund & Boyd, 2015):

- 10.8% in Africa by 2 countries ($2,160 billion)
- 13.4% in North and South America by 9 countries ($2,669 billion)
- 44.0% in Asia by 9 countries ($8,765 billion)
- 19.9 % in Europe by 27 countries ($3,953 billion)
- 11.9% in Oceania by 2 countries ($2,375 billion)

# 6 Projects

This chapter represents some industrial projects here in Norway and other countries in the world. The Norwegian projects are published by (Midttømme, 2005), (Kvalsvik, Midttomme, & Ramstad, 2019), (Pascal et al., 2010) and (Grønlie et al., 1980). The International projects are published by (Menzies et al., 2010) in the Philippines and (Fridleifsson & Albertsson, 2000) in Iceland.

## 6.1 Norwegian Projects

The geology of Norway is crystalline rocks sparsely covered with marine clay and other quaternary deposits. The heat flow is low, and the median heat flow value for mainland Norway. Because of the low-temperature level and gradient, almost all geothermal installations are Ground Source Heat Pumps (GSHP). There is no geothermal power plants or geothermal district heat (DH) plants in Norway.

Norway is situated in the cold climate region through the warm Gulf Stream in the Atlantic gives a milder climate than areas equally far north (Midttømme, 2005). Because of the long coastline and high mountains, there are some variations of regional climates from typical maritime in the western part to continental in the east and more arctic dominated in the northern region.

According to (Midttømme, 2005), Norway is part of the Fennoscandian Shield. The bedrock consists of Precambrian rocks with a belt of Caledonian rocks extending from South West to North Norway. Permian volcanic and intrusive rocks are found in the Oslo region. The porosity of the crystalline bedrock is low. A thin layer of glacial sediments covers the bedrock. In some of the larger valleys, there are groundwater aquifers in alluvial or glacial sediments.

### *6.1.1 Geothermal energy in the Iddefjord granite in Østfold Norway*

The use of geothermal energy sources has been prevalent and has successful review throughout the world. Because of the explosive rise in the cost of conventional energy such as electricity, coal, and petroleum. The Norwegian Department of Petroleum and Energy has supported a project to examine the possibility of utilizing the Iddefjord granite in Østfold (Grønlie et al., 1980).

Because the Iddefjord granite is radioactive above average and produces a substantial amount of heat. They want to know if it is possible to use as hot water geothermal energy

source. The geographical position of the granite is favourable because of its closeness to major cities in Østfold, such as Halden, Moss, Sarpsborg, and Fredrikstad. It will be potential users of a geothermal hot water source.

A gravity study of the Iddefjord granite indicated a relatively thick body (3-5km). There were two holes (123 and 128 m deep) drilled in homogenous granite (holes Nos. 12 and 14, Figure 31) and measured the temperature in 22 water wells deeper than 50 m (Figure 31). Figure 32, shows a few of the temperature/depth plots. All the plots reflect the temperature minimum of last winter at a depth of about 12-15 m. Below the 15 m, there is a more or less linear increase of temperature with depth.

Figure 32:2, 3, 5 and 18 shows some fractures and minor faults in the wells. The water wells are drilled in fractured areas in order to increase permeability and water production. According to (Figure 32, Table 5, Nos. 12 and 14) the best gradients are from the two holes drilled into homogenous granite. Hole No 14 shows the highest value. It was drilled in solid granite, while the lower value in hole No. 12 is caused by the fact that portions of the hole were drilled through gneiss.

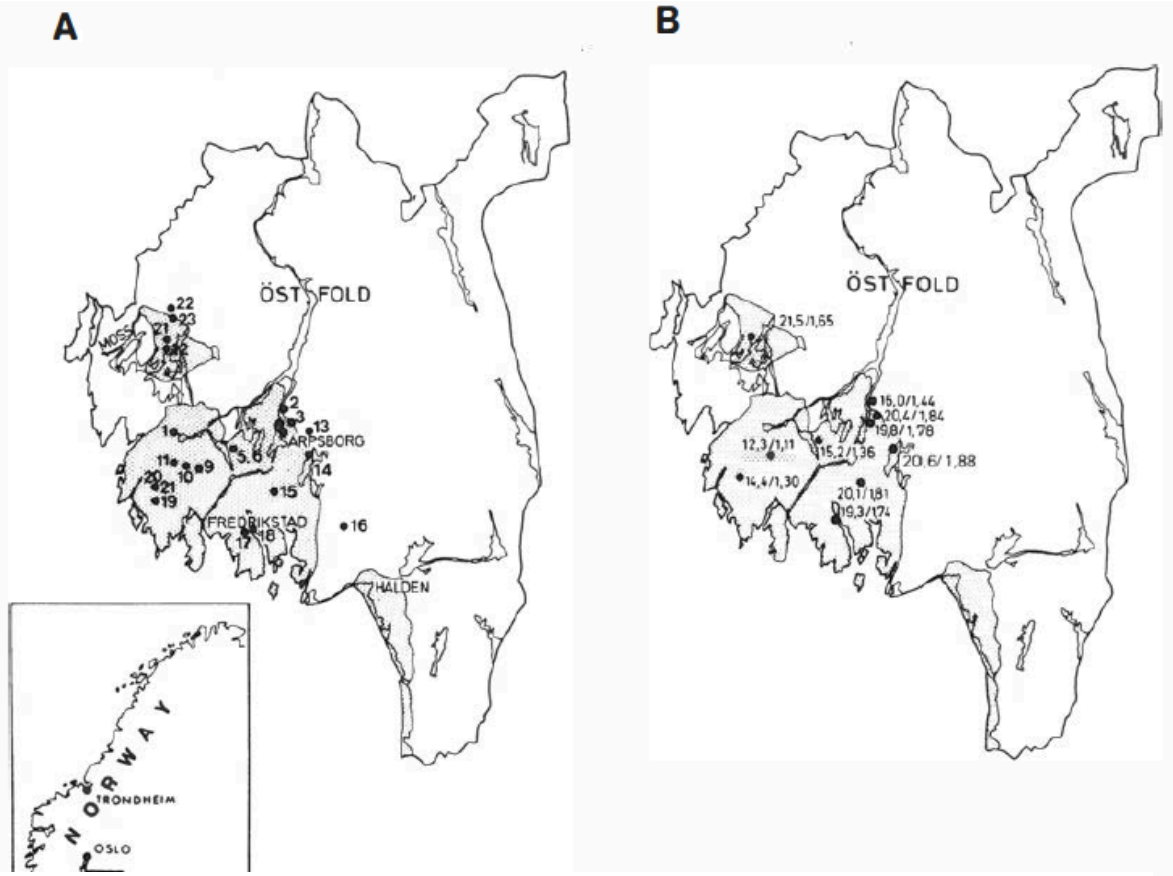


*Figure 31, A: Bore hole localities in Østfold Norway. Dotted area: Iddefjord granite. B: Temperature gradient (°C/km) and heat flow (hfu) from the same localities, (Grønlie et al., 1980)*

According to (Grønlie et al., 1980), the temperature gradients are higher to the east towards the edge of the granite (Figure 31, Table 6), and a maximum of 21.5 °C/km is found in the hole No. 12. The gradients to the west are low (holes Nos. 5,10, and 21) with a minimum of 12.3 °C/km in hole No.10.

The corresponding heat flow values (Figure 31, Table 6) show high importance to the east (maximum 1.88 hfu (78.6 $W/m^2s$) in hole No. 14) and lower values to the west (minimum 1.11 hfu in hole No. 10). The maximum values are 84% higher than the Norwegian heat flow mean, which is 1.020.21 hfu. There was no correction to the temperature gradients for glaciation effects has been made. Because of glaciation cooling effects at 100 m depth for the Båhus granite, there was an increase in the rise of 5-6°C/km.

The variation in geothermal gradient and heat flow observed is closely related to the thickness of the granite and the variation in radioactive mineral content. The granite is thin to the west, according to the gravity model. Therefore, the geothermal gradient and the heat flow interpreted by the gravity data are correct.

On the other hand, the temperature gradient and the heat flow results are fascinating. (Grønlie et al., 1980) suggested working more in order to find the most promising prospective area for possible future geothermal exploitation. And also to define the thickest and most radioactive part of the granite where a new hole should be drilled and measure. (Grønlie et al., 1980) concluded that the immediate future geothermal energy in Norway is not an economical energy alternative yet. However, it might develop more in the coming years as the conventional energy sources.

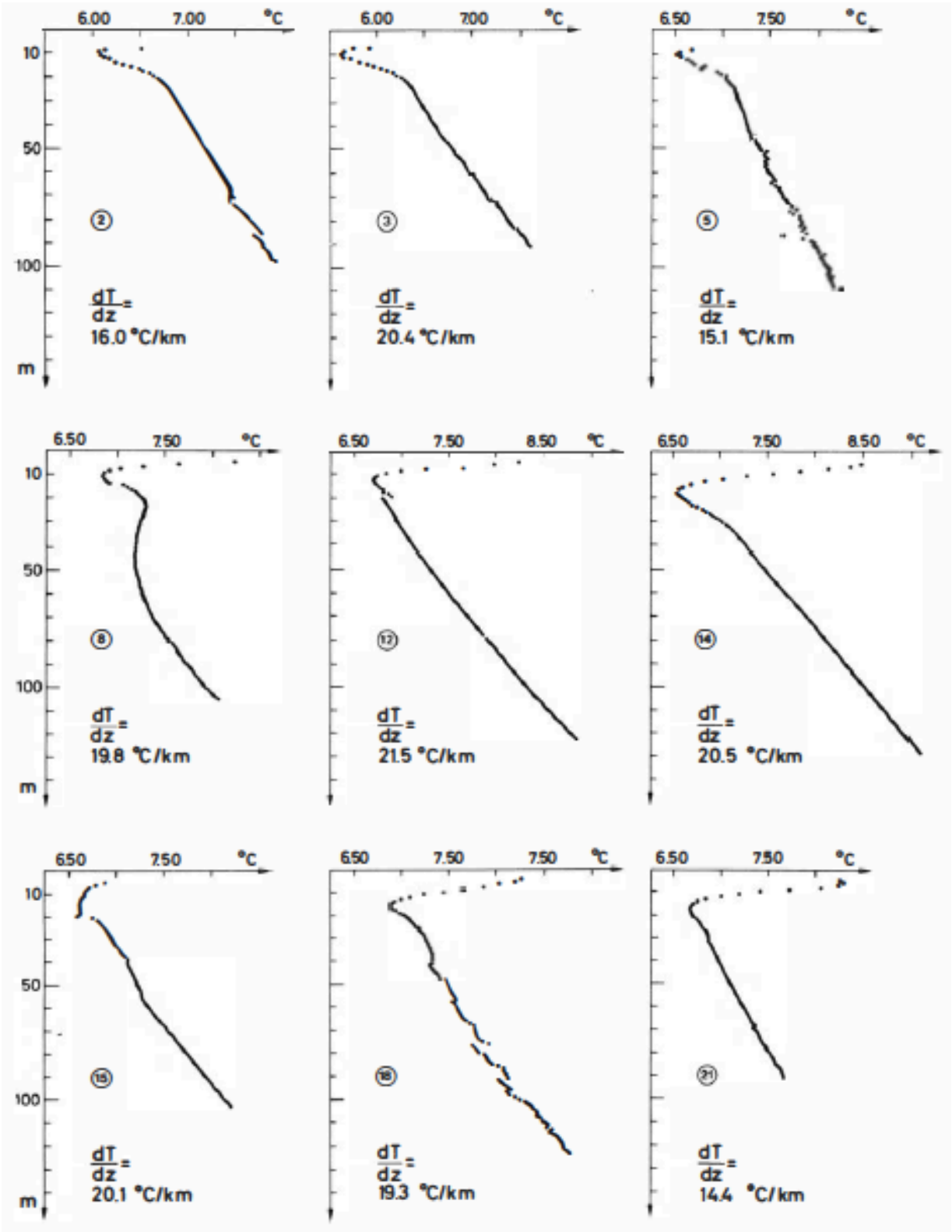


*Figure 32, Temperature verses depth plots from 9 of the location in Figure 33 A. Note the good results in holes Nos. 12 and 14 and the high temperature gradients, (Grønlie, Johansen, Karlstad, & Heier, 1980)*

### 6.1.2 Hot Dry Rock Project in State Hospital in Oslo

In 1999, an attempt was made to develop a Hot Dry Rock pilot plant of 2MW at the new State Hospital in Oslo. The plan was to drill a closed-loop system with two wells connected by horizontal drilling at 5000 m depth. They tested a drilling technique that includes a water-driven percussion hammer and coiled tubing. Figure 33 shows the drilling tools used for the HDR project at the State Hospital in Oslo.

The geology of the area consists of a basement of *gneiss* of *Proterozoic age* covered with *sedimentary rocks* of *Cambrian* to *Silurian age*. Sadly, the site was located in an intense contact *metamorphic* zone with 700 m of hard *hornfels* overlying the *gneiss*. However, the project was abandoned because drilling tools were lost at 1600 m depth. On the bright side, the results obtained hold some promise as to the future development of Hot Dry Rock systems in Norway.

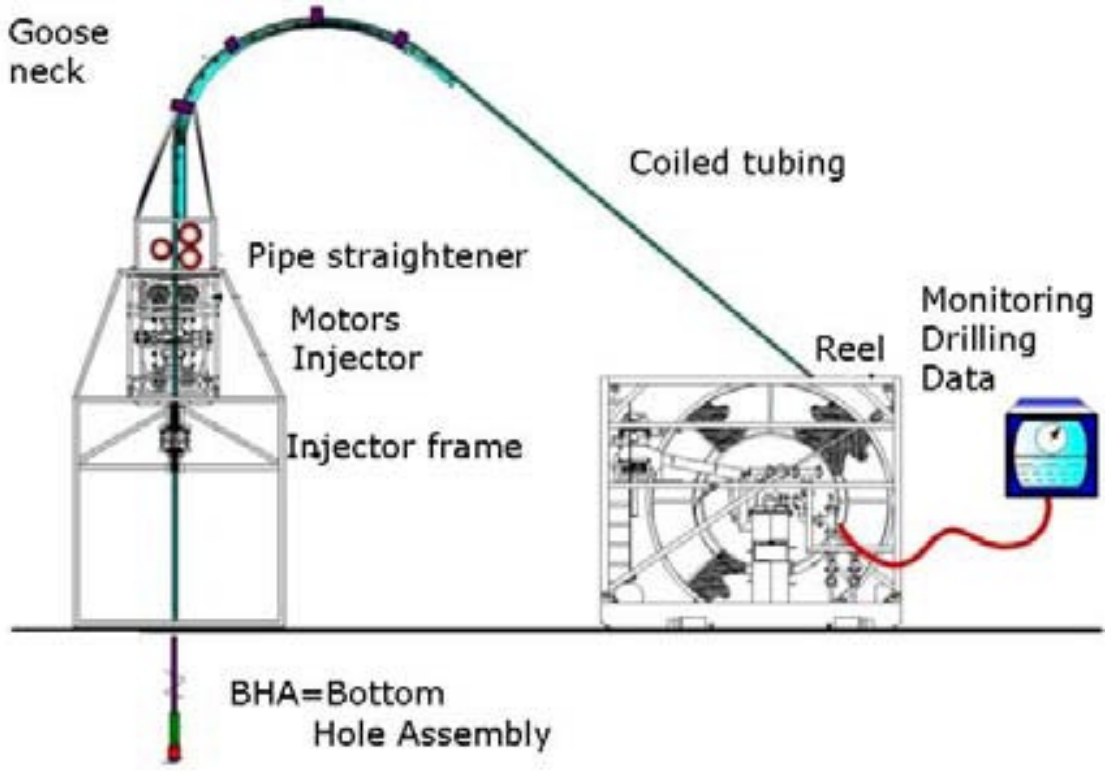


*Figure 33 Drilling tools used for the HDR project at the State Hospital in Oslo,(Midttømme, 2005)*

### 6.1.3 Kontiki project and HeatBar project in Norway

In 2004, NGU (i.e. Geological Survey of Norway) and StatoilHydro initiated the Kontiki project (Pascal et al., 2010). The HeatBar project followed the project in 2006 with additional

support from the Research Council of Norway (i.e NFR). The main goals of both projects were to determine more reliable heat flow values.

The company NGU-NFR and StaoilHydro, they measured temperatures in Kontiki and HeatBar projects. There were 15 deep drill holes located in the Oslo Region (South East Norway), mid-Norway, Nordland (Northern Norway), and Finnmark (Arctic Norway). Most of the drill holes reach the depth 800 m. It allows the identification of paleoclimatic signals in the geothermal gradients and removing them. Figure 34, shows the old heat flow map of Norway (1970s). Most heat flow values were determined from shallow mining wells (i.e. less than 300 m depth) and lake measurements and uncorrected for the potential influence of paleoclimatic variations.

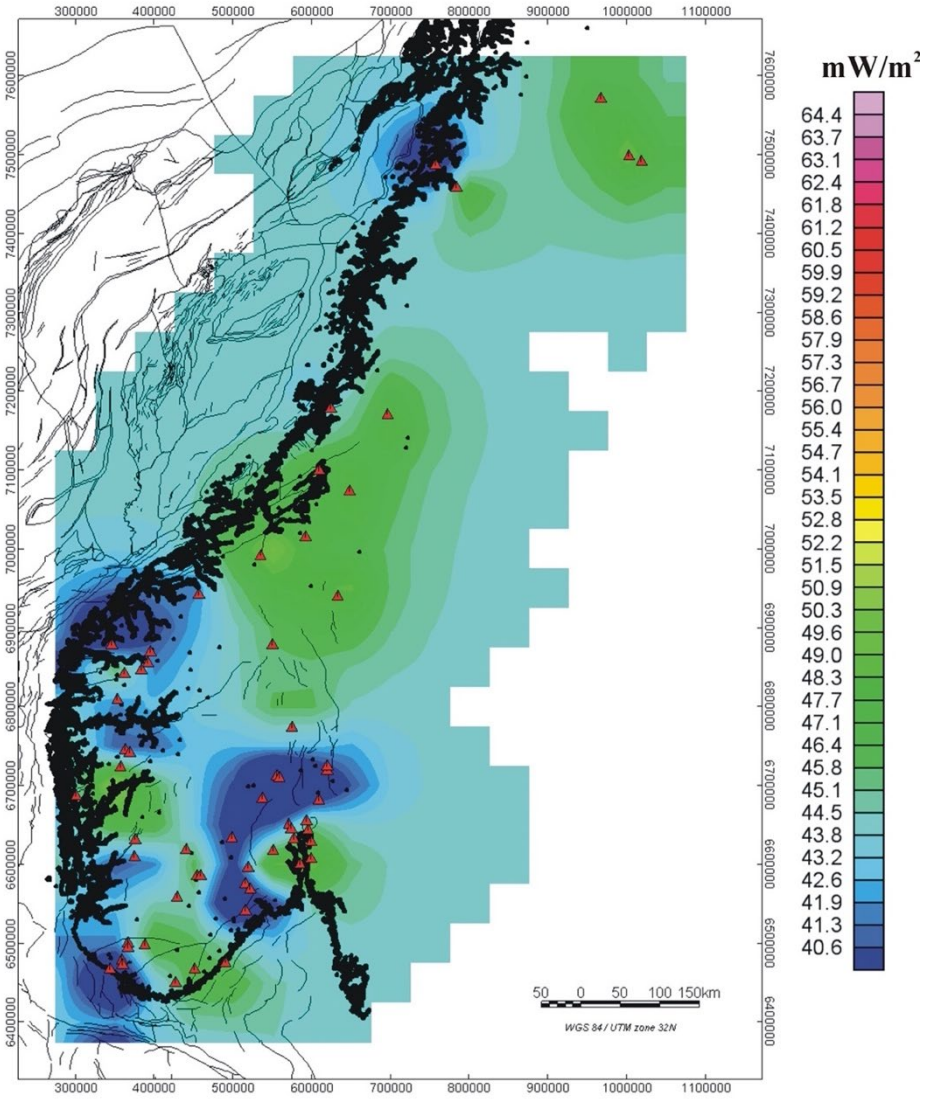


*Figure 34 Heat flow map of Norway from 1970s, (Pascal, Elvebakk, & Olesen, 2010)*

The modern heat flow map of Norway is shown in Figure 35. The heat flow values fall in the range of ~50 to ~70 mW/m$^2$ in excellent agreement with values obtained in the neighbouring country of Sweden. Heat flow reaches its lowest value in northern Norway and its maximum in southern Norway in the Oslo Region. The results from, Table 5, confirmed the visual impression given by Figure 35 and Figure 36. The Oslo Region in southern Norway appears to have the best potential in terms of geothermal prospecting.

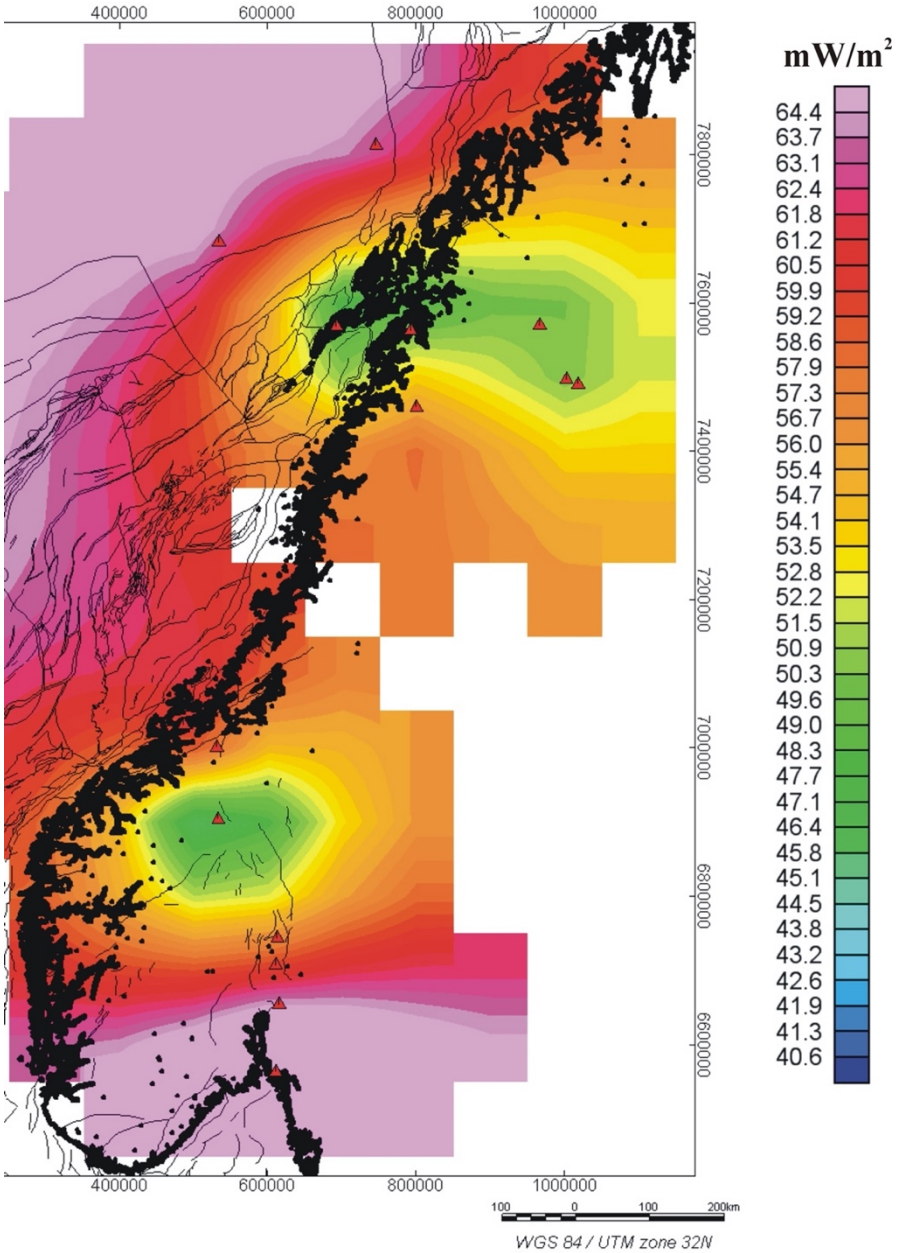


*Figure 35 Modern heat flow map of Norway. Note that the newly determined heat flow values exceed by 10 to 20 mW/m$^2$ (Pascal et al., 2010)*

The progress of the projects was made in the past five years. The framework of the Kontiki and HeatBar projects sheds new light and hope for the geothermal state of Norway. The main finding is that heat flow, and temperature values below the surface are not low as claimed by the old project from the 1970s.

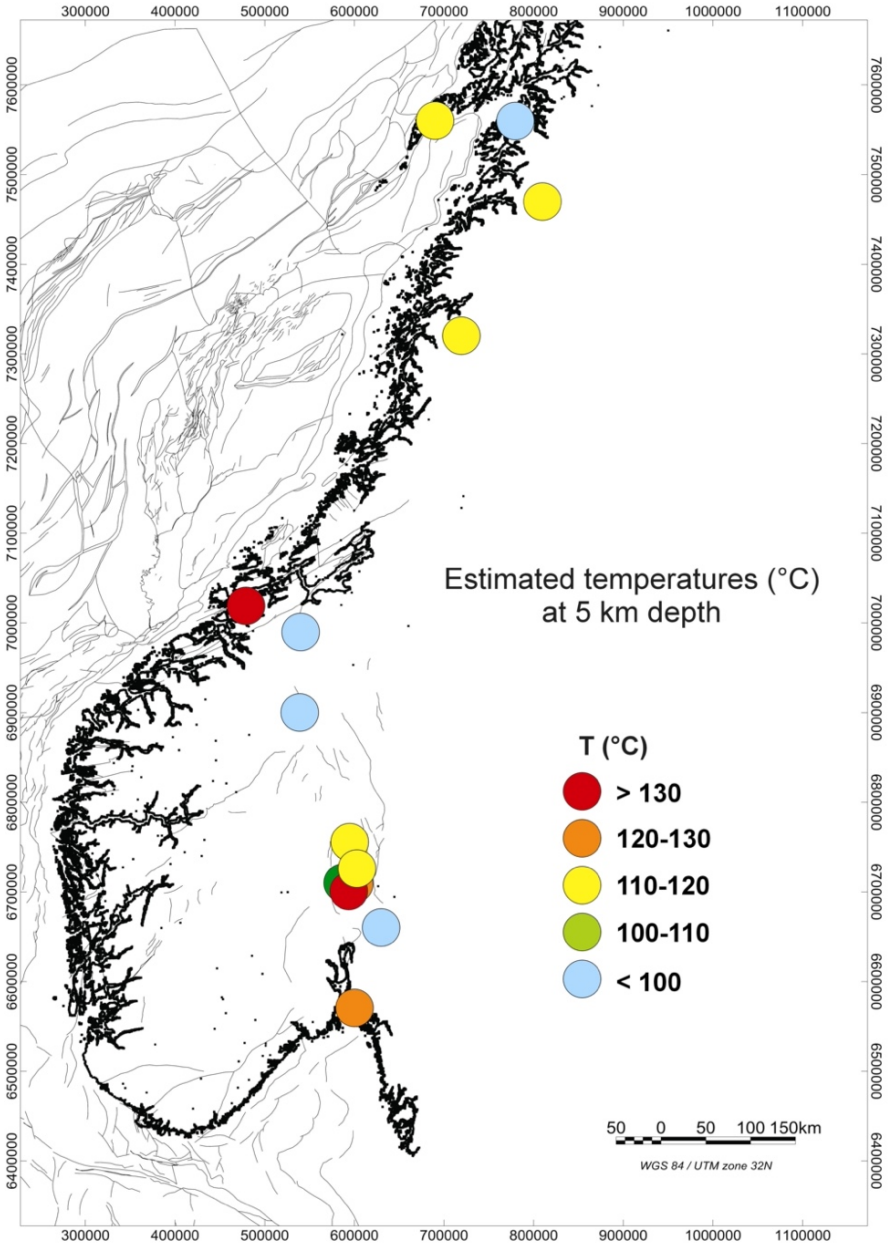


*Figure 36 Estimated temperatures at 5 km depth below the surface, (Pascal et al., 2010)*

## 6.2 The Philippines Project

The Tiwi Geothermal Field began operating on May 15, 1979. It is located on the northeast flank of Mountain Malinao in Albay Province in the Philippines, about 350 km southeast of Manila. According to (Menzies et al., 2010), it is the first National Power Cooperation (NPC) with start-up power of 55 MWe unit. Over the next three years, the installed capacity was increased to 330 MWe.

From 1964 to 1968, the Philippines Commission on Volcanology (COMVOL) with the Philippines Institute of Volcanology and Seismology (PHIVOLCS) evaluated the Tiwi field. It was the first use of geothermal steam for power generation in the Philippines. It includes geologic mapping, geophysical surveys, and drilling of seven temperature gradient holes. In 1970, NPC was given the mandate to develop the Tiwi Geothermal Field for electricity generation under PD 739.

Two years later, on June 4, 1972, the Philippines Geothermal, Inc. (now knowns as CGPHI), conducted a further assessment of the prospect. The well encountered a 270°C liquid-dominated, neutral chloride resource, with low NCG content and sustained steam flow. In 2001, Unit 4 was decommissioned. In 2004-05, Units 1 and 2 (Plant 1) were rehabilitated, with increased capacities of 60MWe each while the capacities of Units 5 and 6 (Plant C) were increased to 57MWe each. Overall, there have now been 156 wells drilled in the Tiwi contract area.

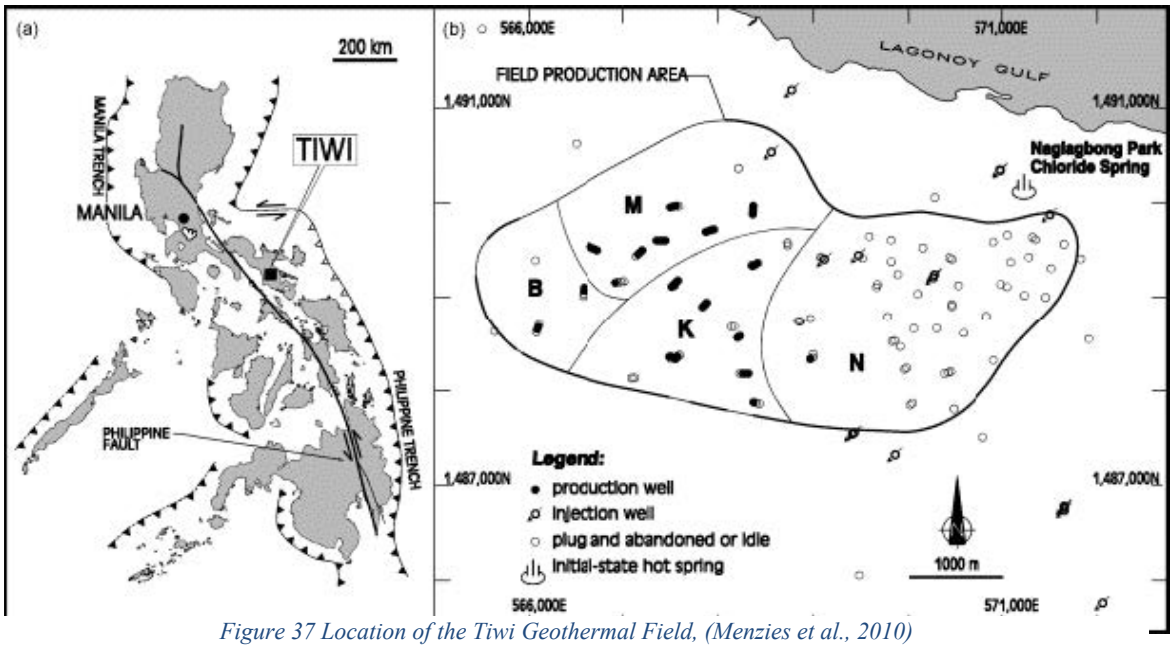


*Figure 37 Location of the Tiwi Geothermal Field, (Menzies et al., 2010)*

(N = Naglagbong, K = Kapipihan, B = Bariis, M = Matalibong

Figure 37 shows the layout of the Tiwi field. It includes a productive area of 12 square km and the four geographic sectors that the field is divided into: Naglabong (Nag), Kapipihan (Kap), Matalibng (Mat) and Bariis (Bar). There are three up-flow zones (Bar, South Kap and Nag) located within the Tiwi field. The heat sources are small dacitic to andesitic domes situated south of the Kap and Bar sectors. The upflows are all neutral-chloride brines with source temperature ranging from 280 to 315°C (NA/KCa-Mg geothermometer). The reservoir chloride concentrations of between 4,000 to 5,200ppm and NCG content in produced steam of 2.0 to 2.5 wt%.

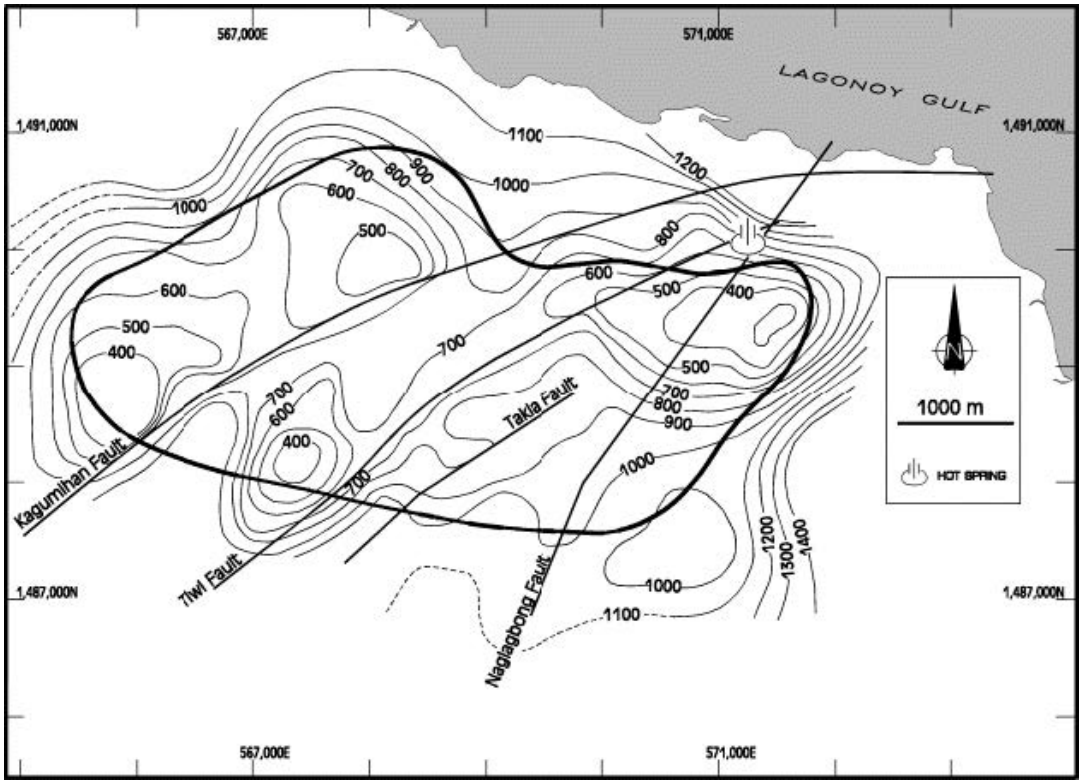


*Figure 38 Reservoir Top and Major Structures in the Tiwi Geothermal Field, (Menzies et al., 2010)*

The cap rock that overlies the productive reservoir is with argillic alteration and dominated by smectite clay. Figure 38 shows the thinnest in the northeast of the Nag sector, where the reservoir top is shallowest. The reservoir top also locates in the North Mat, South Kar, and Bar areas and deepens in the central part of the field between the Kagumihan and Tiwi faults. In the Tiwi field, the most important structures are the fluid flow in the Kagumihan, Tiwi faults, and Naglagbong fault (Figure 39). The strike of these Southwest - Northeast trending faults. They separated the Bar and South Kap / Nag up-flows and divided the reservoir into two or three “compartments”.

After 30 years of commercial production, the biggest challenge was the MR in the Nag area (Menzies et al., 2010). It occurred within the first three years of operation and necessitated the relocation of the entire production system. In 2010, there are 37 production wells in the field. It includes the Bar 11 and Kap 35, where the two wells were completed in 2008. There are 12 used for hot brine injection, 8 are cold brine or condensate injection wells, and 6 were drilled to investigate other potential prospects.

With the successful completion of the two wells, Bar 11 and Kap 35, opens up possibilities for locating future production wells to the south and southwest of the Kap and Bar sectors in the future. However, it will require a significant investment in the existing surface facilities. As it concluded, Tiwi Geothermal Field will continue to be a reliable producer of electrical power to the Philippines national grid for many years to come (Menzies et al., 2010).

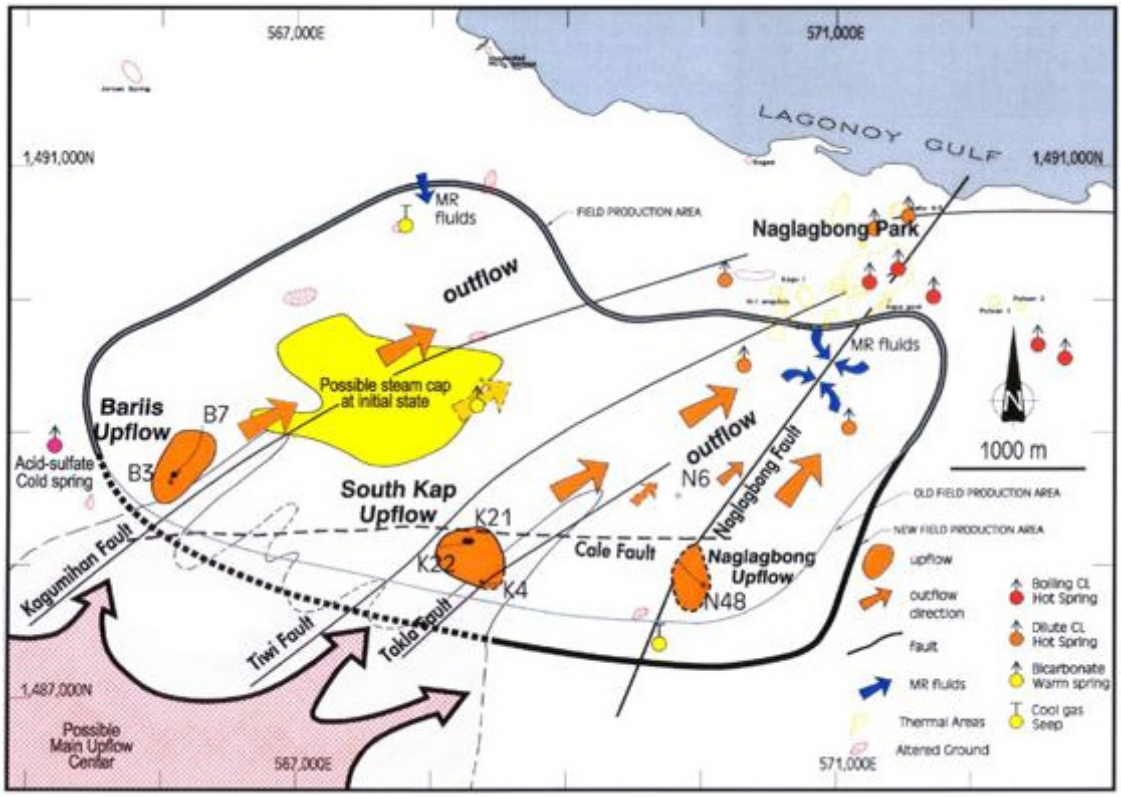


*Figure 39 Initial State Conceptual Model of Tiwi, (Menzies, Villaseñor, & Sunio, 2010)*

## 6.3 Iceland Project

The Icelandic geothermal community had planned to join in a deep geothermal drilling research project on the Reykjanes peninsula. Hitaveita Sudurnesja, Orkuveita Reykjavikur, Landsvirkjun, Federation of Icelandic Energy and Water Works, Iceland Drilling Company

Ltd, Orkustofnun, University of Iceland and other engineering companies in Iceland joined together on this project. They have an idea of using hydrous fluid at supercritical condition. They selected a drillsite in a saline hydrothermal system at the tip of the Reykjanes peninsula. Figure 42 shows the landward extension of the mid-Atlantic ridge.

The geology and surface distribution of the high temperature geothermal system at Reykjanes rift zone is shown in Figure 41 and an aerial view in Figure 42. Subaerial lavas of Holecene age cover the surface. It is where the hyaloclastite ridges of the late Pleistocene age poke the lava fields. The hyaloclastite ridges and the lava fields are hydrothermally altered. It centred within manifestations of fumaroles, mud pools, and hot springs. Figure 41 shows the high resistivity body roughly delineates at 250°C isothermal surface within the high-T system.

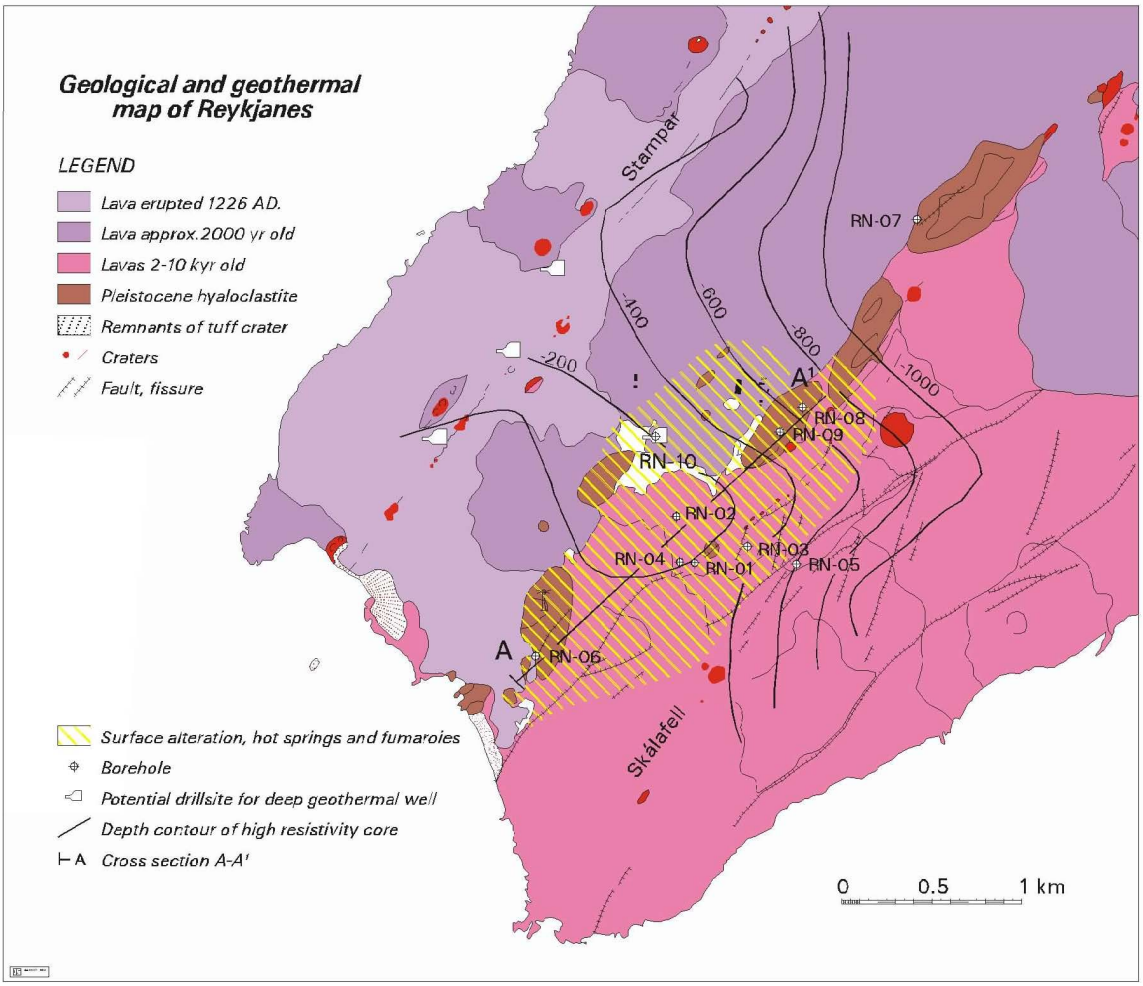


*Figure 40 Geological map of Reykjanes. It shows the drillhole locations, potential drill sites for deep drilling, depth contours to high resistivity core and hydrothermal surface manifestations,(Fridleifsson & Albertsson, 2000)*

In early 1999, the location of drillhole RN-10 (2046 m) drilled (Figure 33). It may consider as a potential drill site for a 4 km deep well, by deepening. It has 13 3/8" cemented production casing down to 692 m depth. It has a slotted 9 5/8" liner to 2030 m within a 12 ¼" hole to 2046 m depth. By deepening well RN-10, the hanging liner needs to be removed, the hole deepened by some 500-1000 m, and a high-resistant cemented casing place in Figure 41. Drilling to the 4 km target depth could continue with 8 ½" drill bit. Well RN-10 is the deepest drill hole on Reykjanes. Table 7 shows a hydrothermal cross-section along the rift axes in the centre of Reykjanes, the location of the profile is shown in Figure 41.

The Nesjavellir field is a part of the active Hengill central volcanic compels. The surface and subsurface geology are characterized by subglacial volcanic formed during glacial periods and lavas formed during interglacial and present. The location of Nesjavellir in shown in Figure 41 and a map of its drill field in Figure 43. Table 7 shows a hydrothermal NW-SE profile across the Nesjavellir drill field. A temperature profile is made inside the drill string, Figure 44, the thermometer only set for 380°C. It shows the well in state of underground blowout below a feed point at 1100 m depth. The feed points accept all the 44-59 1/s of cold water injected.

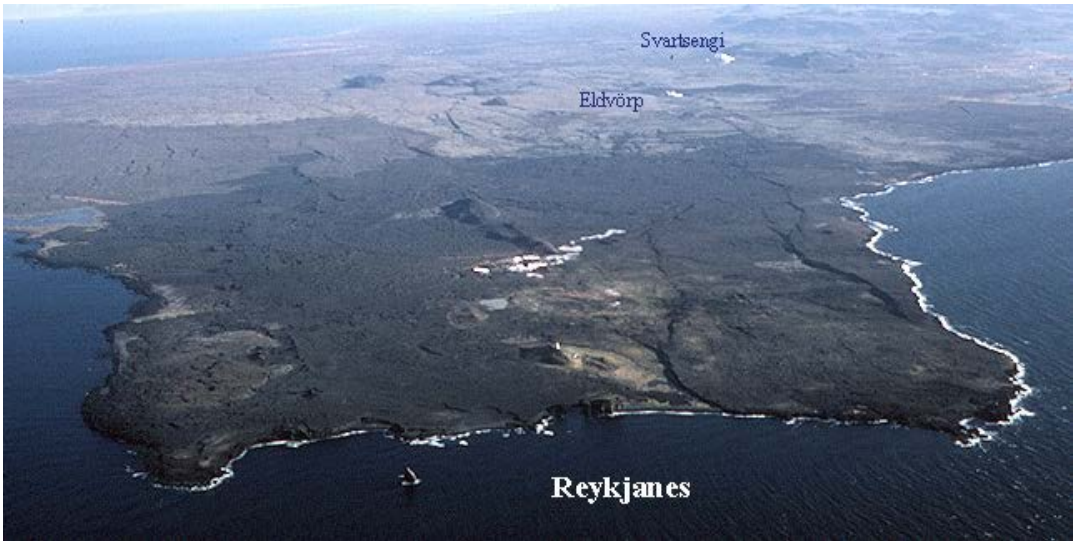


*Figure 41 Reykjanes, the landward extension of the Reykjanes ridge. The drill fields at Reykjanes, Eldvörp and Svartsengi can be seen,(Fridleifsson & Albertsson, 2000)*

A sizeable geothermal system exits within the Krafla central volcano Figure 40. Hitherto, 35 deep drill holes have been sunk into the geothermal system, in one large drill field just north of a power plant. The installed 60 MW electric are produced from about half of the wells at present. The most bottomless well is 2222m. On 1975-1984, there was an active rifting episode took place in the Krafla volcano. It involves 21 cycle of uplifting periods and shorter subside events. The volcanic episode affects the exploited drill field in Krafla. It increased

$CO_2$ to the order of $10^{5.}$ It makes the most active part of the drill field in exploitable for 10-15 years.

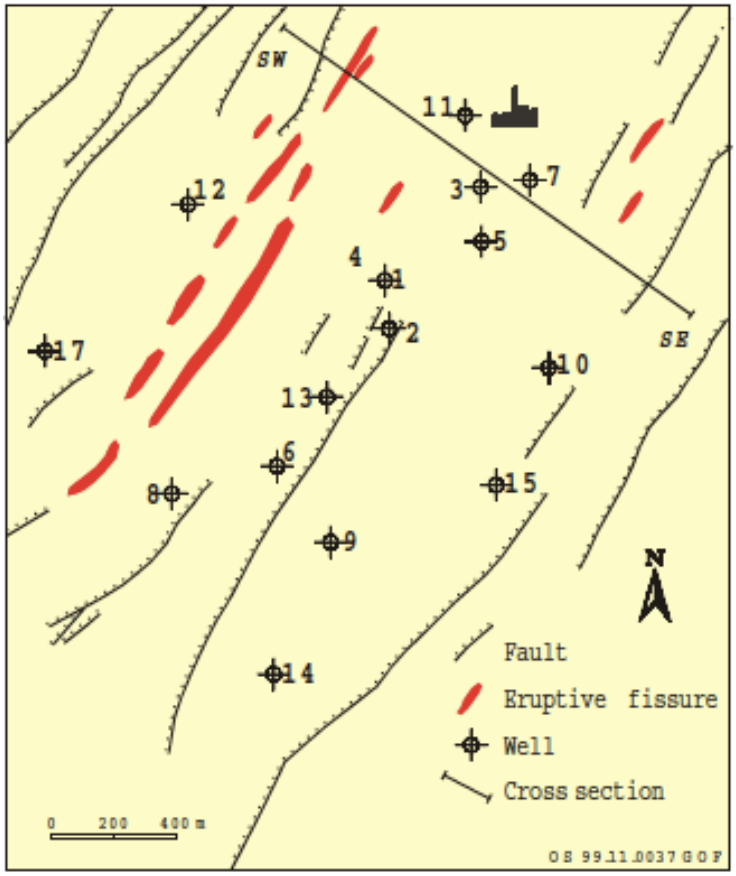


*Figure 42 The Nesjavellir drill field, (Fridleifsson & Albertsson, 2000)*

The high-temperature geothermal systems within the rift zones in Iceland provide several options in finding suitable targets for supercritical fluids. The selected drill sites at Reykjanes flank the surface geothermal manifestations. On the supercritical conditions at Reykjanes, there was a supporting analogue to the time-temperature constraint at a 2000-year-old volcanic fissure at Nesjavellir. It met the supercritical hydrous fluid at 2265 m depth in well NJ-11. The fluid is brought to the surface at supercritical condition into a pilot plant, where the energy and the chemicals will be separated and extracted. The drilling programme in Reykjanes Iceland will take about 2-3 years.

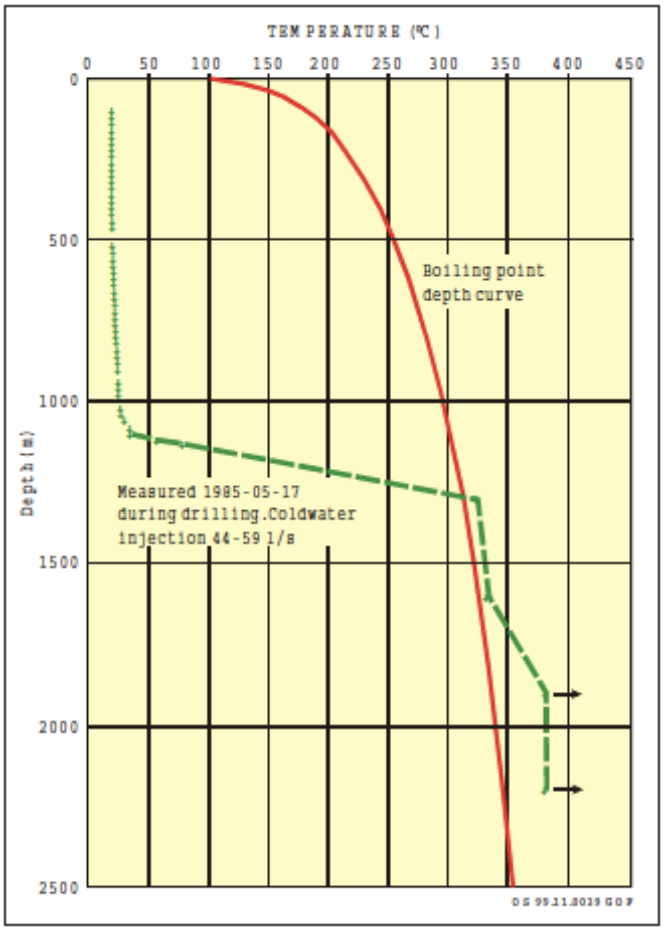


*Figure 43 A temperature profile of well NJ-11 during drilling. The boiling point depth curve for pure water is shown for comparison,(Fridleifsson & Albertsson, 2000)*

# 7 Conclusion

This study gave two overviews about geothermal energy and in geothermal well and drilling. It gave us an exceptional understanding of how to produce and store energy in geothermal resources. Because geothermal energy is the extraction of natural thermal energy from within the earth, it forms energy exploitation that is renewable and environmentally friendly. In 2010, around 587,786 TJ/yr (163,287 GWh/yr) was used in thermal energy (Lund & Boyd, 2015) and in 2016, a total of 13.1 GWe of conventional geothermal energy has been installed worldwide (Matek, 2016).

These discussions gave us the difficulties it faces, such as cost, maintaining optimal subsurface conditions, improving observational methods, etc. With its favour are the following advanced in drilling technology and management, increasing public awareness, positive effect in the environment, etc. Its flaws are installing a well is expensive, injecting high pressure may cost minor seismic activity or small earthquakes etc. On the other hand, it helps us have a more refined perception of how heat is transferred. The heat of the earth is transferred by the formation of the earth or by subsequent radioactive decay of elements in the upper parts of the earth. It is crucial to determine how the overall transfer is producing, which can be estimated from the process variable. By comparing predicted and field casing, we can confirm the basic formulation and applicability of the suggested produces for engineering calculations for heat flow.

Furthermore, this study gave us how to detect geothermal wells and drilling. Preparing for a drilling project is essential to separate the two significant roles, which are – “planning the well” and “designing the well”. With planning a well drilling, it is essential to know the hole size, bit types, all components of bottom-hole, chemical fluids and types, size, weight, problems etc. With designing a well drilling, it is vital to have a great variety of information. Such as the purpose of the well, reservoir conditions, logistical requirements, problems in drilling etc. Finally, it is also considered some industrial projects that used geothermal energy in Norway and other parts of the world, such as the Philippines and Iceland.

These findings indicate geothermal energy is indeed a fundamental renewable resource. It can help minimize the use of fossil fuels, and people are more aware of and appreciate the use of geothermal energy. The main concern in the industry is to recognize the safety of everyone and the environment. We believe this research; would be helpful for many projects in the future.

# References


Allan, M. L., & Kukacka, L. E. (1995). Calcium phosphate cements for lost circulation control in geothermal drilling. *Geothermics, 24*(2), 269-282.

Ármannsson, H., Fridriksson, T., Gudfinnsson, G. H., Ólafsson, M., Óskarsson, F., & Thorbjörnsson, D. (2014). IDDP—The chemistry of the IDDP-01 well fluids in relation to the geochemistry of the Krafla geothermal system. *Geothermics, 49*, 66-75.

baron de Fourier, J. B. J. (1822). *Théorie analytique de la chaleur*: Firmin Didot.

Bellarby, J. (2009). *Well completion design*: Elsevier.

Birch, F., Roy, R., & Decker, E. (1968). Heat flow and thermal history in New England and New York. *Studies of Appalachian Geology: Northern and Maritime*, 437-451.

Boyd, T. L., & Lund, J. W. (2006). *Geothermal heating of greenhouses and aquaculture facilities.* Paper presented at the 2006 ASAE Annual Meeting.

Conover, M. F. (1982). *Designing geothermal power plants to avoid reinventing the corrosion wheel*. Retrieved from

Culver, G. (1998). Drilling and well construction.

Dickson, M. H., & Fanelli, M. (2013). Geothermal energy: utilization and technology.

Ehrlich, R., & Geller, H. A. (2017). *Renewable energy: a first course* (1st Edition ed.): CRC press.

Ellis, I. (1985). Companion study guide to short course on geothermal corrosion and mitigation in low temperature geothermal heating systems.

Finger, J., & Blankenship, D. (2010). Handbook of best practices for geothermal drilling. *Sandia National Laboratories, Albuquerque*.

Fraser, S., Calcagno, P., Jaudin, F., Vernier, R., & Dumas, P. (2013). European Geothermal Risk Insurance Fund EGRIF. *Energy Europe Programme of European Union. http://www. geoelec. eu/wp-content/uploads/2011/09/D-3*.

Fridleifsson, G. Ó., & Albertsson, A. (2000). *Deep geothermal drilling at Reykjanes Ridge: opportunity for an international collaboration.* Paper presented at the Proceedings of the World Geothermal Congress.

Fridriksson, T., & Thórhallsson, S. (2007). Geothermal Utilization: Scaling And Corrosion. *Iceland Geosurvey Course Notes, Iceland*.

Ganguly, S., & Kumar, M. M. (2012). Geothermal reservoirs—A brief review. *Journal of the Geological Society of India, 79*(6), 589-602.

González-Acevedo, Z. I., & García-Zarate, M. A. (2018). Geothermal Energy as an Alternative to Reduce Atmospheric Emissions and Provide Green Energy. In *Green Technologies to Improve the Environment on Earth*: IntechOpen.

Grønlie, G., Johansen, T. E., Karlstad, B., & Heier, K. S. (1980). Prospecting for geothermal energy in the Iddefjord granite, Østfold, Norway. *Norsk Geo/. Tidsskr, 60*, 263-267.

Gunathilake, D. M. C. C., Senanayaka, D.P., Adiletta, G., & Senadeera, W. . (2018). *14 Drying of Agricultural Crops*.

Gunnlaugsson, E., Ármannsson, H., Thorhallsson, S., & Steingrímsson, B. (2014). Problems in geothermal operation–scaling and corrosion. *Goethermal Training Program, United Nations University*, 1-18.

Ichim, A.-C., Teodoriu, C., & Falcone, G. (2017). The influence of remedial cementing on thermal well design with applications to wellbore integrity.

Kabeyi, M. J. B. (2019). Geothermal electricity generation, challenges, opportunities and recommendations. *International Journal of Advances in Scientific Research and Engineering, 5*(8), 53-95.

Kristanto, D., Kusumo, L. P., & Abdassah, D. (2005). *Strategy Development for Corrosion Problem in Geothermal Installations Based on Corrosion Management Technology.* Paper presented at the Proceedings of World Geothermal Congress.

Kvalsvik, K. H., Midttomme, K., & Ramstad, R. K. (2019). *Geothermal energy use, country update for norway.* Paper presented at the European Geothermal Congress.

Lee, K. (1996). *Classification of geothermal resources-an engineering approach*. Retrieved from

Lund, J. W., & Boyd, T. (2015). Direct Utilization of Geothermal Energy 2015 Worldwide Review. *GRC Transactions, 39*, 79-92.
Matek, B. (2016). Annual US & Global Geothermal Power Production Report, Geothermal Energy Association, Washington, USA, 36pp. In.
Menzies, A. J., Villaseñor, L. B., & Sunio, E. G. (2010). *Tiwi geothermal field, Philippines: 30 years of commercial operation.* Paper presented at the Proceedings.
Midttømme, K. (2005). *Norway's geothermal energy situation.* Paper presented at the Proceedings world geothermal congress.
Nathan Amuri, B. (2017). *Heat Recovery Mechanism for Non Condensable Geothermal Fractured Reservoirs by CO2 Injection and Well Heat Insulating.* University of Stavanger, Norway,
Ngugi, P. K. (2008). Geothermal well drilling. *Short Course III on Exploration for Geothermal Resources, Lake Naivasha, Kenya*.
Nordell, B. (2015). Using ice and snow in thermal energy storage systems, book section 8. *Woodhead Publishing Series in Energy, 20*, 187-120.
O'Sullivan, M. J., Pruess, K., & Lippmann, M. J. (2001). State of the art of geothermal reservoir simulation. *Geothermics, 30*(4), 395-429.
Ocampo-Diaz, J. D. D., Valdez-Salaz, B., Shorr, M., Sauceda, M., & Rosas-González, N. (2005). *Review of corrosion and scaling problems in Cerro Prieto geothermal field over 31 years of commercial operations.* Paper presented at the Proceedings of World Geothermal Congress, International Geothermal Association (IGA), Antalya, Turkey.
Pascal, C., Elvebakk, H., & Olesen, O. (2010). *An assessment of deep geothermal resources in Norway.* Paper presented at the Abstracts and Proceedings, World Geothermal Congress, 25–29 April, Bali, Indonesia.
Povarov, O., Tomarov, G., & Semenov, V. (2000). *Physical and chemical processes of geothermal fluid impact on metal of geothermal power plant equipment.* Paper presented at the Proceedings World Geothermal Congress.
Sanada, N., Kurata, Y., Nanjo, H., Kim, H.-s., Ikeuchi, J., & Lichti, K. A. (2000). *IEA Deep Geothermal Resources Subtask C: Materials, Progress with a Database for Materials Performance in Deep and Acidic Geothermal Wells.* Paper presented at the Proc World Geothermal Congress, Kyushu, Tohoku, Japan.
Schweitzer, P. A. (1996). *Corrosion Engineering Handbook, -3 Volume Set*: CRC press.
Shadravan, A., & Shine, J. (2015). *Sustainable zonal isolation under extreme high temperature conditions.* Paper presented at the SPE/IATMI Asia Pacific Oil & Gas Conference and Exhibition.
Sircar, A., Shah, M., Vaidya, D., Dhale, S., Sahajpal, S., Yadav, K., . . . Mishra, T. (2017). Performance simulation of ground source heat pump system based on low enthalpy geothermal systems. *Emerging Trends in Chemical Engineering, 4*(1), 1-12.
Suryanarayana, P., Bowling, J., Sathuvalli, U. B., & Krishnamurthy, R. M. A Design Basis for Geothermal Well Tubulars Subjected to Annular Pressure Buildup from Fluids Trapped in Cement.
Willhite, G. P. (1967). Over-all heat transfer coefficients in steam and hot water injection wells. *Journal of Petroleum technology, 19*(05), 607-615.

# Appendix

| Country | MWt | TJ/yr | GWh/yr | Load Factor |
|---|---|---|---|---|
| Albania | 16.23 | 107.59 | 29.89 | 0.21 |
| Algeria | 54.64 | 1699.65 | 472.25 | 0.99 |
| Argentina | 163.60 | 1,000.03 | 277.81 | 0.19 |
| Armenia | 1.50 | 22.50 | 6.25 | 0.48 |
| Australia | 16.09 | 194.36 | 53.99 | 0.38 |
| Austria | 903.40 | 6,538.00 | 1,816.26 | 0.23 |
| Belarus | 4.73 | 113.53 | 31.54 | 0.76 |
| Belgium | 206.08 | 864.40 | 24.01 | 0.13 |
| Bosnia & Herzegovina | 23.92 | 252.33 | 70.10 | 0.33 |
| Brazil | 360.10 | 6,622.40 | 1,839.70 | 0.58 |
| Bulgaria | 93.11 | 1,224.42 | 340.14 | 0.42 |
| Canada | 1,466.78 | 11,615.00 | 3,226.65 | 0.25 |
| Caribbean Islands | 0.10 | 2.78 | 0.77 | 0.85 |
| Chile | 19.91 | 186.12 | 51.70 | 0.30 |
| China | 17,870.00 | 174,352.00 | 48,434.99 | 0.31 |
| Columbia | 18.00 | 289.88 | 80.50 | 0.51 |
| Costa Rica | 1.00 | 21.00 | 5.83 | 0.67 |
| Croatia | 79.94 | 684.49 | 190.15 | 0.27 |
| Czech Republic | 304.50 | 1,790.00 | 497.26 | 0.19 |
| Denmark | 353.00 | 3,755.00 | 1,043.14 | 0.34 |
| Ecuador | 5.16 | 102.40 | 28.45 | 0.63 |
| Egypt | 6.80 | 88.00 | 24.45 | 0.41 |
| El Savador | 3.36 | 56.00 | 15.56 | 0.53 |
| Estonia | 63.00 | 356.00 | 98.90 | 0.18 |
| Ethiopia | 2.20 | 41.60 | 11.56 | 0.60 |
| Finland | 1,560.00 | 18,000.00 | 5,000.40 | 0.37 |
| France | 2,346.90 | 15,867.00 | 4,407.85 | 0.21 |
| Georgia | 73.42 | 695.16 | 193.12 | 0.30 |
| Germany | 2,848.60 | 19,531.30 | 5,425.80 | 0.22 |
| Greece | 221.88 | 1,326.45 | 368.49 | 0.19 |
| Greenland | 1.00 | 21.00 | 5.83 | 0.67 |
| Guatemala | 2.31 | 56.46 | 15.68 | 0.78 |
| Honduras | 1.93 | 45.00 | 12.50 | 0.74 |
| Hungary | 905.58 | 10,268.06 | 2,852.47 | 0.36 |
| Iceland | 2,040.00 | 26,717.00 | 7,422 | 0.42 |
| India | 986.00 | 4,302.00 | 1,195.10 | 0.14 |
| Indonesia | 2.30 | 42.60 | 11.83 | 0.59 |
| Iran | 81.50 | 1,103.12 | 306.45 | 0.43 |
| Ireland | 265.54 | 1,240.54 | 344.62 | 0.15 |
| Israel | 82.40 | 2,193.00 | 609.22 | 0.84 |
| Italy | 1,014.00 | 8,682.00 | 2411.90 | 0.27 |
| Japan | 2,186.17 | 26,130.08 | 7,258.94 | 0.38 |
| Jordan | 153.30 | 1,540.00 | 427.81 | 0.32 |
| Kenya | 22.40 | 182.62 | 50.73 | 0.26 |

| | | | | |
|---|---|---|---|---|
| Korea (South) | 835.80 | 2,682.65 | 745.24 | 0.10 |
| Latvia | 1.63 | 31.81 | 8.84 | 0.62 |
| Lithuania | 94.60 | 712.90 | 198.04 | 0.24 |
| Macedonia | 48.68 | 601.11 | 166.99 | 0.39 |
| Madagascar | 2.81 | 75.59 | 21.00 | 0.85 |
| Mexico | 155.82 | 4,171.00 | 1,158.70 | 0.85 |
| Mongolia | 20.16 | 340.46 | 94.58 | 0.54 |
| Morocco | 5.00 | 50.00 | 13.89 | 0.32 |
| Nepal | 3.32 | 81.11 | 22.53 | 0.78 |
| Netherlands | 790.00 | 6,426.00 | 1,785.14 | 0.26 |
| New Zealand | 487.45 | 8,621.00 | 2,394.91 | 0.56 |
| Norway | 1,300.00 | 8,260.00 | 2,294.63 | 0.20 |
| Pakistan | 0.54 | 2.46 | 0.68 | 0.14 |
| Papua New Guinea | 0.10 | 1.00 | 0.28 | 0.32 |
| Peru | 3.00 | 61.00 | 16.95 | 0.64 |
| Philippines | 3.30 | 39.58 | 11.00 | 0.38 |
| Poland | 488.84 | 2,742.60 | 761.89 | 0.18 |
| Portugal | 35.20 | 478.20 | 132.84 | 0.43 |
| Romania | 245.13 | 1,905.32 | 529.30 | 0.25 |
| Russia | 308.20 | 6,143.50 | 1,706.66 | 0.63 |
| Saudi Arabia | 44.00 | 152.89 | 42.47 | 0.11 |
| Serbia | 115.64 | 1,802.48 | 500.73 | 0.49 |
| Slovak Republic | 149.40 | 2,469.60 | 686.05 | 0.52 |
| Slovenia | 152.75 | 1,137.23 | 315.93 | 0.24 |
| South Africa | 2.30 | 37.00 | 10.28 | 0.51 |
| Spain | 64.13 | 344.85 | 95.80 | 0.17 |
| Sweden | 5,600.00 | 51,920.00 | 14,423.38 | 0.29 |
| Switzerland | 1,733.08 | 11,836.80 | 3,288.26 | 0.22 |
| Tajikistan | 2.93 | 55.40 | 15.39 | 0.60 |
| Thailand | 128.51 | 1,181.20 | 328.14 | 0.29 |
| Tunisia | 43.80 | 364.00 | 101.12 | 0.26 |
| Turkey | 2,886.30 | 45,126.00 | 12,536.00 | 0.50 |
| Ukraine | 10.90 | 118.80 | 33.00 | 0.35 |
| United Kingdom | 283.76 | 1,906.50 | 529.63 | 0.21 |
| United States | 17,415.91 | 75,862.20 | 21,074.52 | 0.14 |
| Venezuela | 0.70 | 14.00 | 3.89 | 0.63 |
| Vietnam | 31.20 | 92.33 | 25.65 | 0.09 |
| Yemen | 1.00 | 15.00 | 4.17 | 0.48 |
| **GRAND TOTAL** | **70,328.98** | **587,786.43** | **163,287.07** | 0.27 |

*Table 1 - Summary of direct-use data worldwide in 2015, (Lund & Boyd, 2015)*

**Capacity, MWt**

| | 2015 | 2010 | 2005 | 2000 | 1995 |
|---|---|---|---|---|---|
| Geothermal Heat Pumps | 49,898 | 33,134 | 15,384 | 5,275 | 1,854 |
| Space Heating | 7,556 | 5,394 | 4,366 | 3,263 | 2,579 |
| Greenhouse Heating | 1,830 | 1,544 | 1,404 | 1,246 | 1,085 |
| Aquaculture Pond Heating | 695 | 653 | 616 | 605 | 1,097 |
| Agricultural Drying | 161 | 125 | 157 | 74 | 67 |
| Industrial Uses | 610 | 533 | 484 | 474 | 544 |
| Bathing and Swimming | 9,140 | 6,700 | 5,401 | 3,957 | 1,085 |
| Cooling / Snow Melting | 360 | 368 | 371 | 114 | 115 |
| Others | 79 | 42 | 86 | 137 | 238 |
| **Total** | **70,329** | **48,493** | **28,269** | **15,145** | **8,664** |

**Utilization, TJ/yr**

| | 2015 | 2010 | 2005 | 2000 | 1995 |
|---|---|---|---|---|---|
| Geothermal Heat Pumps | 325,028 | 200,149 | 87,503 | 23,275 | 14,617 |
| Space Heating | 88,222 | 63,025 | 55,256 | 42,926 | 38,230 |
| Greenhouse Heating | 26,662 | 23,264 | 20,661 | 17,864 | 15,742 |
| Aquaculture Pond Heating | 11,958 | 11,521 | 10,976 | 11,733 | 13,493 |
| Agricultural Drying | 2,030 | 1,635 | 2,013 | 1,038 | 1,124 |
| Industrial Uses | 10,453 | 11,745 | 10,868 | 10,220 | 10,120 |
| Bathing and Swimming | 119,381 | 109,410 | 83,018 | 79,546 | 15,742 |
| Cooling / Snow Melting | 2,600 | 2,126 | 2,032 | 1,063 | 1,124 |
| Others | 1,452 | 955 | 1,045 | 3,034 | 2,249 |
| **Total** | **587,786** | **423,830** | **273,372** | **190,699** | **112,441** |

**Capacity Factor**

| | 2015 | 2010 | 2005 | 2000 | 1995 |
|---|---|---|---|---|---|
| Geothermal Heat Pumps | 0.207 | 0.19 | 0.18 | 0.14 | 0.25 |
| Space Heating | 0.370 | 0.37 | 0.40 | 0.42 | 0.47 |
| Greenhouse Heating | 0.462 | 0.48 | 0.47 | 0.45 | 0.46 |
| Aquaculture Pond Heating | 0.546 | 0.56 | 0.57 | 0.61 | 0.39 |
| Agricultural Drying | 0.400 | 0.41 | 0.41 | 0.44 | 0.53 |
| Industrial Uses | 0.543 | 0.70 | 0.71 | 0.68 | 0.59 |
| Bathing and Swimming | 0.414 | 0.52 | 0.49 | 0.64 | 0.46 |
| Cooling / Snow Melting | 0.229 | 0.18 | 0.17 | 0.30 | 0.31 |
| Others | 0.583 | 0.72 | 0.39 | 0.70 | 0.30 |
| **Total** | 0.265 | 0.28 | 0.31 | 0.40 | 0.41 |

*Table 2 - Summary of the various categories of direct-use worldwide for the period of 2015, 2010, 2005, 2000 and 1995, (Lund & Boyd, 2015)*

| | |
|---|---|
| Hole size: | 9.625 in. |
| Casing (7 in., 26 lb, J-55): | |
| OD | 7.000 in. |
| ID | 6.276 in. |
| Tubing (2⅞ in., 6.4 lb, J-55): | |
| OD | 2.875 in. |
| ID | 2.441 in. |
| $k_e$: | 1.4 Btu/hr ft °F |
| $k_{cem.}$: | 0.51 Btu/hr ft °F |
| $k_{ins.}$: | $0.0256 + (T-50)(3.67 \times 10^{-5})$ Btu/hr ft °F |
| $\alpha$: | 0.04 sq ft/hr |
| $\varepsilon_{to} = \varepsilon_{ci}$ (mill scale): | 0.9 |
| $\varepsilon_{to}$ (aluminum paint): | 0.4 |
| $T_e$: | 80F |

*Table 3 - Parameters for Variation of $U_{to}$, (Willhite, 1967)*

| Material | Thermal Conductivity (Btu/hr · ft · °F) |
|---|---|
| **Steel** | 25.0 |
| **Insulation (calcium silicate)** | 0.02 to 0.06 |
| **Cement:** | |
| **Wet (at completion)** | 0.5 to 0.6 |
| **Dry** | 0.2 to 0.4 |

*Table 4 - Thermal Conductivity of Wellbore Materials, (Willhite, 1967)*

| HOLE NO | DEPTH m | TEMP. GRADIENT °C/km | CONDUCTIVITY $10^{-3}$ cal/cm s °C | HEAT FLOW hfu | HEAT FLOW W/m$^2$s |
|---|---|---|---|---|---|
| 2 | 98 | 16.0 | 9.00* | 1.44 | 60.2 |
| 3 | 91 | 20.4 | 9.00* | 1.84 | 76.9 |
| 5 | 109 | 15.2 | 9.00* | 1.36 | 56.8 |
| 8 | 106 | 19.8 | 9.00* | 1.78 | 74.4 |
| 10 | 91 | 12.3 | 9.00* | 1.11 | 46.4 |
| 12 | 123 | 21.5 | 7.37 | 1.65 | 69.0 |
| 13 | 101 | 16.7 | 9.00* | 1.51 | 63.1 |
| 14 | 128 | 20.6 | 9.01 | 1.88 | 78.6 |
| 15 | 103 | 20.1 | 9.00* | 1.81 | 75.7 |
| 18 | 124 | 19.3 | 9.00* | 1.74 | 72.7 |
| 21 | 91 | 14.4 | 9.00* | 1.30 | 54.3 |
| Average Norway | | | | 1.02 | 42.6 |

*Table 5 - Temperature gradient, conductivity and heat flow from 11 holes in the Iddefjord granite, Østfold, Norway. Conductivity only measured in holes Nos. 12 and 14 (*: estimated conductivity), (Grønlie et al., 1980)*

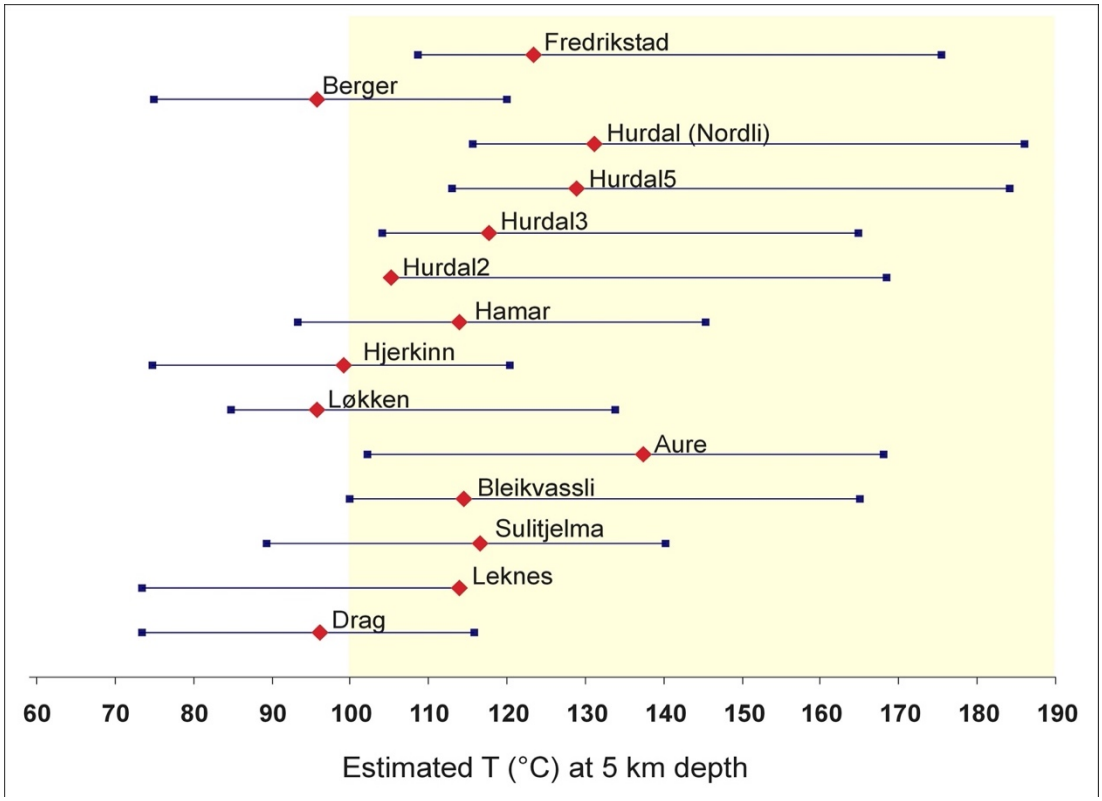


*Table 6 - Estimated temperatures at 5km depth below the surface for each selected heat flow site in Norway, (Midttømme, 2005)*

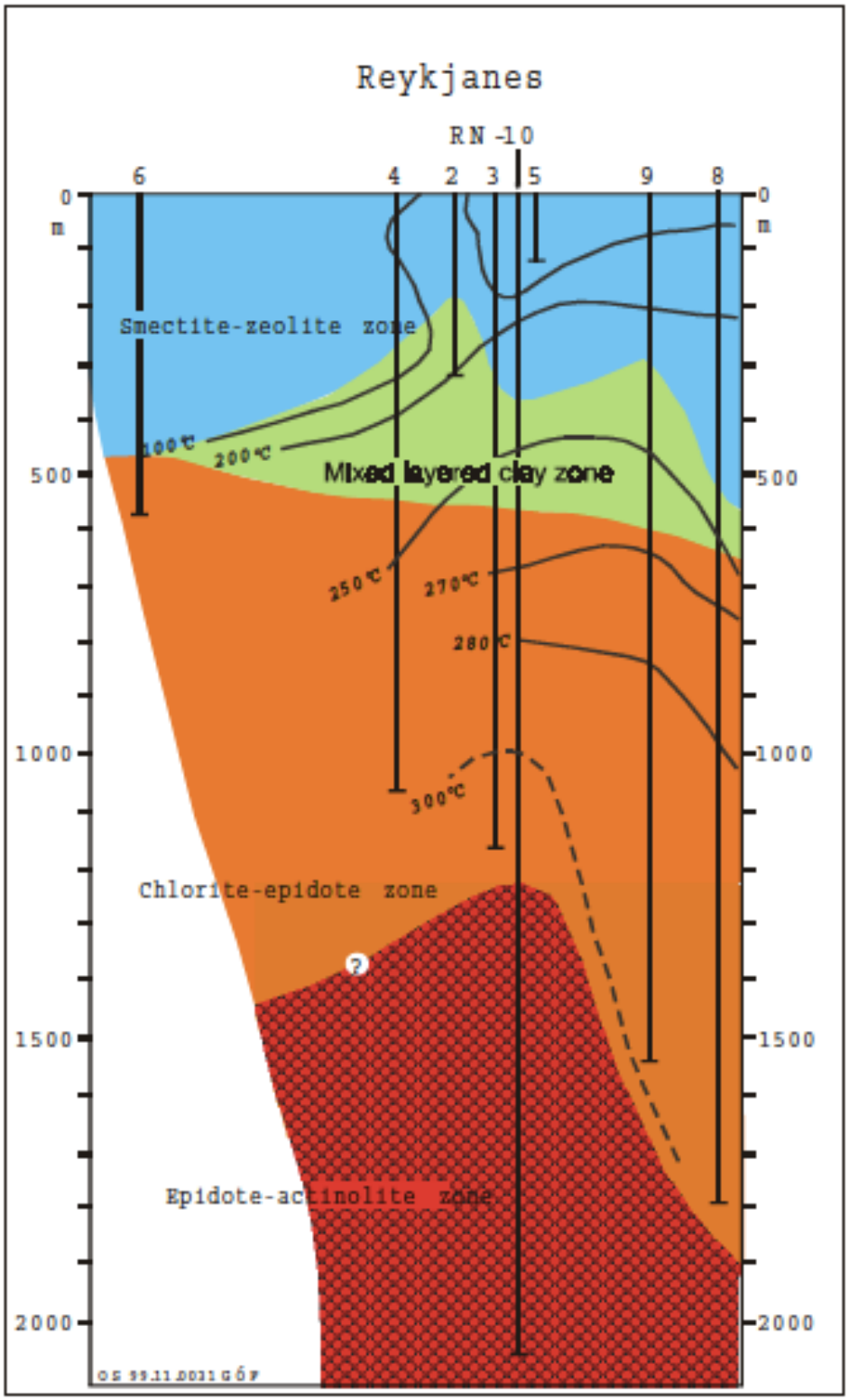


*Table 7 - Hydrothermal section along the rift axes at Reykjanes, inclunding all deep drill holes,(Fridleifsson & Albertsson, 2000)*

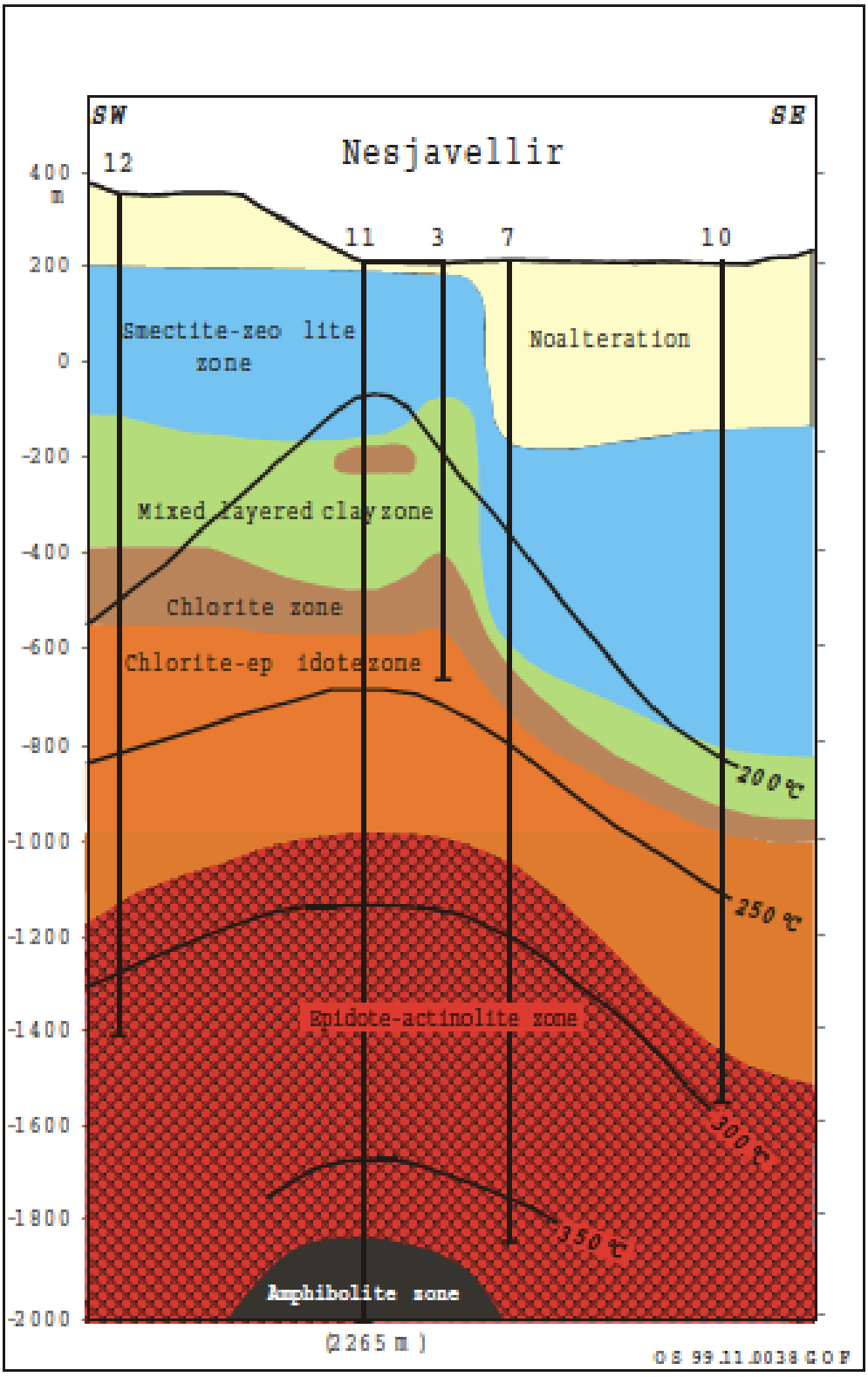


*Table 8 - Hydrothermal cross section across the rift zone at Nesjavallir, including well NJ-11,(Fridleifsson & Albertsson, 2000)*

| Hole Diameter, cm | Casing Diameter, cm | Setting Depth, m |
|---|---|---|
| 66 | 55.9 | 91 |
| 52 | 40.6 | 457 |
| 37.5 | 29.8 | 1524 |
| 27 | Openhole | 3048, 3 times |

*Table 9 - Steam Well Borehole Profile, (Finger & Blankenship, 2010)*

| Bit Diameter, cm | No. Bits Used | Avg. ROP, m/hr | Avg. Life, m |
|---|---|---|---|
| 66 | 1 | 11.6 | 91+ |
| 52 | 2 | 6.4 | 183 |
| 37.5 | 4 | 5.2 | 1 @ 610<br>3 @ 152 |
| 27 | 17 | 29 | 335 |

*Table 10 - Steam Well Bit Summary, (Finger & Blankenship, 2010)*

| Hole Diameter, cm | Casing Diameter, cm | Setting Depth, m |
|---|---|---|
| 102 | 91.4 | 30.5 |
| 44.5 w/91.4 ur* | 76.2 | 91 |
| 44.5 w/76.2 ur | 61 | 305 |
| 44.5 w/61 ur | 50.8 | 457 |
| 44.5 w/55.9 ur | 40.6 | 640 |
| | 34 Ti | 640 |
| 37.5 | openhole | 1524 |
| *ur = underreamer | | |

*Table 11 - Brine Well Borehole Profile (Finger & Blankenship, 2010)*

| Bit Diameter, cm | No. Bits Used | Avg. ROP, m/hr | Avg. Life, m |
|---|---|---|---|
| 44.5 | 1 | na | 640 |
| 37.5 | 7 | 4.6 | 122 |

*Table 12 - Brine Well Bit Summary, (Finger & Blankenship, 2010)*